CENTRE DE RECERCA MATEMÀTICA

Title:	*Advanced Course on Piecewise Smooth Dynamical Systems*
Journal Information:	*CRM Preprints*,
Author(s):	Advanced Course on Piecewise Smooth Dynamical Systems.
Volume, pages:	*1-101*, DOI:[--]

CENTRE DE RECERCA MATEMÀTICA

Advanced Course on Piecewise Smooth Dynamical Systems

Quaderns

Number 75 / April 2016

Advanced Course on

Piecewise Smooth Dynamical Systems

April 11 to 15, 2016

Acknowledgements. This program is made possible in part by the generous support from the Simons Foundation, Generalitat de Catalunya, Società italiana Caos e Complessità (Italian Society for Chaos and Complexity), EPSRC (Engineering and Physical Sciences Research Council), Universitat Politècnica de Catalunya, Societat Catalana de Matemàtiques, wiris, BREUDS (Brazillian-European partnership in Dynamical Systems).

Contents

The notes contained in this booklet were printed directly from files supplied by the autors before the course.

Foreword

These are notes prepared for the Advanced School on *Piecewise Smooth Dynamical Systems*, organized in the Centre de Recerca Matemàtica (Bellaterra, Catalonia), during 11-15 April, 2016. The School has been organized with support from the EPSRC (Engineering and Physical Sciences Research Council), the Societat Catalana de Matemàtiques, WIRIS, and the IMA (Institute for Mathematics and its Applications). The Course comes in three parts: flows, maps, and applications.

An *Introduction to the dynamics of piecewise smooth maps* will be given by Paul Glendinning. After a discussion of why pieceiwse smooth maps are interesting, the course moves into their phenomenology, and reviews some techniques from smooth theory. The main topics are then: basic stability analysis, piecewise monotonic maps of the interval, rotation-like maps, gluing bifurcations (aka Big Bang bifurcations and period-adding), an introduction to renormalization, decomposition theorems and a brief guide to kneading theory, piecewise smooth maps of the plane including the Lozi and border collision normal form, piecewise isometries, bounding regions, periodic orbits and resonance, robust chaos, and two-dimensional attractors. The course concludes with a discussion of challenges in higher dimensions, particularly concerning periodic orbits, N-dimensional attractors, and analogies with smooth cases.

An *Introduction to the dynamics of piecewise smooth flows* will be given by Mike Jeffrey. We start with a few key points in the history & applications of discontinuities from mechanics and control systems, and some of the key figures in setting up a general theory for differential equations with 'discontinuous righthand sides'. The methods of inclusions versus combinations are discussed, after which we introduce the elementary dynamics of crossing and sliding at a discontinuity surface. The analytical methods of switching layers and layer variables are presented for one switch and then for multiple switches. The concepts of discontinuity-induced phenomena and determinacy breaking are introduced, along with the (problematic) definitions of stability, equivalence, & bifurcation in piecewise smooth flows. We end by introducing some of the novel attractors and bifurcations that offer a hint at what remains to be discovered, including the present state of zoology of singularities in the plane.

The last part of the course will be a series of guest lectures, introducing course participants to some of the current research topics in applications of piecewise smooth dynamics. The guest lecturers will be researchers in residence at the Intensive Research Program on Advances in Nonsmooth Dynamics at the CRM, 1 February – 29 April 2016.

Mike Jeffrey (University of Bristol)
Paul Glendinning (University of Mancehster)

Introduction to the dynamics of piecewise smooth maps

by

Paul Glendinning

School of Mathematics, University of Manchester, Manchester M13 9PL, U.K.

Abstract. These are preliminary notes for the Advanced Course on Piecewise Smooth Dynamical Systems 11–15 April 2016 at the CRM, Barcelona as part of the CRM Intensive Research Program in Nonsmooth Dynamics.

1. Introduction

This course is about piecewise smooth (PWS) maps. If the phase space (typically $\mathbb{R}^n$) is partitioned into N disjoint open regions such that the union of the closures of these regions is the whole space, then a PWS map is a map on this partition which is defined by a different smooth function on each region. Note that a PWS map may be discontinuous across boundaries, or it may be continuous but the Jacobian matrix is discontinuous. Other classes exist, but these two form the basis for most studies. The decision about how to define dynamics on the boundaries of the regions can be a bit awkward and will involve us in some little technical issues later.

Given this description you may think that these maps are really rather special and uninteresting, so the first question you should ask about the study of piecewise smooth maps is: why bother?

1.1. PWS maps are interesting. PWS maps are interesting. So interesting that the ideas, examples and techniques involved in their study have been rediscovered by different groups at different times. This is in some sense irritating (it is hard to know what has been done, and the same phenomenon is called by a different name in different groups making comparisons hard), but it also emphasises how central PWS systems are in the study of dynamics. Despite the range of modern applications the area is still seen from the outside as quite a narrow interest group. On the other hand, as Mike Field says, engineers (both mechanical and electronic) have spent the last 50 years working with systems containing jumps, whilst the dynamical systems community has spent the last 50 years perfecting the theory of smooth dynamical systems. It is time for a change!

The list below gives an idea of the groups that have been interested in PWS systems. It is neither complete, nor accurate (and I apologise in advance to those who think I have put them in the wrong group), but it gives an impression of the diversity of approaches and interests in the area.

- (Mechanics, 1990s) Budd, di Bernardo, Champneys, Dankowitz, Nordmark, Hogan (from 1980s!).

- (Electronics, applied dynamical systems, 1990s) Banerjee, Grebogi, Nusse, Ott, Yorke.
- (Ergodic Theory, 1980s and 2000s) Young, Misieurewicz; Buzzi, Keller, Saussol, Tsujii.
- (Classification of flows on manifolds and rational billiards, 1960s) Viana
- (Non-invertible maps, 1980s) Avrutin, Gardini, Lozi, Mira, Schanz, Shushko.
- (Homoclinic bifurcations, 1970s) Gambaudo, Glendinning, Holmes, Lorenz, Procaccia, Tresser.
- (Structure Theorems, 1970s) Alseda, Guckenheimer, Llibre, Milnor, Misiurewicz, Rand, Thurston, Williams.
- (Rotations, 1980s) Herman, Kadanoff, Keener, Lanford, Rhodes, Thompson.
- (Modern Nonsmooth, 2000s) Colombo, Granados, Jeffrey, Simpson.

I could go on, but you get the point.

1.2. Motivating examples. There are a number of standard examples that give a sense of the many models that can be described via PWS systems. Here are a few.

A bouncing ball

Suppose a ball is dropped and starts bouncing. Let v_n be the speed (upwards) immediately after the n^{th} bounce at time t_n. It will rise to height h_n with $2gh_n = v_n^2$ after time v_n/g and then return to the ground at time $t_{n+1} = t_n + 2v_n/g$ with the same speed v_n. The collision with the ground instantaneously reverses the direction of the the velocity and reduces its magnitude by a factor $r \in (0,1)$, so $v_{n+1} = rv_n$.

This impacting system therefore has a jump in the velocity at each collision but the equations describing the change over each bounce are

$$v_{n+1} = rv_n, \quad t_{n+1} = t_n + 2v_n/g, \quad 0 < r < 1.$$

Thus although the dynamics is piecewise smooth with jumps in phase space, the modelling map is smooth and is *not* of the sort that will concern us here. Indeed, they can be solved:

$$\begin{aligned} v_n &= r^n v_0, \\ t_n &= t_0 + \tfrac{2v_0}{g}(1 + r + r^2 + \cdots + r^{n-1}) = t_0 + \tfrac{2v_0(1-r^n}{g(1-r)}. \end{aligned} \tag{1}$$

As $n \to \infty$, $t_n - t_0 \to \frac{2v_0}{g(1-r)}$, i.e., there are an infinite number of bounces in finite time for this model system.

A grazing bifurcation

Consider a differential equation in the plane defined so that in $x < 0$ the system (extended into $x > 0$) has a circular stable periodic orbit of radius a bit larger than 1 enclosing an unstable focus at $(-1, 0)$, whilst in $x > 0$ the system is defined by a differential equation having trajectories that are locally parabolic about of the form $x = c - (y - \epsilon)^2$ for some small $\epsilon > 0$ and with the direction of time chosen so that $\dot{y} > 0$. These systems are 'glued'

together across the discontinuity (switching) line $x = 0$. For example, this is the case for the differential equations

$$\begin{aligned} \dot{x} &= (1+a)(x+1) - y - (x+1)((x+1)^2 + y^2) \\ \dot{y} &= x + 1 + (1+a)y - y((x+1)^2 + y^2) \text{if } x < 0 \end{aligned} \tag{2}$$

and

$$\begin{aligned} \dot{x} &= 2(y - \epsilon) \\ \dot{y} &= 1 \text{if } x > 0. \end{aligned} \tag{3}$$

Geometrically, an important point on the switching line is the grazing point at which $\dot{x} = 0$. An elementary calculation shows that this is $y_* \approx a$ when a is small. Choose a return section $y = y_*$ near the origin. Solutions in $x < 0$ simply move up (increasing x) until they strike the y-axis with $y \leq y_*$ at which time they switch to the parabolic flow, striking $y = y_*$ at some point in $x > 0$ and then pass back into $x < 0$ with $y > y_*$ and then travel again round a loop in $x < 0$. This generates a return map on $x = 0$ but with an interesting feature.

Let (x_0, y_*), $x_0 < 0$, denote the initial condition such that the next intersection of the trajectory through (x_0, y_*) with $y = y_*$ is at the grazing point $(0, y_*)$. A solution with an initial condition a little to the left of (x_0, y_*) on $y = y_*$ will next intersect the return line just to the left of $x = 0$ without entering $x > 0$ and do a further loop close to the grazing orbit in $x < 0$ before striking $x = 0$ an using the parabolic flow to intersect the $y = y_*$ at some point x_1.

However, a solution with an initial condition a little to the right of (x_0, y_*) on $y = y_*$ will strike $x = 0$ just below $(0, y_*)$ and then the parabolic flow will lead to an intersection with $y = y_*$ at some point x_2. For appropriate choices of parameter $x_2 < x_1$ and, assuming sufficient contraction near the periodic orbit of the $x < 0$ system, the return map will have slope less than on (attraction) and a jump at $x = 0$ reflecting the two possible images of the grazing point.

In this case the return map derived on $y = y_*$ has a discontinuity at the due to the geometry of the two flows that make up the nonsmooth flow defined in (2, 3).

The Lorenz semiflow

The Lorenz equations provide one of the early examples of differential equations with chaotic attractors (although the proof that the attractor really is chaotic is relatively recent). Guckenheimer and Williams [**32, 51**] developed mathematical abstractions of the equations, assuming that the flow lies on the branched manifold of Figure 1a. In this case the chaos is due to solutions falling one one or other side of the stable manifold of a saddle and being swept round a loop to the left or to the right. The return map of the model flow takes the form shown in Figure 1b. It has a discontinuity at the origin (the stable manifold of the saddle) and the slope goes to infinity like $|x|^\alpha$, $0 < \alpha < 1$ at the point of discontinuity. We will return to maps like these in later sections.

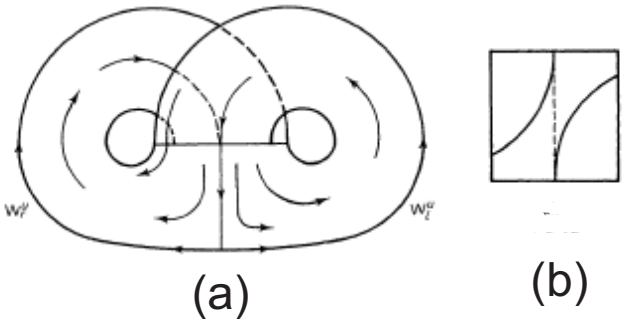

FIGURE 1. Lorenz semiflow and the associated one-dimensional map, from [**51**].

1.3. Phenomenology. In many cases the interest is not in a particular map, but in a family of maps. Thus many results aim to describe the structure of dynamics as a function of parameter, i.e., the bifurcation theory of these maps. One feature that stands out in PWS systems because it is not present in smooth systems is period-adding. In period-adding bifurcations there is usually a sequence of bifurcations in which a constant is added to the period of the orbit at each bifurcation. An example is shown in Figure 2. Sometimes the bifurcations are clean, in the sense that there are no intermediary bifurcations, and sometimes more complicated, with bands of chaos separating the added orbits. This diagram shows solutions of Nordmark's square root map asa function of the parameter μ. The map is continuous but non-differentiable at a single point:

$$x_{n+1} = \begin{cases} \mu + ax_n & \text{if } x < 0 \\ \mu - b\sqrt{x_n} & \text{if } x \geq 0 \end{cases} \tag{4}$$

with $a = 0.5$ and $b = 2$ We will look at another way such sequences can be generated in section 4b.

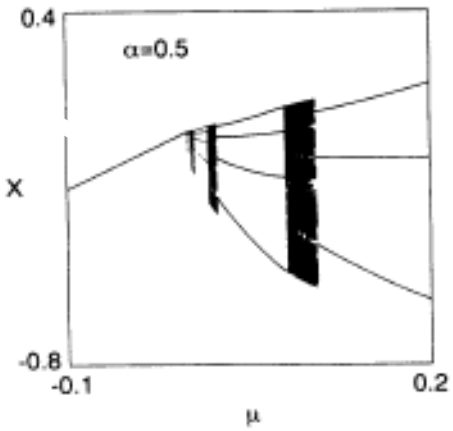

FIGURE 2. Period adding cascade with chaotic bands, from [**40**].

In many circumstances more than one parameter is present, and the sensitivity to changes in the parameter can be mind-boggling. Figure 3 shows the result of a numerical simulation by Avrutin *et al.* [**3**] showing very complicated regions of dynamics in a two parameter example. This level of complexity make it hard to decide what feature is worth concentrating upon in any analysis.

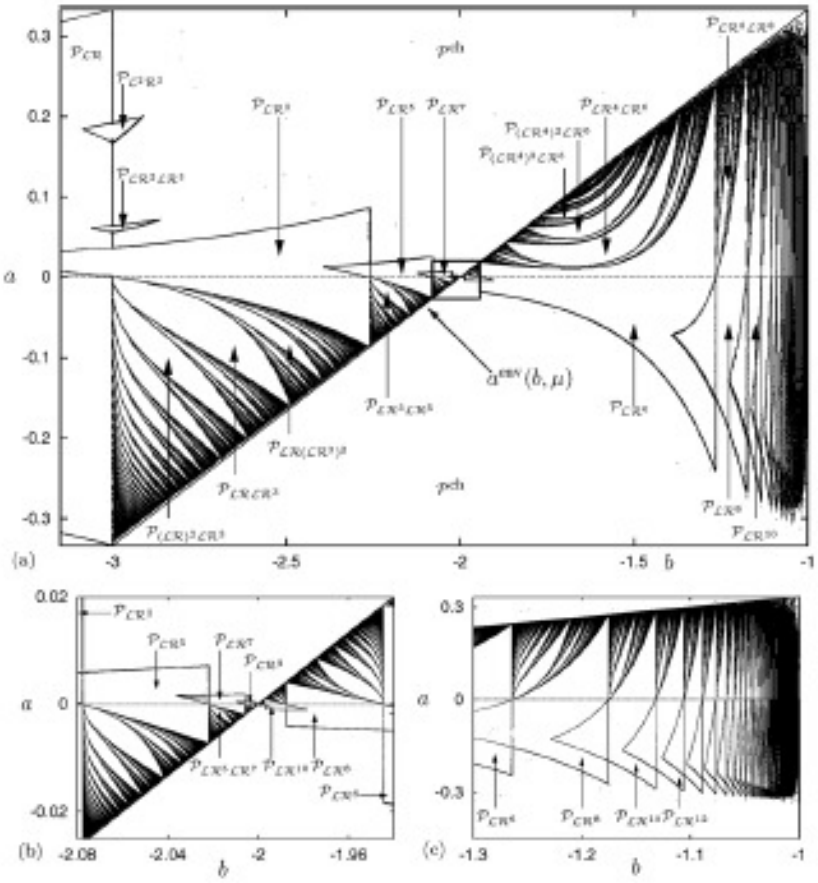

FIGURE 3. Bifurcation curves in a two parameter piecewise smooth map of the interval, from [**3**].

These two examples bring out an important feature of the non-smooth world. The number of possible behaviours seems to be huge, and the complexity of the bifurcation diagrams and their sensitivity to changes in other parameters ca be quite bewildering. For the mathematician used to tidy classifications this can be a problem. One of the recurring themes of this lecture series is that 'less is more'. In a world of extraordinary complexity it may not be either useful or possible to obtain a complete list of theoretical possibilities, and that a less complete description may be more useful.

1.4. Less is more. Figure 3 and the results of e.g., [**29**] suggest that the level of complexity of bifurcations in even quite simple PWS systems is much greater than that for smooth flows. In the theory of smooth systems it is standard to give quite general bifurcation theorems which reflect the

important local features of the dynamics. It seems likely that there is a proliferation of cases for PWS systems which means that detailed bifurcation theorems are much less useful, and it is then a matter of judgement about how much detail should be given.

These lectures reflect this attitude. I will use some standard examples to illustrate techniques rather than attempt to provide a detailed description of every bifurcation in the literature. This might make the use of a small number of examples appear unbalanced, but (I hope) that the techniques described here can be applied to many of the examples that might be met in applications. For more detail of 'less is more' see [**27, 28**].

1.5. Smooth Theory. By definition a PWS system is smooth in regions, so any dynamics that does not interact with a boundary can be described using smooth theory. This includes the existence and stability of fixed points and periodic orbits in smooth regions and their bifurcations (in section 2.4 we will look at some elementary new bifurcations involving the boundary).

A fixed point of a smooth map $f\colon \mathbb{R}^n \to \mathbb{R}^n$ is a solution of

$$x = f(x) \tag{5}$$

and it is stable (or more accurately, linearly stable) if all the eigenvalues of the Jacobian matrix

$$Df(x) = \begin{pmatrix} \frac{\partial f_1}{\partial x_1} & \frac{\partial f_1}{\partial x_2} & \cdots & \cdots & \frac{\partial f_1}{\partial x_n} \\ \frac{\partial f_2}{\partial x_1} & \frac{\partial f_2}{\partial x_2} & \cdots & \cdots & \frac{\partial f_2}{\partial x_n} \\ \vdots & \vdots & \vdots & \vdots & \vdots \\ \frac{\partial f_n}{\partial x_1} & \frac{\partial f_n}{\partial x_2} & \cdots & \cdots & \frac{\partial f_n}{\partial x_n} \end{pmatrix} \tag{6}$$

evaluated at the fixed point lie inside the unit circle (i.e., have modulus less than one).

A point is periodic of period p if

$$x = f^p(x) \tag{7}$$

where $f^p(x) = f(f^{p-1}(x))$, i.e., it denotes the p^{th} iterate of f,

$$f^p = f \circ f \circ \cdots \circ f \quad (p \text{ times}),$$

and not the p^{th} power of $f(x)$ which we will denote by $[f(x)]^p$ or similar. If x is a point of period p then the periodic orbit containing x is

$$\{x, f(x), \ldots, f^{p-1}(x)\}$$

and if all the points are distinct then it is sometimes worth emphasising that p is the minimal possible period of the orbit (though usually this is left unstated). Note that if x has period p then it also has period mp for all $m > 1$.

Since a periodic point can be viewed as a fixed point of f^p, the linear stability of a periodic orbit is determined by the eigenvalues of the Jacobian matrix

$$Df^p(x) = Df(f^{p-1}(x))Df(f^{p-2}(x)) \ldots Df(x).$$

Bifurcations occur is an eigenvalue passes through the unit circle, so there are three generic cases: a simple eigenvalue of $+1$, a simple eigenvalue of $+1$, or a pair of simple eigenvalues $e^{\pm i\theta}$, $\theta \neq m\pi$, $m \in \mathbb{Z}$.

The Centre Manifold Theorem implies that these cases can be classified in the same way regardless of the dimension of the phase space, a feature that is not true of PWS bifurcations). An eigenvalue of $+1$ implies that for small changes of parameter there is typically a saddle-node bifurcation in which as a parameter is varied a pair of fixed points come together at the bifurcation parameter and do not exist thereafter. Symmetries or the non-generic vanishing of some derivatives of the Taylor expansion of the map can imply that a saddlenode bifurcation does not happen and there may be a transcritical bifurcation (exchange of stability) or a pitchfork bifurcation.

An eigenvalue of -1 leads to a period-doubling bifurcation: as parameters vary a fixed point changes stability at the bifurcation value and an orbit of period two is created. If this period two orbit is stable it is called a supercritical period-doubling bifurcation.

A pair of eigenvalues $e^{\pm i\theta}$, $\theta \neq m\pi$, $m \in \mathbb{Z}$ leads to a Hopf, or Niemark-Sacker bifurcation. The fixed point changes stability and an invariant curve bifurcates on which there can be other attractors (e.g., periodic orbits) near resonances when θ is a rational multiple of 2π.

1.6. Markov partitions and chaos. There are a number of results which make the analysis of one-dimensional systems significantly easier than higher dimensional dynamics. The first result describes the dynamics of monotonic maps.

Lemma 1. *Suppose $f\colon \mathbb{R} \to \mathbb{R}$ is a continuous map. If f is increasing then every bounded orbit is either a fixed point or tends to a fixed point. If f is decreasing then every bounded orbit is either a fixed point or a point of period two or tends to a fixed point or a point of period two.*

Proof. Suppose that f is increasing, i.e., $x < y$ implies that $f(x) \leq f(y)$. Take $x \in \mathbb{R}$. Then either

$$f(x) = x, \quad \text{or} \quad f(x) > x, \quad \text{or} \quad f(x) < x.$$

In the first case x is a fixed point. In the second case $x < f(x)$ implies that $f(x) \leq f^2(x)$ using the increasing property, and hence by induction $(f^k(x))$ is an increasing sequence. It is therefore either unbounded or bounded above. If it is bounded above then the sequence tends to a limit, ℓ, and hence $(f^{k+1}(x))$ tends to $f(\ell)$. But the two sequences are the same (by continuity of f) and hence $\ell = f(\ell)$, i.e., ℓ is a fixed point. In the third case $f(x) < x$ implies that $f^2(x) \leq f(x)$ and so $(f^k(x))$ is a decreasing sequence. It is therefore unbounded or bounded below, in which case by the same argument as in the second case the limit is a fixed point.

If f is decreasing then $x < y$ implies that $f(x) \geq f(y)$ and hence $f^2(x) \leq f^2(y)$. Hence f^2 is increasing and since fixed points of f^2 are either fixed points or points of period two for f the second part of the lemma holds. □

Lemma 1 describes simple behaviour – we now describe how to treat some chaotic dynamics. The first idea is the transition matrix. Throughout this section f will be a continuous map $f\colon \mathbb{R} \to \mathbb{R}$.

Definition 2. If J and K are is a closed intervals then J f-covers K if $K \subseteq f(J)$.

Lemma 3. *If J f-covers itself then J contains a fixed point of f.*

PROOF. Let $J = [a, b]$. Since J f-covers itself there exist y and z in $[a, b]$ such that $f(y) \leq a$ and $f(z) \geq b$. Let $g(x) = f(x) - x$ which is also continuous and $g(y) \leq 0$ and $g(z) \geq 0$. Applying the Intermediate Value Theorem to g on the interval between x and y there exists u such that $g(u) = 0$, i.e., u is a fixed point of f. □

Definition 4. Let $J_1, \ldots, J_m$ be closed intervals with disjoint interiors. A Markov graph of f is a directed graph with vertices $1, \ldots, m$ and a directed edge from i to j iff J_i f-covers J_j. The transition matrix associated with this graph is the $m \times m$ matrix T with

$$T_{ij} = \begin{cases} 1 & \text{if } J_i \ f-\text{covers } J_j \\ 0 & \text{otherwise.} \end{cases}$$

A path in a directed graph is an ordered sequence of vertices $a_0 a_1 \ldots a_k$ such that there is a directed edge from a_i to a_{i+1} for each $i = 0, \ldots, k-1$. The length of the path is the number of edges traversed (i.e., k in the example). Note that if there is a path from a_0 to a_k of length k if and only if $T^k_{a_0 a_k} \neq 0$.

Lemma 5. *If there is a path of length k from $a_0 \ldots a_k$ in the Markov graph then there exists a closed interval $L \subset J_{a_0}$ such that $f^k(L) = J_{a_k}$ and $f^r(L) \subseteq J_{a_r}$.*

PROOF. The proof is by induction on k.

If $f(J_{a_0}) \subseteq J_{a_1}$ then since f is continuous there exists $L \subseteq J_{a_0}$ such that $f(L) = J_{a_1}$. (If this is not obvious, look at the interior of J_{a_1} and note f^{-1} of an open interval is a union of open intervals.)

Now suppose that the lemma is true for $k = m$ and consider a path of length $m + 1$, $a_0 \ldots a_{m+1}$. By the induction hypothesis, since $a_1 \ldots a_{m+1}$ is a path of length m there exists $L' \subseteq J_{a_1}$ such that $f^m(L') \subseteq J_{a_{m+1}}$ and $f^r(L') \subseteq J_{a_{r+1}}$, $r = 1, \ldots, m$.

Since J_{a_0} f-covers J_{a_1}, J_{a_0} f-covers L' and hence there exists $L \subseteq J_{a_0}$ such that $f(L) = L'$. A quick check confirms that $f^{k+1}(L) = f^k(L')$ and so L has the desired property. □

Corollary 6. *If $a_0 a_1 \ldots a_p$ is a path of length p with $a_0 = a_p$ then f has a periodic orbit of period p.*

Corollary 7. *If $a_0 a_1 \ldots$ is an infinite path in the Markov graph then there exists $x \in J_{a_0}$ such that $f^r(x) \in J_{a_r}$ for all $r \geq 0$.*

PROOF. Take an infinite intersection of nested closed intervals L of Lemma 5 for each finite path $a_0 \ldots a_r$. □

This is the basic tool for proving classic theorems such as Sharkovskii's Theorem. It also provides a motivation for the definition of a one-dimensional horseshoe.

Definition 8. f has a horseshoe if there exist closed intervals J_0 and J_1 with disjoint interiors such that J_0 f-covers both J_0 and J_1 and J_1 f-covers both J_0 and J_1.

Theorem 9. *If f has a horseshoe then for any sequence of 0s and 1s $a_0a_1\ldots$ there exists $x \in J_{a_0}$ such that $f^r(x) \in J_{a_r}$ for all $r > 0$.*

This is sometimes described as f having dynamics equivalent to a full shift on two symbols.

Note that these results only need f to be continuous on the intervals J_k; what happens between these intervals is immaterial. This means that the methods are often applicable in PWS systems.

2. PWS maps of the interval

The next four sections describe properties of one-dimensional PWS maps. In this section we describe some properties and analyse some simple examples. We need a technical convention about how to work with closed intervals if a map has a discontinuity.

Let $J = [a, b]$ be a closed interval and suppose that f is continuous on the interior of J. Then define

$$f(a) = \lim_{x \downarrow a} f(x) \quad \text{and} \quad f(b) = \lim_{x \uparrow a} f(x).$$

Note that when applying this to an iterate of J we may effectively be using two values of the map at the discontinuity.

2.1. Transitivity and chaos. We start with a generalization of a horseshoe for PWS maps which we will use as our definition of chaos.

Definition 10. Suppose $f\colon I \to I$ is a PWS map of the interval I. f is chaotic if there exist closed intervals J_0 and J_1 with disjoint interiors and $n_0, n_1 > 0$ such that $f^{n_k}|J_k$ is continuous and J_k f^{n_k}-covers J_0 and J_1.

Two further definitions will be useful.

Definition 11. Suppose $f\colon I \to I$ is a PWS map of the interval I. f is transitive if for every open interval $J \subseteq I$ there exists $N < \infty$ such that

$$I = \mathrm{c}\ell \bigcup_{k=0}^{N} f^k(U).$$

Note that this implies another definition of transitivity, that for all open intervals U and V in I there exists $k \geq 0$ such that $f^k(U) \cap V \neq \emptyset$. Moreover it can be used to prove that the non-wandering set of a map is the interval I itself.

Definition 12. Suppose $f\colon I \to I$ is a PWS map of the interval I. A point is wandering if there exists an open set u with $x \in U$ such that $f^n(U) \cap U = \emptyset$ for all $n \geq 1$. If x is not a wandering point then x is a non-wandering point. The non-wandering set of f, $\Omega(f)$, is the set of all non-wandering points of f.

Lemma 13. *Suppose $f\colon I \to I$ is a PWS map of the interval I. If f is transitive on I then $\Omega(f) = I$.*

PROOF. If f is transitive then for any interval U there exists $N < \infty$ such that $I = \cup_0^N f^r(U)$ and hence $m \leq N$ such that $f^m(U) \cap U \neq \emptyset$; in other words no point can be wandering. □

A stronger definition of the expansion of intervals makes all the consequences easy to establish.

Definition 14. Suppose $f\colon I \to I$ is a PWS map of the interval I with M continuous, monotonic branches on the open intervals $J_1, \dots J_M$.. Then f is locally eventually onto (LEO) if for every open interval $U \subseteq I$ there exist open intervals $L_k \subseteq U$ and $n_k \geq 0$ such that $f^{n_k}|L_k$ is monotonic and continuous and $f^{n_k}(L_k) = J_k$, $k = 1, \dots, M$.

Note that the conditions that $f^{n_k}|L_k$ are continuous imply that all the standard smooth dynamical results can be imported to the PWS case.

Lemma 15. *Suppose $f\colon I \to I$ is a PWS map of the interval I. If f is LEO then it is transitive and chaotic.*

PROOF. Transitivity is obvious as for any open U there exist $L_k \subseteq U$, $k = 1, \dots, M$ as in the definition such that $\cup_1^M f^{n_k}(L_k) = \cup_1^M J_k$ and by definition the closure of the union of the monotonic branches is the whole interval.

For chaos (definition 10), take two disjoint open intervals U and V in the same monotonic branch interval J_c. Then there exis $L_0 \subseteq U$ and $L_1 \subseteq V$ and $n_0, n_1 \geq 1$ such that $f^{n_k}|L_k$, $k = 0, 1$, is continuous and $f^{n_k}(L_k) = J_c$. Since $L_k \subset J_c$, f is chaotic by using the closed set convention to extend to the closures of L_k. □

2.2. Tent maps. An interesting example is provided by the (symmetric) tent maps. This is a family of continuous PWS maps of the interval $T_s\colon [0,1] \to [0,1]$ defined for $s \in (1,2]$ by

$$T_s(x) = \begin{cases} sx & \text{if } 0 \leq x \leq \frac{1}{2} \\ s(1-x) & \text{if } \frac{1}{2} \leq x \leq 1. \end{cases} \tag{8}$$

Let the length of an interval U be denoted by $|U|$. There are three immediate remarks worth making to start with:

(a) There are no stable periodic orbits (the slope of the map has modulus $s > 1$).

(b) For every open interval $U \subset (0,1)$ there exists $n > 0$ such that $\frac{1}{2} \in T_s^n(U)$ (if not then T^s is linear so $|T_s(U)| = s|U|$ and by induction $|T_s^n(U)| = s^n|U|$; but since the interval must have length less than 1 this is a contradiction).

(c) Let $I_0 = [T_s^2(\frac{1}{2}), T_s(\frac{1}{2}]$, then $\Omega(f) = \{0\} \cup \Omega(T_s|I_0)$ (0 is a fixed point so in $\Omega(T_s)$; the interval I_0 is invariant and any opn interval outside I_0 must map into I_0 eventually by (b)).

Lemma 16. *If $\sqrt{2} < s \leq 2$ and I_0 as in (c) above then*

$$\Omega(T_s) = \{0\} \cup I_0.$$

These sets are disjoint unless $s = 2$, when 0 is the left end-point of I_0.

PROOF. We will show that $T_s|I_0$ is LEO and hence that $\Omega(T|I_0) = I_0$. By direct calculation $I_0 = [x_1, x_2]$ where

$$x_1 = \frac{s}{2}(2-s), \quad x_1 = \frac{s}{2}. \tag{9}$$

Note that if $s = 2$ then $I_0 = [0, 1]$ and the last statement of Lemma 16 is shown.

Consider any open interval $U \subset I_0$. If $\frac{1}{2} \notin U$ then $|T_s(U)| = s|U|$ and so (cf. remark (b) above) there exists n_0 such that $\frac{1}{2} \in T_s^{n_0}(U)$. Let $T_s^{n_0}(U) = V_0 \cup \{\frac{1}{2}\} \cup V_1$ with V_0 in $x < \frac{1}{2}$ and V_1 is in $x > \frac{1}{2}$. Then there exists $\alpha \in (0, 1)$ such that

$$|V_0| = \alpha |T_s^{n_0}(U)|, \quad |V_1| = (1-\alpha)|T_s^{n_0}(U)|.$$

Both intervals $T_s(V_k)$ have $T_s(\frac{1}{2}) = x_2$ as their right end-point and so one contains the other (or both are equal). Thus

$$|T_s^{n_0+1}(U)| = \max_k\{|T_s(V_k)|\} = (\max\{\alpha s, (1-\alpha)s\})\,|T_s^{n_0}(U)|.$$

The maximum of αs and $(1-\alpha)s$ is greater than or equal to $\frac{1}{2}s$ since if $\alpha \neq \frac{1}{2}$ then one of the two terms α or $1-\alpha$ is greater than $\frac{1}{2}$. Hence

$$|T_s^{n_0+1}(U)| \geq \frac{s}{2}|T_s^{n_0}(U)|. \tag{10}$$

Choose $U_0 \subseteq U$ such that V_k where $T_s^{n_0}(U_0) = V_k$ is the interval with larger image, so $T_s^{n_0+1}|U_0$ is monotonic and $T_s^{n_0+1}(U_0) = T_s^{n_0+1}(U)$. If $\frac{1}{2} \notin T_s^{n_0+1}(U_0)$ then

$$|T_s^{n_0+2}(U_0)| \geq \frac{s^2}{2}|T_s^{n_0}(U_0)| > |T_s^{n_0}(U)| \tag{11}$$

and so the length continues to expand. This cannot continue indefinitely so after a finite number of further passages including $\frac{1}{2}$ (at which we define smaller intervals $U_1, U_2, \ldots U_m$ in U such that $|T_s^{n_r+1}(U_r)| = |T_s^{n_r+1}(U)|$ and $T_s^{n_r+1}|U_r$ is monotonic) we arrive at an interval U_m such that

$$\frac{1}{2} \in T_s^{n_m+1}(U_m) \quad \text{and} \quad \frac{1}{2} \in T_s^{n_m+2}(U_m).$$

But the first of these implies that $T_s(\frac{1}{2}) \subseteq T_s^{n_m+2}(U_m)$, so U_m contains an open interval $\tilde{U}$ such that $T_s^{n_m+2}|\tilde{U}$ is monotonic and $T_s^{n_m+2}(\tilde{U}) = (\frac{1}{2}, \frac{s}{2})$. Thus $T_s^{n_m+3}|\tilde{U}$ is monotonic and $T_s^{n_m+3}(\tilde{U}) = (\frac{s}{2}(2-s), \frac{s}{2})$ and so T_s is LEO on I_0. □

The next step is probably the most important in this course: it involves looking at a higher iterate of T_s on a subinterval of $[0, 1]$. This is the idea behind renormalization and induced maps. We will make this explicit in the next subsection, but for the moment we will see it in action as we extend Lemma 16 to $1 < s \leq \sqrt{2}$.

Theorem 17. *If $\sqrt{2} < s^{2^n} \le 2$, $n \ge 0$, then*

$$\Omega(T_s) = \{0\} \cup I_n \cup \left(\bigcup_{k=1}^{n} P_k \right)$$

where the right union is empty if $n = 0$. The set P_k is an unstable periodic orbit of period 2^k, $k = 1, 2, \ldots n$ and I_n is a union of 2^n closed intervals. These intervals are disjoint unless $s^{2^n} = 2$ in which case they intersect pairwise on the periodic orbit P_n.

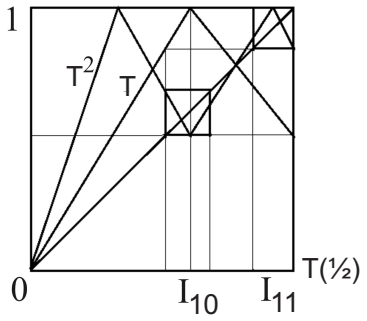

FIGURE 4. $s < \sqrt{2}$: the tent map and its second iterate.

PROOF. If $n = 0$ the theorem is proved by Lemma 16. If $s \le \sqrt{2}$ consider the second iterate of the map, T_s^2 which has the form shown in Figure 4. It has turning points at $\frac{1}{2}$ and the two preimages of $\frac{1}{2}$, i.e., $c_\pm$ where $sc_- = \frac{1}{2}$ and $s(1 - c_+) = \frac{1}{2}$, solving gives

$$c_- = \frac{1}{2s}, \quad c_+ = \frac{2s-1}{2s}.$$

There is a non-trivial fixed point of T_s in $x > \frac{1}{2}$ with at $x_* = \frac{s}{s+1}$ and this has a preimage in $x < \frac{1}{2}$, y_-, where $sy_- = x_*$, and this in turn has a preimage in $x > \frac{1}{2}$, y_+, with $s(1 - y_+) = y_-$. Direct calculation yields

$$y_- = \frac{1}{s+1} = 1 - \frac{s}{s+1}, \quad y_+ = \frac{s^2+s-1}{s(s+1)}. \tag{12}$$

Consider $T_s^2|[y_-, x_*]$. This is symmetric about $\frac{1}{2}$ and the modulus of the slope is s^2. T_s^2 maps the interval $[y_-, x_+]$ into itself provided $T_s^2(\frac{1}{2}) \ge y_-$ which is equivalent to $s^2 \le 2$ after some algebra. Thus if $s^2 \le 2$ the map $T_s^2|[y_-, x_*]$ is equivalent by an affine change of variable to $T_{s^2}|[0, 1]$.

Thus if $\sqrt{2} < s^2 \le 2$, $\Omega(T_s^2|[y_-, x_*]) = \{x_*\} \cup J_0$ where J_0 is an interval disjoint from x_* except in the case $s^2 = 2$ when x_* is an endpoint of J_0. Let $I_1 = J_0 \cup T_s(J_0)$ and $P_1 = \{x_*\}$. Then this establishes

$$\Omega(T_s) = \{0\} \cup I_1 \cup P_1, \quad \sqrt{2} < s^2 \le 2,$$

where I_1 is a union of two intervals joined pairwise on P_1 if $s^2 = 2$.

To complete the proof use induction on n. If $s^2 \le \sqrt{2}$ then consider the second iterate of T_s^2 on $[y_-, x_*]$, which has slopes of modulus $s^4 = s^{2^2}$ and

the same structure provided $\sqrt{2} < s^4 \leq 2$, and so on. We leave the details to the reader. □

2.3. Renormalization and Induced maps. The previous example is our first sight of a really important idea: renormalization, i.e., the consideration of induced maps. This will be central to much of the theoretical analysis we do here.

Definition 18. Suppose $f\colon [0,1] \to [0,1]$ is a PWS map and there exists $c \in (0,1)$ such that f is monotonic and continuous on $(0,c)$ and on $(c,1)$. f is renormalizable if there exist positive integers n_0 and n_1 with $n_0 + n_1 > 2$ and non-trivial intervals $J_0 = (x_1, c)$ and $J_1 = (c, x_2)$ such that $f^{n_k}|J_k$ is continuous and monotonic, $k = 0, 1$ and

$$f^{n_k}(J_k) \subseteq J_0 \cup \{c\} \cup J_1, \quad k = 0, 1. \tag{13}$$

In some sense, apart from stable periodic orbits, renormalization is the only obstruction to transitivity in PWS maps with two monotonic branches.

Theorem 19. *Suppose $f\colon [0,1] \to [0,1]$ is a PWS map with two monotonic branches separated by $c \in (0,1)$. If there exists $s > 1$ such that $|f'(x)| \geq a$ for all $x \in (0,1)\backslash\{c\}$ then either f is transitive or f is renormalizable. If f is renormalizable on an interval J containing c then $\Omega(f) = T \cup R$ where T is described by a Markov graph and R is the nonwandering set of the induced map on J and its iterates under f.*

Proof. Without loss of generality assume that $[0,1]$ is the smallest interval mapped into itself by f. Note that f has no stable periodic orbits.

Take any open interval U. By the expansion argument of (b) above Lemma 16 there exists $n_0 \geq 0$ such that $c \in f^{n_0}(U) = U_0$ and follow both branches to their next intersection with c, i.e., let $U_0 = V_0 \cup \{c\} \cup V_1$ in the standard way and choose the smallest m_k, $k = 0, 1$ such that $c \in f^{m_k}(V_k)$, $k = 0, 1$ (these exist by the expansion argument). If $f^{m_k}(V_k) \subseteq U_0$ then f is renormalizable. Otherwise set $U_1 = f^{m_0}(V_0) \cup f^{m_1}(V_1) \cup U_0$ and note $U_0 \subset U_1$.

Now repeat the argument using U_1 and note that the equivalent of the return times for U_1 are less than or equal to the return times m_k for U_0. Either f is renormalizable or there exists U_2 with $U_1 \subseteq U_2$ which is a union of iterates of subsets of U.

Either there exists $m < \infty$ such that $U_m = (0,1)$ and so U satisfies the transitivity condition (but not necessarily all U satisfy the condition) or $U_n \to U_\infty$ as $n \to \infty$ and by continuity appropriate iterates of f map U_∞ into itself.

Hence once again either f is renormalizable or $U_\infty = (0,1)$. But since the return times are decreasing, they also tend to a limit, m_k^∞, $k = 0, 1$, and these are reached in finite steps. Thus if $U_n \neq (0,1)$ for all $n > N_0$ (transitivity again) the minimality of $(0,1)$ implies that $U_n \cup f(U_n) = (0,1)$ for large enough n; the transitivity condition again.

Thus for each U either U satisfies the transitivity condition or f is renormalizable. Hence either f is renormalizable or f is not renormalizable and every open U satisfies the transitivity condition and hence f is transitive.

If f is renormalizable let J_k be the intervals as in the definition and choose the maximal intervals satisfying (13). Let

$$K = J_0 \cup \left(\bigcup_1^{n_0} f^r(J_0) \right) \cup \{c\} \cup J_1 \cup \left(\bigcup_1^{n_1} f^r(J_1) \right)$$

and let $L = I \backslash K$. Then L is a (possibly empty) finite union of closed intervals and since the sets K are mapped to themselves if $f(L_i) \cap L_j \neq \emptyset$ then $L_j \subseteq f(L_i)$, i.e., L_i f-covers L_j and so the dynamics in L can be described by a Markov graph. Setting $T = \Omega(f) \cap L$ and $R = \Omega(f) \cap c\ell(K)$ produces the stated descomposition of the non-wandering set. □

2.4. Boundary Bifurcations. In the previous sections we have been concerned with chaos and expansion. Now we consider how periodic orbits can be created or destroyed by non-smooth effects. To do bifurcation theory we need to consider families of maps, and this leads to problems about how to talk about 'continuous' families of discontinuous mappings! In the next section we will look at some more sophisticated approaches, but for now we are concerned only with local phenomena and so we will work with locally fixed families.

Definition 20. A family of PWS mappings $f(x, \mu)$, $f\colon [0,1] \times \mathbb{R} \to [0,1]$ is locally fixed if there exists $\epsilon > 0$ such that the set of discontinuities, d_k, and the set of critical points, c_k are fixed for all $\mu \in (-\epsilon, \epsilon)$ and f is C^2 functions of both variables on the intervals J_k.

Thus for a locally fixed family, there exist fixed intervals bounded by the discontinuities and critical points on which f is smooth. For most families this can be achieved locally by a change of coordinates.

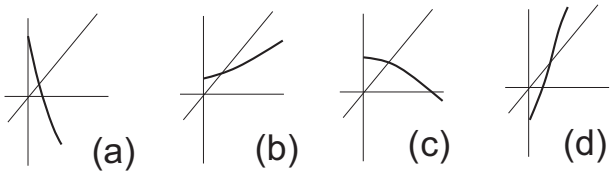

FIGURE 5. The four cases for elementary border bifurcations: (a) $a < -1$; (b) $-1 < a < 0$; (c) $0 < a < 1$; (d) $a > 1$.

Theorem 21. *If $f\colon I \times (-\epsilon, \epsilon) \to I$ be a locally fixed family of PWS maps and suppose that d is a point of discontinuity. If there is a neighbourhood $J = (d, d+\delta)$, $\delta > 0$, such that f is smooth (C^2)*

$$\lim_{x \downarrow d} f(x,0) = d, \quad \lim_{x \downarrow d} |f'(x,0)| = a \neq 1 \tag{14}$$

then there exists $\delta, \eta > 0$ such and $b \in \{+1, -1\}$ such that if μ is between 0 and $b\eta$ then f has a fixed point in $(b, b+\delta)$ and no other locally recurrent dynamics, whilst if μ is between 0 and $-b\eta$ then f has no locally recurrent dynamics. The fixed point is stable if $a < 1$ and unstable if $a > 1$.

Thus the effect of a boundary bifurcation is to create or destroy a fixed point. Of course the same result holds for periodic orbits by replacing f by f^p. Global features of the maps can create more dynamics in the intervals – the theorem only refers to dynamics locally, i.e., that remain in the interval J for all time. The proof is elementary and is left as an exercise. The four cases are illustrated in Figure 5.

3. Lorenz maps and rotations

This section is devoted to PWS maps of the interval with a single discontinuity such that both continuous branches are increasing. These include Lorenz maps and rotations. If $f\colon [0,1] \to [0,1]$ is a PWS map with increasing branches and a single discontinuity at $c \in (0,1)$ with $f(c_-) = 1$ and $f(c_+) = 0$ there are three separate cases:

- Rotations: $f(0) = f(1)$.
- Gap maps: $f(0) > f(1)$.
- Overlap maps: $f(0) < f(1)$.

Rotations have a distinguished history going back to the classic results of Julia and Denjoy in the early twentieth century. Gap maps have many similarities and some beautiful general results are due to Keener [**34**] and Rhodes and Thompson [**43, 44**]. Overlap maps allow the possibility of chaos and include the many studies of Lorenz maps.

3.1. Rotations. A rigid rotation is a map $r_\alpha\colon [0,1) \to [0,1)$ with $\alpha \in [0,1)$ defined by

$$r_\alpha(x) = x + \alpha \pmod 1. \tag{15}$$

The function $R_\alpha\colon \mathbb{R} \to \mathbb{R}$ defined by $R_\alpha(x) = x + \alpha$ is an example of a lift of r_α, and $R_\alpha(x+1) = R_\alpha(x) + 1$. The dynamics of the map r_α can be recovered from R_α by projecting modulo 1, hence r_α has a periodic point of period q iff there exists $x \in \mathbb{R}$ such that $R_\alpha^q(x) = x + p$ for some $p \in \mathbb{Z}$ (so $x + p = x \bmod 1$). But

$$R_\alpha^q(x) = x + q\alpha \tag{16}$$

so x is periodic if and only if $q\alpha = p$, or $\alpha = \frac{p}{q} \in \mathbb{Q}$, and in this case all points are periodic. If $\alpha \notin \mathbb{Q}$ then the orbit is dense on the circle (see e.g., Devaney). Thus for rigid rotations there is a simple dichotomy

- $\alpha \in \mathbb{Q}$ and all points are periodic; or
- $\alpha \notin \mathbb{Q}$ and orbits are dense on the circle.

Note also that (15) can be seen as a map of the interval with a discontinuity: given $\alpha \in (0,1)$ define $f_\alpha\colon [0,1] \to [0,1]$ by

$$f_\alpha(x) = \begin{cases} x + \alpha & \text{if } 0 \le x < 1 - \alpha \\ x + \alpha - 1 & \text{if } 1 - \alpha < x < 1 \end{cases} \tag{17}$$

with our usual convention about the discontinuity. We will exploit this connection more in the next section, but first we describe some of the classic results for homeomorphisms of the circle.

The generalization of α to homeomorphisms is the idea of a rotation number which describes an average angular velocity around the circle. If f_α is a circle map then F_α

Definition 22. If f is a circle map with lift F then provided the limit exists

$$\rho(F,x) = \lim_{n\to\infty} \tfrac{1}{n}(F^n(x) - x) \tag{18}$$

is called the rotation number of x under F.

The following sequence of theorems are the classic results of Julia and Denjoy. Proofs use simple real analysis and can be found in Devaney.

Theorem 23. *If F is the lift of a homeomorphism of the circle f then $\rho(F,x)$ exists and is independent of x.*

It is usual to talk about the rotation number of f in this case, denoted $\rho(f)$ as $\rho(F,x)$ modulo 1.

Theorem 24. *Suppose f is a homeomorphism of the circle.*

(a) *If $\rho(f) \in \mathbb{Q}$ then f has at least one periodic orbit.*
(b) *If $\rho(f) \notin \mathbb{Q}$ then f has no periodic orbits and if f is C^2 then every orbit is dense in the circle.*

If f is not C^2 then it is possible to create attracting Cantor sets with irrational rotation numbers, these are the Denjoy counter-examples.

Families of circle maps can be defined via their lifts: a continuous family of smooth circle maps is a family with lifts F_μ which can be chosen such that such that

$$\lim_{\mu\to\mu_0} |F_\mu(x) - F_{\mu_0}(x)| = 0$$

for all $x \in \mathbb{R}$.

Theorem 25. *If (f_μ) is a continuous family of continuous circle homeomorphisms then $\rho(f_\mu) = \rho(\mu)$ varies continuously. If there exist $\mu_1 < \mu_2$ such that $\rho(\mu_1) < \frac{p}{q} < \rho(\mu_2)$ then typically $\rho(\mu) = \frac{p}{q}$ on an interval of parameter values.*

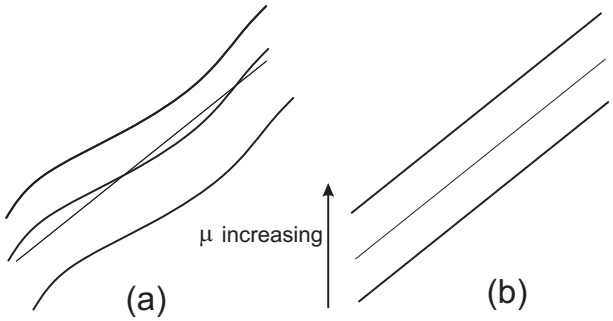

FIGURE 6. Part of the graph of f as μ increases illustrating why there is (a) persistency of intersections with the diagonal in the general case; and (b) degeneracy in the slope one case.

Again, we will not give proofs for the circle maps case – see [**12**]. The continuous variation of $\rho(\mu)$ implies that the irrational rotation numbers do appear in examples. The interval of values with rational rotation numbers is often referred to as mode locking. It is easy to see why this occurs typically. If $\rho(\mu) = p/q$ then (Theorem 24a) there exists a periodic point, i.e a solution to $F^q(x) = x + p$. If $\rho(\mu) < \frac{p}{q}$ then $F^q(x) < x + p$ for all $x \in \mathbb{R}$ whilst if $\rho(\mu) > \frac{p}{q}$ then $F^q(x) > x + p$ for all $x \in \mathbb{R}$. Thus (see Figure 6) either there is a range of parameters such that the graph of $F^q(x) - x$ passes across p, or there is one parameter at which $F^q_\mu(x) - x \equiv p$ for all x. But this latter condition is very unlikely (the q^{th} iterate would be identically linear).

3.2. Rotation renormalization and codings. Suppose $f\colon [0,1] \to [0,1]$ is a rotation-like PWS map, i.e., there exists $c \in (0,1)$ such that f is continuous and strictly increasing on $(0,c)$ and on $(c,1)$ with

$$\lim_{x\uparrow c} f(x) = 1, \quad \lim_{x\downarrow c} f(x) = 0, \quad f(0) = f(1).$$

Then we can associate f with a circle homeomorphism with lift F defined by

$$F(x) = \begin{cases} f(x) & \text{if } 0 \le x < c \\ 1 & \text{if } x = c \\ f(x) + 1 & \text{if } c < x < 1 \end{cases} \tag{19}$$

and $F(x+1) = F(x) + 1$. Thus we can talk about the rotation number of f, though F is not necessarily C^2 at integer values, so a little care needs to be taken about bifurcations (this will be considered in the next subsection). The rotation number can also be thought of as

$$\rho(f) = \lim_{n\to infty} \tfrac{1}{n}\#\{r \mid f^r(x) > c,\ r = 1, 2, \ldots, n\}$$

since the lift moves solutions into the next interval $(m, m+1)$ if and only if $x > c$.

There is a natural renormalization for circle maps that can help describe the dynamics of examples.

First note that there is a simple trichotomy:

- $f(0) = c$; or
- $f(0) > c$; or
- $f(0) < c$.

If $f(0) = c$ then $f((0,c) = (c,1)$ and $f(c,1) = (0,c)$ so $\rho(f) = \frac{1}{2}$.

If $f(0) > c$ then $f((0,c)) \subset (c,1)$ and hence $f^2|(0,c)$ is continuous and monotonic. Either f has a fixed point (and hence rotation number zero or one) or consider the induced map

$$g(x) = \begin{cases} f^2(x) & \text{if } 0 \le x < c \\ f(x) & \text{if } c < x \le f(0). \end{cases} \tag{20}$$

This is has two monotonic continuous branches and the image of the left end point, 0, is $g(0) = f^2(0)$ whilst the image of the left end-point, $f(0)$, is

$g(f(0)) = f^2(0)$, so the two end-points map to the same point. Rescaling back to the interval $[0,1]$ we obtain the renormalized (induced) map

$$f_1(x) = \begin{cases} \frac{1}{a} f^2(ax) & \text{if } 0 \le x < \frac{c}{a} \\ \frac{1}{a} f(ax) & \text{if } \frac{c}{a} < x \le 1 \end{cases} \tag{21}$$

where $a = f(0)$.

This new map is in the same class as f and so has a well defined rotation number. We would now like to relate the rotation number of f_1, ρ_1, with the rotation number of f, ρ_0.

Consider an orbit of f_1 and suppose that in length n it has m_n iterations in $x > c_1 = c/a$ (and so $n - m_n$ iterates in $x < c_1$. Then

$$\rho_1 = \lim_{n\to\infty} \frac{m_n}{n}.$$

Now that same orbit translates to an orbit of f for which every iterate in $x < c_1$ for f_1 is two iterates, one in $x < c$ and one in $x > c$ for f, whilst every iterate in $x > c_1$ for f_1 corresponds to one iterate in $x > c_1$ for f. Hence the first n iterates under f_1 with m_n iterates in $x > c_1$ corresponds to and orbit segment of length $2(n - m_n) + m_n = 2n - m_n$ of f with n iterates in $x > c$, giving

$$\rho_0 = \lim_{n\to\infty} \frac{n}{2n - m_n} = \lim_{n\to\infty} \frac{1}{2 - \frac{m_n}{n}}.$$

Thus if ρ_1 is known the rotation number of f can be recovered using the transformation

$$\rho_0 = \frac{1}{2 - \rho_1}. \tag{22}$$

If $f(0) = a > c$ then $f((c,1)) \subset (0,c)$ and hence $f^2|(c,1)$ is continuous and monotonic. Either f has a fixed point (and hence rotation number zero or one) or we define

$$g(x) = \begin{cases} f(x) & \text{if } a \le x < c \\ f^2(x) & \text{if } c < x \le 1. \end{cases} \tag{23}$$

By the same argument as before this is in the same class as f but on the interval $[a,1]$ and so we rescale

$$f_1(x) = \begin{cases} \frac{1}{1-a}(f(a + (1-a)x) - a) & \text{if } 0 \le x < \frac{c-a}{1-a} \\ \frac{1}{1-a}(f^2(a + (1-a)x) - a) & \text{if } \frac{c-a}{1-a} < x \le 1 \end{cases} \tag{24}$$

Now if $\rho_1 = \lim m_n/n$ as before then each iteration in $x > c_1 = (c-a)/(1-a)$ corresponds to two iterates for f and so the length of the orbit for f is $(n - m_n) + 2m_n$ but there is no change in the number of iterates in $x > c$ and so

$$\rho_0 = \lim_{n\to\infty} \frac{m_n}{n + m_n}$$

and equating limits gives

$$\rho_0 = \frac{\rho_1}{1 + \rho_1}. \tag{25}$$

Renormalization has a very natural interpretation in terms of the continued fraction expansion of the rotation numbers. Any number between 0 and 1 has a continued fraction expansion

$$[a_0, a_1, a_2 \dots] = \frac{1}{a_0 + \frac{1}{a_1 + \frac{1}{a_2 + \dots}}}$$

with $a_i \in \mathbb{N}$. If $a_0 = 1$ then the number is bigger than $\frac{1}{2}$ and if $a_0 \geq 2$ then the number is less than $\frac{1}{2}$.

Theorem 26. *Suppose $\rho(f) = [a_0, a_1, \dots]$. If $a_0 = 1$ then $\rho(f) > \frac{1}{2}$ and the renormalized map f_1 is as defined in* (21) *and*

$$\rho(f_1) = \begin{cases} [1, a_1 - 1, a_2, \dots] & \text{if } a_1 \geq 2 \\ [a_2 + 1, a_3, \dots] & \text{if } a_1 = 1. \end{cases} \tag{26}$$

If $a_0 \geq 2$ then $\rho(f) < \frac{1}{2}$ and (24) *defines the renormalized map and*

$$\rho(f_1) = [a_0 - 1, a_1, a_2, \dots]. \tag{27}$$

Proof. First note that if $x = [a_0, a_1, \dots]$ then $x^{-1} = a_0 + [a_1, a_2, \dots]$. Define $\rho_0 = \rho(f)$ and $\rho_1 = \rho(f_1)$.

If $\rho_0 > \frac{1}{2}$, i.e., $a_0 = 1$ in the continued fraction expansion of ρ_0 and

$$\rho_0 = [1, n, a_2, \dots]$$

and (22) implies

$$\rho_1 = 2 - \rho_0^{-1}.$$

Hence using the remark about the continued fraction expansion of x^{-1} at the start of this proof

$$\rho_1 = 1 - [n, a_2, \dots] = 1 - \frac{1}{n+s} = \frac{n-1+s}{n+s} \tag{28}$$

where $s = [a_2, a_3, \dots]$. If $n = 1$ then

$$\rho_1 = \frac{s}{s+1} = \frac{1}{1+s^{-1}} = \frac{1}{1 + a_2 + [a_3, a_4, \dots]} = [a_2 + 1, a_3, a_4, \dots]$$

as required. If $n \geq 2$ then (28) implies that the claim of the theorem is that

$$\frac{n-1+s}{n+s} = [1, n-1, a_2, a_3, \dots].$$

The second term is

$$\frac{1}{1 + \frac{1}{n-1+s}} = \frac{1}{\frac{n+s}{n-1+s}} = \frac{n-1+s}{n+s}$$

establishing the required result.

If $\rho < \frac{1}{2}$, i.e., $a_0 = n \geq 2$ in the continued fraction expansion of ρ_0 then (25) implies that

$$\rho_0 = \frac{1}{1 + \rho_1^{-1}}$$

and so if $\rho_1 = [b_0, b_1, b_2, \dots]$ then $\rho_0 = \frac{1}{1 + b_0 + [b_2, b_3, \dots]}$ and so $\rho_0 = [b_0 + 1, b_1, b_2, \dots]$. Hence $b_0 = n - 1$ and $b_k = a_k$ if $k \geq 1$, establishing the required relationship. □

This connection means that knowing the rotation number the set of renormalizations is determined and vice versa. This can often be useful when looking at examples.

Another way of looking at the renormalization maps is that if $\rho < \frac{1}{2}$ the coding of orbits for the induced or renormalized map can be used to obtain the coding for the original map by the replacement operation

$$0 \to 0, \quad 1 \to 10.$$

In other words, every symbol 1 for the map is followed by a zero. Similarly if $\rho > \frac{1}{2}$ then the replacement operation is

$$0 \to 01, \quad 1 \to 1,$$

i.e., every 0 is followed by a 1. This process continues and the symbol sequences obtained in this way have many beautiful properties that have been discovered and rediscovered many times. One particularly nice property is that these sequences are minimax. Let $\Sigma_{p,q}$ with $0 < p < q$ denote all the infinite sequences s of 0s and 1s with period q and which have p 1s in every q symbols, so it has rotation number p/q. Let σ be the standard shift map. Now define

$$s_{p,q} = \min_{s \in \Sigma_{p,q}} \left(\max_{1 \le k < q} \sigma^k s \right). \tag{29}$$

Such a sequence is called a minimax sequence of length q.

Then every periodic point with rotation number p/q has a symbolic description that is a shift of the minimax sequence $s_{p,q}$. These sequences are sometimes called rotation compatible sequences, and limits as $p/q \to \omega$ for irrational numbers ω can be taken to define rotation compatible sequences with irrational rotation numbers.

3.3. Gap maps. Consider maps $f\colon [0,1] \to [0,1]$ such that there exists $c \in (0,1)$ such that f is continuous and strictly increasing on $90, c)$ and on $(c,1)$, and

$$\lim_{x \uparrow c} f(x) = 1, \quad \lim_{x \downarrow c} f(x) = 1, \quad f(0) < f(1). \tag{30}$$

The final condition of (30) explains why these maps are called gap maps: there is an interval $(f(0), f(1))$ which has no preimages under f. As with circle maps we can associate f with a lift F as in (19), but this time there is a discontinuity at integer values of x. (Note that as a map of the interval the discontinuity is at $x = c$, but as a map of the circle it is the gap condition that creates the discontinuity:

$$\lim_{x \uparrow 1} F(x) = 1 + f(1) < 1 + f(0) = \lim_{x \downarrow 1} F(x).$$

However, although the lift of f is discontinuous, the function F is monotonic increasing regardless of the choice made for the value at $x = p$ between the two limiting choices determined by continuity. It is therefore natural to ask whether the results for standard circle maps holds for these discontinuous lifts.

Theorem 27. *If F is the lift of a gap map then $\rho(F)$ exists and is independent of both x and the choice of $F(1) \in (1 + f(0), 1 + f(1))$.*

Note that this result is no longer true for maps with gaps and plateaus (intervals on which F is constant), but it remains true if F is strictly increasing and has a countable set of discontinuities.

Definition 28. (f_μ) is a continuous family of gap maps for $\mu \in (\mu_1, \mu_2) = \mathcal{M}$ if for all $\mu_0 \in \mathcal{M}$ and all $x \in \mathbb{R}$

$$\lim_{\mu \to \mu_0} |F_\mu(x) - F_{\mu_0}(x)| = 0.$$

Rhodes and Thompson prove that the bifurcation structure in terms of continuity of rotation numbers and mode-locking is also retained for continuous families of gap maps.

Theorem 29. *If (f_μ) is a continuous family of gap maps then $\rho(f_\mu) = \rho(\mu)$ varies continuously. If there exist $\mu_1 < \mu_2$ such that $\rho(\mu_1) < \frac{p}{q} < \rho(\mu_2)$ then typically $\rho(\mu) = \frac{p}{q}$ on an interval of parameter values.*

As before, this implies that if the rotation number varies then non-periodic (irrational rotation number) behaviour is possible though this will be on a Cantor set. These can be very hard to observe numerically, and there was at one stage some confusion as to whether they exist or not.

3.4. Overlap Maps. An overlap map is a map satisfying the conditions for a gap map but for which the last criterion of (30) is replaced by

$$f(0) < f(1). \tag{31}$$

Thus rather than having a gap there is a set of points with two preimages under f. These maps can be chaotic and the non-wandering set can be described by kneading theory (e.g., Glendinning and Hall) or the less detailed decomposition theorem of section 5. In this section we will continue the analogy with circle maps to provide a different view of the effect of overlap. The analogy is with continuous non-invertible circle maps. For these maps the idea of a rotation number is replaced by a rotation interval.

Definition 30. The rotation set of a lift F is the set

$$\rho(F) = \{\alpha \mid \rho(x, f) = \alpha \text{ for some } x \in \mathbb{R}\}.$$

Theorem 31. *If f is an overlap map with lift F then $\rho(F)$ is a closed interval (possibly a point).*

Proof (sketch). First note that the lift of f jumps down at integers, for example at $x = 1$ the jump is from $1 + f(1)$ to $1 + f(0)$, so it is no longer strictly increasing and the previous results cannot be used. However, the graph is bounded by two continuous monotonic (but not strictly monotonic) lifts:

$$F_0(x) = \inf_{y>x} F(y), \quad F_1(x) = \sup_{y<x} F(x). \tag{32}$$

Clearly (see Figure 7) $F_0(x) \leq F_1(x)$ and $F_k(x)$ are increasing and continuous. We will treat the simple case in which there is only one plateau in each period of the lift. Now, F_k can be seen as the inverses of gap maps, and

hence (or by direct verification) have well-defined rotation numbers with $\rho(F_0) \leq \rho(F_1)$. Moreover,

$$F_0(x) \leq F(x) \leq F_1(x)$$

implies that for all x such that $\rho(x, F)$ exists then $\rho(F_0) \leq \rho(x, F) \leq \rho(F_1)$ (indeed we can take limsups and liminfs of $\frac{1}{n}(F^n(x) - x)$ and these will both lie between $\rho(F_0)$ and $\rho(F_1)$). Thus

$$\rho(F) \subseteq [\rho(F_0), \rho(F_1)].$$

To finish we need to show that for all $y \in [\rho(F_0), \rho(F_1)]$ there exists x such that $\rho(x, F) = y$. We begin by interpolating between F_0 and F_1 creating a continuous family F_μ, $0 \leq \mu \leq 1$ of monotonic circle maps as shown in Figure 7. Each of these has a unique rotation number $\rho_\mu \in [\rho(F_0), \rho(F_1)]$ and ρ_μ varies continuously with μ by Theorem 29. Thus for every $r \in [\rho(F_0), \rho(F_1)]$ there exists $\mu \in [0, 1]$ such that $\rho_\mu = r$. To complete the proof we will show that for each monotonic circle map f_μ with lift F_μ and plateau with open arc P there exists $x \in \mathbb{T}$ such that $f_\mu^n(x) \notin P$ for all $n \geq 0$ and hence, since $f(x) = f_\mu(x)$ if $x \notin P$ then the orbit of x under f_μ is the orbit of x under f and since $\rho(F_\mu) = \rho_\mu$ exists and is independent of x, $\rho(F, x) = \rho_\mu$.

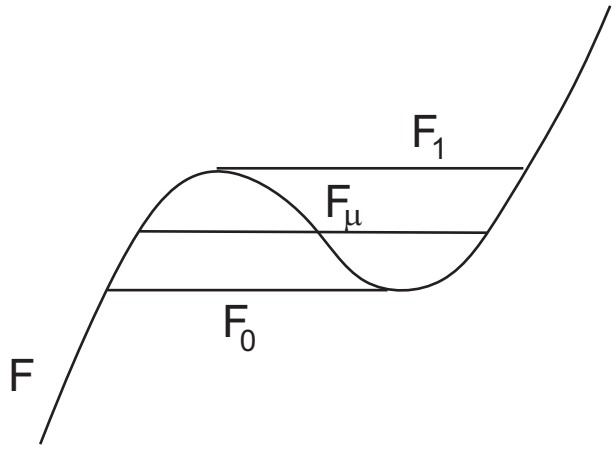

FIGURE 7. Part of the graph of the lift F showing the construction of the maps F_1, F_μ and F_1 which differ from F only on the plateaus.

Let

$$\Gamma_n = \{x \in \mathbb{T} \mid f^k(x) \notin P,\ k = 0, 1, \ldots, n\}.$$

Then since P is open and f_μ and f_μ^{-1} are continuous on $\mathbb{T}\backslash P$, Γ_n is closed and $\Gamma_{n+1} \subseteq \Gamma_n$, hence provided $\Gamma_n \neq \emptyset$ for some n, the limit $\cap\Gamma_n$ is closed and non-empty. Points in this countable intersection have precisely the required property.

So suppose that there exists $m > 0$ such that $\Gamma_m = \emptyset$, i.e for all $x \in \mathbb{T}$ there exists $k \leq m$ such that $f^k(x) \in P$. Now, $f_\mu(P) = y$ is a point, and hence $\cup_{k \geq 0} f_\mu^k(P) = P \cup C$, where C is a countable set of points, and in particular $P \cup C \neq \mathbb{T}$. But by assumption, for all $x \in \mathbb{T}$, $f_\mu^m(x) \in P \cup C$, i.e., $f_\mu^m(\mathbb{T}) \subseteq P \cup C$. But f_μ is a surjecttion, so $f_\mu^m(\mathbb{T}) = \mathbb{T}$, hence we have a contradiction. □

4. Gluing Bifurcations

Gluing bifurcations describe the dynamics of piecewise monotonic maps near codimension two points for maps that are locally contracting. There are three cases determined by the orientation of each continuous branch of the map. These codimension two bifurcations have been described by various authors, e.g., [**20, 31**], in recent years, but as a historical curiosity we will follow the account of Glendinning [**21**] from 1985. This was work done with Gambaudo and Tresser intended to form part of the sequel to [**16**], but which was never completed. The analysis was in the context of homoclinic bifurcations related to the Lorenz semi-flows of section 1.2.

Thus the remainder of this chapter is taken verbatim from [**21**]. Where there is reference to work elsewhere in the dissertation, or where the context may be unclear I have added commentary in italics inside square brackets [*thus*].

START of excerpt from [21].

In the general case we have two parameters which, as usual, can be thought of as parameterising the x-coordinate of the first intersection of the two branches of the unstable manifold of the stationary point with a surface inside a small neighbourhood of the stationary point. recall that the one dimensional map used to model the flow is a piecewise monotonic function with a single discontinuity (at $x = 0$):

$$x' = \begin{cases} -\mu + ax^{\delta} & x > 0 \\ \nu - b(-x)^{\delta} & x < 0 \end{cases} \tag{33}$$

[*the assumption that $\delta > 1$ was part of the chapter introduction; all the results below depend upon is local monotonicity and contraction.*] Note that the signs of μ and ν have been changed so that the interesting behaviour arises when the parameters are positive. Once again there are four cases depending on the signs of the constants a and b, i.,e. whether the global reinjections are orientable (positive signs) or non-orientable (negative signs). Regardless of the signs of a and b we can see from the graph of the map that $\mu < 0$, $\nu < 0$ there is a pair of stable fixed points of the map and so, at least locally, these are the only periodic orbits of the map. The remainder of the parameter space varies according to the signs of a and b so the various cases will be treated separately.

(a) The Orientable case: $a > 0$, $b > 0$

The curve in parameter space given by $\mu = 0$ (resp. $\nu = 0$) corresponds to a line of homoclinic orbits [*i.e., border bifurcations as in section 2.4*] involving the positive (resp. negative) branch of the unstable manifold of the origin. Hence (cf. section 2.1) we know that on crossing this curve a periodic orbit is generated. From the graph of the model map it is clear that this periodic orbit corresponds to the fixed point in $x > 0$ (resp. $x < 0$) which exists for $\mu < 0$ (resp. $\nu < 0$). Since the slope of the map is always positive and less than one any orbit that enters $x > 0$ when $\mu < 0$ (resp. $x > 0$ when $\nu < 0$) tends directly to the fixed point. Using the standard

coding of orbits, 0 for points in $x < 0$ and 1 for points in $x > 0$, these facts imply that the only periodic orbits are

$$\begin{array}{ll} 0 \text{ and } 1 & \text{if } \mu < 0 \text{ and } \nu < 0 \\ 0 & \text{if } \mu > 0 \text{ and } \nu < 0 \\ 1 & \text{if } \mu < 0 \text{ and } \nu > 0 \end{array}$$

If μ and ν are both positive then situation is considerably more complicated. We shall prove the following theorem.

Theorem 32 (Theorem 3.2)**.** *For $\mu > 0$ and $\nu > 0$ the periodic orbits of* (33) *have the following properties:*

(i) *there is at most one periodic orbit*
(ii) *periodic orbits have codes which are rotation compatible, i.e., minimax*
(iii) *the rotation number of periodic orbits varies monotonically with one parameter when the other is held fixed.*

Statements (i) and (ii) are a simple consequence of the theorems of section 3.1 [*those of chapter 3 above*]. The important new part is (iii). This statement implies that there are parameter values in a neighbourhood of $(0, 0)$ for which the system has a periodic orbit with any given minimax code, and also that there are parameter values at which the rotation number of a periodic orbit is irrational, i.e., there are aperiodic orbits which are stable (and so not chaotic). [*That could have been phrased better!*] From the geometry of the flow it is clear that the orbits lie on a torus with a hole. This is precisely the property of Cherry flows which have been studied by many pure mathematicians (e.g., Palis and de Melo, 1984 [**42**]). It is curious that these apparently abstract flows arise naturally near pairs of homoclinic orbits.

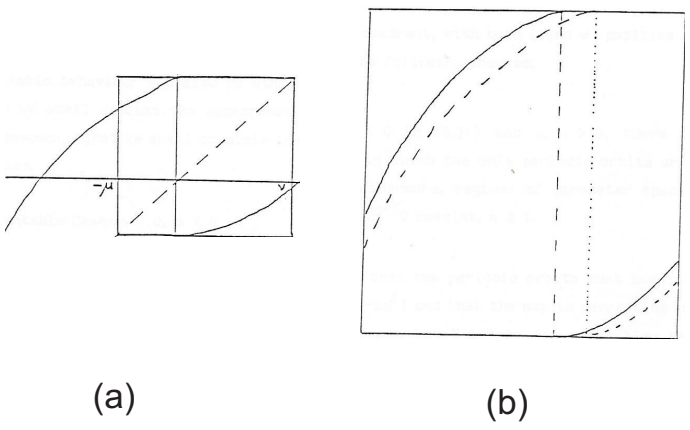

FIGURE 8. (Fig. 65 of [**21**].) (a) The return map with $\mu, \nu > 0$ showing the region $[-\mu, \nu]$ in which the orbits of 0^+ and 0^- remain. (b) The map $g_{\mu,\nu}$ for two values of the parameter ν. The associated lift is monotonic.

To prove statement (iii) we begin by rescaling the map so that the important dynamics (and in particular the orbits of 0^+ and 0^- [*the limits as* 0

is approached from above or below respectively]) is contained in the interval $[-1, 1]$. The iterates of 0^+ and 0^- remain in the interval $[-\mu, \nu]$ (see Fig. 65 [*i.e., Figure 8 here*] so we look for a change of coordinates of the form $z = p + qx$ such that

$$-1 = p - q\mu$$

and

$$1 = p + q\nu$$

so that when $x = -\mu$, $z = -1$ and when $x = \nu$, $z = 1$. This gives

$$\begin{aligned} p &= (\mu - \nu)/(\mu + \nu) \\ q &= 2/(\mu + \nu) \end{aligned}$$

i.e.,

$$z = \{\mu - \nu + 2x\}/(\mu + \nu) \tag{34}$$

In the new coordinates we have the map $g_{\mu,\nu}\colon [-1, 1] \to [-1, 1]$ given by

$$\begin{aligned} g_{\mu,\nu} &= -1 + a[(z - \frac{\mu - \nu}{\mu + \nu})/2]^\delta \quad \text{if } \frac{\mu - \nu}{\mu + \nu} < z < 1 \\ &= 1 - b[(z - \frac{\mu - \nu}{\mu + \nu})/2]^\delta \qquad \text{if } -1 < z < \frac{\mu - \nu}{\mu + \nu}. \end{aligned} \tag{35}$$

This new map has all the properties of $f_{\mu,\nu}$ and in particular orbits have the same rotation number. Note that $g_{\mu,\nu}$ is piecewise increasing with a single discontinuity and so it can be viewed as a discontinuous map of the circle to itself. Hence we can associate a lift $G_{\mu,\nu}\colon \mathbb{R} \to \mathbb{R}$ with $g_{\mu.\nu}$ and so define a rotation number in the usual way. Viewing $g_{\mu,\nu}$ as an application [*map in French*] of the circle we have, from Theorem 1 of Gambaudo and Tresser (1985) [**18**]

- to all $x \in [-1, 1]$ there is a unique rotation number $\rho_{\mu,\nu}$ (this follows from the piecewise monotonicity of the mapping)
- for all $\rho_{\mu,\nu}$ there is a rotation compatible orbit with that rotation number

Given the uniqueness of the rotation number for given values of the parameters and the existence of a rotation compatible orbit with this rotation number we obtain (i) and (ii) of the theorem.

Gambaudo and Tresser (1985) [**18**] also show that if the lift of a map depending on a single parameter is increasing with the parameter, then the rotation number is increasing and continuous with the parameter [*for continuous families as shown described in chapter 3; obvious for this family* (33) *but needs stating for the more general case*]. A direct application of this result gives part (iii) of the theorem noting that $G_{\mu,\nu}$ is increasing with ν (Fig. 65) [*Figure 8 here*].

Q.E.D.

Outside the region of validity of this local analysis, outside some neighbourhood of the codimension two homoclinic bifurcation, the appearance of chaotic behaviour can also be studied in a similar way. In the next section we shall discuss the appearance of chaos and look at a simple example.

However, first we shall complete the local analysis for the remaining two cases.

(b) The Semi-orientable case: $a > 0$, $b < 0$.

Here the right hand reinjection ($x > 0$) is orientable whilst the other is non-orientable. Using the techniques above we can show from the one-dimensional map that

- in $\mu < 0$, $\nu < 0$ the only periodic orbits have codes 1 and 0
- in $\mu < 0$, $\nu > 0$ the only periodic orbit has code 1
- in $\mu > 0$, $\nu < 0$ the periodic orbit with code 0 exists throughout the quadrant, and in $\nu > b\mu^\delta$ there is also a periodic orbit with code 10.

The final quadrant, with both μ and ν positive is more complicated. We shall prove the following theorem:

Theorem 33 (Theorem 3.3)**.** *For $a > 0$, $b < 0$ in (33) and $\mu, \nu > 0$, there is a neighbourhood of $(\mu, \nu) = (0, 0)$ in which the only periodic orbits are those with codes 1^n0, $n \geq 1$ and further more, regions of parameter space in which orbits with codes 1^n0 and $1^{n+1}0$ coexist, $n \geq 1$.*

[*This statement is seriously ungrammatical: as the proof below shows it is intended that there are regions with just code 1^n0 and regions with the stated coexistence.*]

First note that the periodic orbits must have all their points in $[-\mu, \nu - b\mu^\delta]$ and that the map is decreasing and positive in $x < 0$, and increasing in $x > 0$. Let $N \geq 2$ be the first time that $f^N(x) < 0$ for some $x \in [-\mu, 0)$ and note that parameter values can be found such that any given value of N (≥ 2) can be realised, with $N = 2$ for μ/ν large and $N \to \infty$ as $\mu/\nu \to 0$. Now consider the map

$$h(x) = \begin{cases} f(x) & \text{if } x > 0 \\ f^N(x) & \text{if } x < 0 \end{cases} \tag{36}$$

Since $f'(x) > 0$ in $x > 0$ and $f(x) > 0$ for $x < 0$ we have $f^N(0^-) < f^N(x)$ for x in $[-\mu, 0)$ and, by the definition of N, $f^N(0^-) < 0$. Hence $h(x)$ looks like $f(x)$ (upside down) in the region of parameter space with $\mu > 0$ and $\nu < 0$. The remarks made above for this quadrant of parameter space hold: there is a periodic orbit with code 0 and, in some cases, a periodic orbit with code 10, for h. In terms of f this translates into the existence of a periodic orbit with code 01^{N-1} and, in some cases, a periodic orbit with code 01^N coexists with this first orbit. It should be clear that on a line in parameter space with ν constant both possibilities must be realized, hence the theorem.

Now, the homoclinic orbit associated with a periodic orbit of code 10 occurs when $f(\nu) = -\mu + a\nu^\delta = 0$, i.e., $\mu = a\nu^\delta$. This gives the bifurcation diagram in Fig. 66 [*Figure 9 here*], where the shaded regions indicate the coexistence of two periodic orbits [*note to younger self: you forgot to do any shading*].

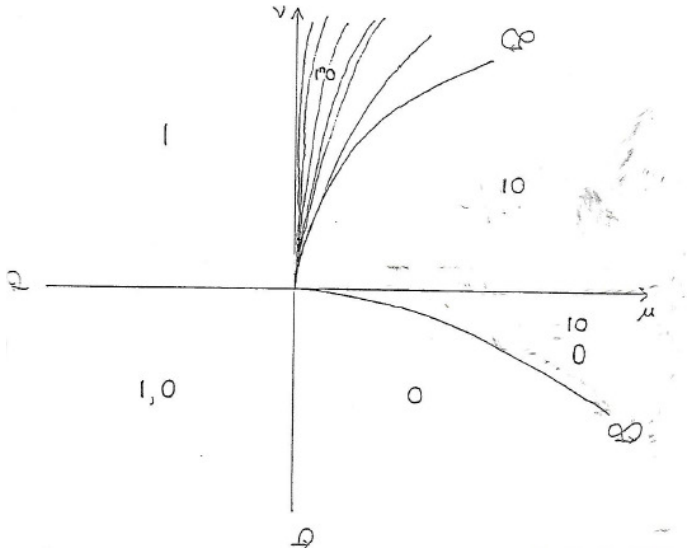

FIGURE 9. (Fig. 66 of [**21**].) (μ, ν) parameter for the semi-orientable case.

(c) The Non-orientable Case: $a < 0$, $b < 0$.

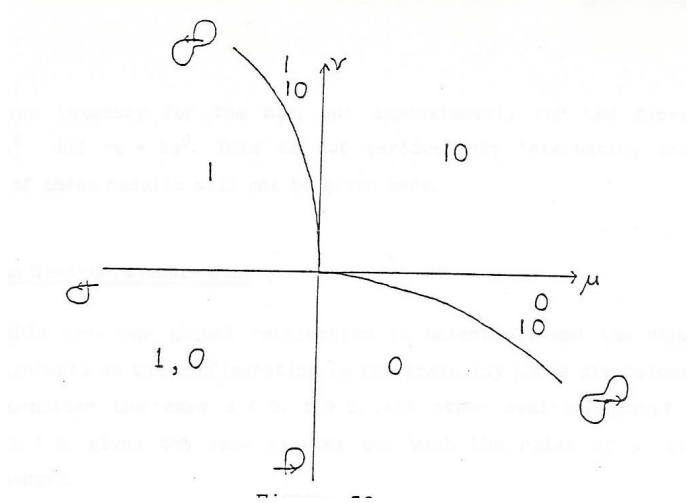

FIGURE 10. (Fig. 53 of [**21**].) (μ, ν) parameter space showing the homoclinic curves and the codes of periodic orbits for the orientable case [*of the figure eight configuration*].

When both the global reinjections are non-orientable the dynamics of the local map is relatively simple and we obtain essentially the same diagram as Fig. 53 [*Figure 10 ere*] for the orientable figure eight. It follows directly from the one-dimensional map (33) that

- if $\mu < 0$ and $\nu < 0$ the only periodic orbits have codes 1 and 0
- if $\mu > 0$ and $\nu < 0$ the periodic orbit with code 0 exists throughout the region and a periodic orbit with code 01 coexists with it if $-\mu > a\nu^{\delta}$

- if $\mu < 0$ and $\nu > 0$ the periodic orbit with code 1 exists throughout the region and a periodic orbit with code 10 coexists with it if $-\nu > b\mu^{\delta}$
- if $\mu > 0$ and $\nu > 0$ the periodic orbit with code 01 exists throughout the region and is the only periodic orbit of the local analysis.

This completes the local bifurcation pictures for the butterfly configuration of homclinic orbits.

END of excerpt from [21].

The extract above is an early draft and could obviously be improved (it was written to a deadline). But it does indicate the results we understood at that time. Further details including diagrams for the orientable case and links with differential equations can be found in [**17**] and the cases were described again in [**15**].

5. A Decomposition Theorem

Kneading Theory as developed by Milnor and Thurston, [**38**] which was circulating in preprint form from 1977, can be used to provide a decomposition of the non-wandering sets of piecewise smooth maps of the interval, and an early application was the decomposition theorem of Jonker and Rand [**33**] for smooth unimodal maps. However, the techniques of kneading theory are less well-known now, though the potential application to maps of great interest in the applied community is clear. In this paper we describe how to obtain an equivalent decomposition for maps with a single discontinuity or turning point using elementary observations.

These results hold for any map of the interval that has two monotonic continuous branches. Thus it includes all the maps considered in detail by Avrutin, Schanz and co-workers. They show just how complicated the detailed description of dynamics in parameter space can be. The philosophy behind the approach taken here is to avoid the temptation to describe the dynamics in detail whilst retaining sufficient information to be useful in applications. In particular it draws out the similarities of the dynamics of these maps rather than concentrating on differences.

WARNING: This chapter is work in progress. Though the ideas are standard I have not had time to go through it carefully and check the details (any comments gratefully received).

5.1. Background and Statement of Results. Let $f_i \colon \mathbb{R} \to \mathbb{R}$ be continuous, monotonic functions. Fix $c \in \mathbb{R}$ and suppose that there exists a largest non-trivial interval I containing c in its interior such that

$$g(x) = \begin{cases} f_0(x) & \text{if } x < c \\ f_1(x) & \text{if } x > c \end{cases}$$

maps I into itself. We shall call $g \colon I \to I$ a maximal two branch map. Note that the boundaries of the interval I are typically subsets of the fixed points of g and their preimages, or points of period two. Similarly g is a minimal two branch map if I is the smallest possible interval containing c

in its interior which g maps to itself. In interesting cases the end points of I wil lbe subsets of the orbit of c approached from above or below.

Two points are equivalent, $x \sim y$ if all the images of the open interval (x, y) are disjoint from c. The interval $J = (x, y)$ is then called a homterval, so $c \notin f^n(J)$ for all $n = 0, 1, 2, \ldots$. The images of x and y are equivalent in the sense that coding their orbits via sequences of 0s and 1s according to whether the n^{th} iterate lies to the left or the right of c cannot distinguish between the two points. All the classification below is up to orbit equivalence, $x \sim y$.

A point is wandering if there exists a neighbourhood U of x such that $f^n(U) \cap U = \emptyset$, otherwise it is non-wandering (and returns arbitrarily close to itself infinitely often). An interval J is wandering if $f^n(J) \cap J = \emptyset$ for all n, otherwise it is a non-wandering interval. The structure theorem we prove concerns the non-wandering set, $\Omega(g)$, of g. An open interval is transitive if for all $\epsilon > 0$ and all $y \in I$ there exists $x \in U$ and $n(\epsilon) \geq 0$ such that $|g^n(x) - y| < \epsilon$. The map g is transitive if for every interval U that is not a homterval, $\cup_0^\infty f^n(U) = \text{int}(I)$.

Theorem 34. *If $g\colon I \to I$ is a minimal two branch map then there exists N, $0 \leq N \leq \infty$ such that if $N = 0$ then $\Omega(g)$ is either a union of one or two periodic orbits (up to equivalence), a zero entropy Cantor set, or g is transitive on I; whilst if $1 \leq N < \infty$ then*

$$\Omega(g) = \bigcup_0^N \Omega_k$$

where if $k < N$ then Ω_k is either a union of one or two periodic orbits (up to equivalence) or a set equivalent to the dynamics defined by a finite transition matrix, and Ω_N is either a union of one or two periodic orbits (up to equivalence) or g is transitive on V_N; whilst if $N = \infty$ then an infinite decomposition holds with Ω_k, $k < \infty$ as before and Ω_∞ may be a chaotic or nonchaotic set on a Cantor set (up to equivalence).

5.2. Homtervals. An open interval J is a homterval if it contains no preimages of c, i.e., if $f^n|J$ is a homeomorphism for all $n \geq 0$. There are two types of homtervals – wandering intervals and intervals in the basin of attraction of a stable periodic orbit. It is often useful to consider maximal homtervals, the largest homterval containing J.

The following lemma is one of the standard theorems of undergraduate course on dynamical systems (see e.g., [**12**]).

Lemma 35. *If $f_I \to I$ and f is a homeomorphism then every point is either a fixed point, or a period two orbit, or in the basin of attraction of a fixed point or period two orbit.*

Homtervals are either wandering or basins of attraction of periodic orbits.

Lemma 36. *If J is a homterval then either J contains a union of basins of attraction of a stable periodic orbit or $f^n(J) \cap J = \emptyset$ for all $n > 0$.*

PROOF. Supose J is a homterval and $f^k(J) \cap J \neq \emptyset$ for some $k > 0$ (choose the smallest such). Then $f^n|f^k(J)$ and $f^n|J$ are homeomorphisms and so $J_1 = f^k(J) \cap J$ is a homterval and $f^k(J_1) \cap J_1 \neq \emptyset$. Set

$$J_\infty = \bigcup_{n=1}^{\infty} f^{nk}(J).$$

Then J_∞ is a homterval (as it is the union of homtervals) and $f^k(J_\infty) \subseteq J_\infty$ (simply apply f^k to the definition). Thus $c\ell(J_\infty)$ contains at least one stable periodic orbit, and J_∞ is a union of periodic orbits and basins of attraction of periodic orbits. □

The problem of homtervals from the point of view of structure theorems is that all points in a homterval have the same symbolic sequence attached to them, and this means that symbolic descriptions are ambiguous. In some elementary cases they can be ruled out.

Lemma 37. *Suppose $g\colon I \to I$ is a minimal two branch map and each branch of g is differentiable and there exists $\epsilon > 0$ such that for all $x \in I$, $|g'(x)| > 1 + \epsilon$. Then I contains no homtervals*

PROOF. If J is a homterval then the derivative condition and the Mean Value Theorem imply that $|g^n(J)| \geq (1+\epsilon)|g^{n-1}(J)|$ and hence $|g^n(J)| \geq (1+\epsilon)^n|J|$. Thus for all $|J| > 0$ there exists n such that $|g^n(J)| > |I|$, an obvious contradiction. □

A huge amount of effort has gone into proving the non-existence of wandering intervals and multiple (more than two) stable periodic orbits at higher iterates, see Berry and Mestel and de Melo and van Strien [**35**]. We will simply live with the possibility.

5.3. Renormalization and induced maps. If $g\colon I \to I$ is a minimal two branch map then it is *renormalizable* if there exists $J \subset I$ with $c \in J$ and n_k, $n_0 + n_1 > 2$, such that c divided J into two intervals J_k and $g^{n_k}(J_k) \subseteq J$, $c \notin g^r(J_k)$, $r = 1, \ldots, n_k - 1$.

Note that if g is renormalizable then the induced map

$$\tilde{g}(x) = \begin{cases} g^{n_0}(x) & \text{if } x \in J_0 \\ g^{n_1}(x) & \text{if } x \in J_1 \end{cases}$$

is a two branch map from J to itself.

Lemma 38. *If g is a minimal two branch map then $\Omega(g) = \Omega_0 \cup \Omega_1$ where Ω_0 is semi-conjugate to the dynamics of a finite Markov partition and Ω_1 is the non-wandering set of the induced map $\tilde{g}$ and its iterates under g. Either $\Omega_0 \cap \Omega_1 = \emptyset$ or the intersection is a union of one or two periodic orbits.*

PROOF. Choose J to be the smallest closed interval on which the induced map is degined, so $\tilde{g}$ is a minimal two branch map. Let $\omega = \Omega(\tilde{g})$, $\omega = \omega_0 \cup \omega_1$ and define

$$K = \left(\bigcup_0^{n_0-1} g^k(J_0) \right) \cup \left(\bigcup_0^{n_1-1} g^k(J_1) \right)$$

and

$$L = I \backslash K.$$

Then L is a finite union (possibly empty) of open intervals L_i on which g is continuous, and the left and right end-points of each interval map into K; hence if $g(L_i) \cap L_j \neq \emptyset$ then $L_j \subseteq L_i$, i.e., either $g(L_i) \cup L_j \neq \emptyset$ or L_i g-covers L_j. Thus the partition by K generates a finite Markov partition for the dynamics of g restricted to L. Let $\Omega_0 = \Omega(g) \cap c\ell(L)$, so Ω_0 is determined by the finite Markov partition just described.

Finally, $\Omega_1 = \Omega(g) \cap K$, and note that if $\omega = \omega_0 \cup \omega_1$ be the non-wandering set of $\tilde{g}$ in J, then

$$\Omega_1 = \left(\bigcup_0^{n_0-1} g^k(\omega_0) \right) \cup \left(\bigcup_0^{n_1-1} g^k(\omega_1) \right). \qquad \square$$

5.4. Non-chaotic maps. Suppose that g is a non-chaotic. This case has been treated in detail in [**24**]. Either g is not renormalizable, in which case $\Omega(g)$ is a finite union of periodic orbits, or it is renormalizable and $\Omega(g) = \Omega_0 \cup \Omega_1$ as described in Lemma 38, and Ω_0 is a finite union of periodic orbits modulo equivalence. Since g is not chaotic, the induced map $\tilde{g}$ is not chaotic, hence either it is renormalizable again, or not. If it is not renormalizable then $\Omega(\tilde{g})$ is a finite union of periodic orbits, and if it is renormalizable then we generate a new set (possibly empty) of periodic orbits and a new induced map.

Either this process stops, in which case $\Omega(g)$ is a finite union of periodic orbits, or every induced map is renormalizable. In this latter case there are nested intervals $J^{(r)}$ containing c and a countable set of periodic orbits, a finite set in each set $L^{(r)}$, together with $\Omega_\infty = c\ell \cap g^n(J_\infty)$ where $J_\infty = \cap_J^{(r)}$. Note that J_∞ is non-empty as it contains at least c, and Ω_∞ is typically a Cantor set on which the dynamics is non-chaotic.

This establishes the decomposition for the non-chaotic case.

Note that a great deal more detail could be given – there are an uncountable set of possibilities for Ω_∞ and the coexisting periodic orbits have well-defined sets of periods. See [**24**] for more detail.

5.5. The chaotic case. In the chaotic case there are uncountably many different symbol sequences. We will say that an interval is an *essential* interval if it contains uncountably many symbol sequences, i.e., if the set of dynamical conjugacy classes uner $\sim$ is uncountable. This is the natural object to consider, and we will say that a map is essentially transitive if $\cup_0^\infty g^n(U) = I$ for every essential interval U.

Lemma 39. *If g is a chaotic minimal two branch map and if g is not renormalizable then g is essentially transitive.*

PROOF. Let $U =< a, b >$ be an essential interval. Then there exists a smallest $n \geq 0$ such that there exists $x \in U$ such that $g^n(x) = c$ and both $c \in g^n(U)$ and both (a, x) and (x, b) are essential. Let $V_b \subseteq U$ be the maximal subset of U such that $g^n | V_b$ is monotonic. Let $V = g^n(V_b) = V_0 \cup V_1$ and note that both V_0 and V_1 are essential.

Hence there exist smallest n_0 and n_1 such that $g^{n_k}(V_k) \cap V \neq \emptyset$. Moreover, as g is minimal and not remormalizable then if $g^{n_k}(V_k) \subseteq V$, $k - 0, 1$ either $V = I$ (i.e., g is essentially transitive) or we get a contradiction. Thus if g is not essentially transitive at least one of the inclusions is not satisfied and

$$V \subset V^{(1)} = g^{n_0}(V_0) \cap V \cap g^{n_1}(V_1).$$

Now continue inductively: either g is essentially transitive or there exist $V^{(r+1)} \subseteq V^{(r)}$ such that $c \in V^{(r)}$ and $V^{(r)}$ is a union of iterates of V. Taking limits, $V^{(r)} \to V_\infty$, and either g is essentially transitive or $c \in V_\infty$ and there exist m_0, m_1 such that $g^{m_k}(V_\infty) \subseteq V_\infty$.

(The last inclusion follows because clearly m_0 and m_1 giving an intersection exist, and the inclusion follows from the limiting process.) Thus either $m_0 = m_1 = 1$ and $V_\infty = I$ as g is a minimal two branch map (and hence g is essentially transitive), or $m_0 + m_1 > 2$ and g is renormalizable (a contradiction). □

5.6. Proof of the Theorem. In this section we will complete the (sketch) proof of Theorem 34. We begin with a simple dichotomy.

Either

(a) g is renormalizable; or
(b) g is not renormalizable.

By Lemma 39 if g is not renormalizable then g is essentially transitive and the non-wandering set is I, thus it is case (a) that needs further thought.

Here there is either a finite number of renormalizations possible, in which case there exists a minimal interval J containing c for renormalization and the induced map on this interval is either zero entropy or not renormalizable with positive entropy (essentially transitive). Iterates of J define a Markov partition and dynamics outside the union of the iterates of the interval on which the induced map is defined is conjugate to a subshift of finite type.

If the map is infinitely renormalizable then there is an infinite set of unions of intervals in which the dynamics is described by a subshift of finite type (possibly empty as in the case of circle renormalizations) and there is a limiting set (typically a Cantor set). □

6. PWS maps of the plane

The results in pervious sections rely heavily on the order property of the real line, and maps in the plane are much harder to analyze. In many ways this section is a list of results and techniques without a strong overarching theory underpinning it. We will start with some examples and phenomenolgy.

6.1. The Lozi map. The Lozi map is a natural extension of tent maps to the plane. If the family of tent maps is written in the form

$$x_{n+1} = 1 - a|x_n|, \quad a \in (1, 2] \tag{37}$$

then the Lozi map is the map of the plane defined by

$$\begin{aligned} x_{n+1} &= 1 - a|x_n| + y_n \\ y_{n+1} &= bx_n. \end{aligned} \tag{38}$$

If $b \to 0$ then $|y_n| \to 0$ and so the x evolution is the tent map (37). If $b \neq 0$ is small then the attractor looks like a set of folded lines as shown in Figure 11. The Lozi map has uniform expansion and contraction properties, and this makes it a good example to test our ability to prove the existence of strange attractors.

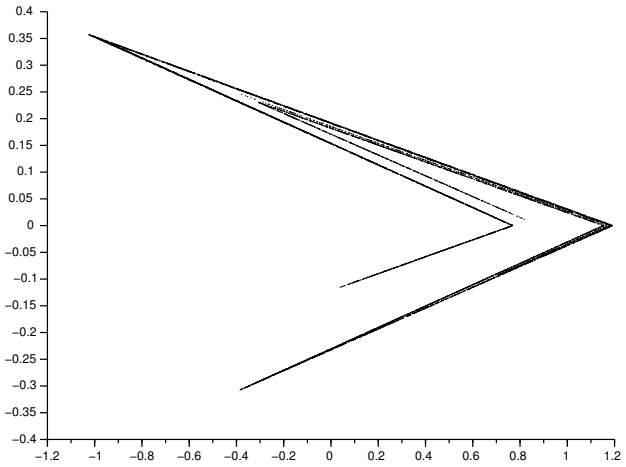

FIGURE 11. Numerically computed attractor of the Lozi map with $a = 1.7$ and $b = 0.3$.

6.2. The border collision normal form. The border collision normal form (BCNF) is a generalization of the Lozi map that describes the local behaviour of PWS maps for which a fixed point of one of the smooth systems defining the map hits a boundary on which that system is defined as parameters are varied. It is usually written as

$$\begin{pmatrix} x_{n+1} \\ y_{n+1} \end{pmatrix} = \begin{cases} f_0(x_n, y_n) & \text{if } x < 0 \\ f_1(x_n, y_n) & \text{if } x_n > 0 \end{cases} \tag{39}$$

with

$$f_k(x, y) = \begin{pmatrix} T_k & 1 \\ -D_k & 0 \end{pmatrix} \begin{pmatrix} x_n \\ y_n \end{pmatrix} + \begin{pmatrix} \mu \\ 0 \end{pmatrix}, \quad k = 0, 1. \tag{40}$$

The constants T_k and D_k are the trace and determinant of the matrix and μ is
the bifurcation parameter. Note that by scaling x and y the parameter μ can be taken in the set $\{-1, 0, +1\}$ so the idea that μ varies continuously is unnecessary.

The BCNF is continuous, but (assuming that $T_0 \neq T_1$ or $D_0 \neq D_1$) the Jacobians are different. Even so, the number of different phenomena that

can be observed is huge. Figure 12 shows a number of different possible bifurcations. With all this complexity it can be very difficult to decide what to analyze mathematically. Rather than attempt a complete classification we will give examples of the sort of thing that can be done in each of the three cases: periodic, one-dimensional and two-dimensional attractors in the next section.

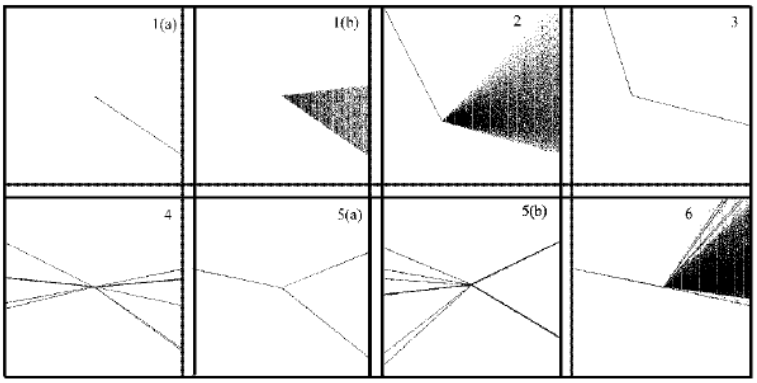

FIGURE 12. From [**4**]. Some bifurcations of the BCNF (only attractors are mentioned): μ is plotted horizontally and the projection of attractors onto the x-axis vertically. 1(a) no attractor to fixed point; 1(b) no attractor to chaos; 2 fixed point to chaos; 3 fixed point to fixed point; 4 coexisting fixed point and period 3 to coexisting fixed point and period 4; 5(a) fixed point to period two; 5(b) fixed point and period 11 to period 2; 6 fixed point to period 5 and chaotic attractor.

7. Periodic orbits and resonance

Suppose that one fixed point of the border collision normal form exists and the Jacobian has complex eigenvalues. In that case the motion on one side of the switching surface is like a rotation, with orbits spiralling in or out of the fixed point. It is then natural to look for periodic orbits that can be described by sequences of 1s and 0s (reflecting iterates in $x > 0$ and $x < 0$ respectively) that come from the order of rotations described in section 3. It turns out that this can be carried out exactly, giving equations determining when these orbits exist.

7.1. Fixed points and period two. Before considering the more complicated orbits it clearly makes sense to look at simplest orbits: fixed points and points of period two. For non-degenerate systems solutions to linear equations are unique, and so the only period two orbits that we will look for ar those with one point in $x < 0$ and one point in $x > 0$.

A fixed point exists in $x > 0$ if there is a solution to $f_1(x, y) = (x, y)$ with $x > 0$, i.e., if

$$T_1 x + y + \mu = x, \quad -D_1 x = y, \quad x > 0.$$

Solving these simple linear equations gives

$$x = \frac{\mu}{1 + D_1 - T_1}, \quad y = -\frac{D_1\mu}{1 + D_1 - T_1} \tag{41}$$

and so provided $1 + D_1 - T_1 \neq 0$ there is a fixed point for an appropriate sign of μ: $\mu > 0$ if $1 + D_1 - T_1 > 0$ and $\mu < 0$ if $1 + D_1 - T_1 < 0$.

A precisely analogous manipulation shows that there is a fixed point in $x < 0$ provided $\mu > 0$ if $1 + D_0 - T_0 < 0$ and $\mu < 0$ if $1 + D_0 - T_0 > 0$. Moreover, a fixed point is stable if the modulus of every eigenvalue of the Jacobian is less than one. This translates to the conditions $|D_0| < 1$ and $|T_0| < 1 + D_0$ in $x < 0$. This condition can also be written as

$$0 < 1 + D_0 - |T_0|.$$

Precisely analogous conditions hold in $x > 0$.

Putting the two branches of solutions together we see that if

$$(1 + D_0 - T_0)(1 + D_1 - T_1) > 0 \tag{42}$$

then the two fixed points exist for opposite signs of μ whilst if

$$(1 + D_0 - T_0)(1 + D_1 - T_1) < 0 \tag{43}$$

then the two fixed points exist for the same sign of μ (rather like a smooth saddle-node bifurcation).

Except in the degenerate case that a Jocobian has an eigenvalue of -1, in which case there can be a degenerate line of orbits of period two, an orbit of period two has one point on each side of $x = 0$. The equations are a little more messy, but still linear. Going through the detailed calculation period two points are at (x_0, y_0) with $x_0 < 0$ and (x_1, y_1) with $x_1 > 0$ and

$$\begin{aligned} x_0 &= \mu + y_1 + T_1 x_1 \qquad & y_0 &= -D_1 x_1 \\ x_1 &= \mu + y_0 + T_0 x_0 \qquad & y_1 &= -D_0 x_0 \end{aligned} \tag{44}$$

which imply

$$(x_k, y_k) = \left(\frac{1 + T_{1-k} + D_{1-k}}{(1 + D_0)(1 + D_1) - T_0 T_1}\mu, -D_{1-k}x_{1-k} \right), \quad k = 0, 1. \tag{45}$$

These lie on the 'correct' side of the y-axis for one sign of μ provided

$$(1 + T_0 + D_0)(1 + T_1 + D_1) < 0 \tag{46}$$

and if this inequality does not hold then there are no non-degenerate points of period two.

Stability is determined by the trace and determinant of the product of the linear parts of the BCNF:

$$\begin{pmatrix} T_0 & 1 \\ -D_0 & 0 \end{pmatrix} \begin{pmatrix} T_1 & 1 \\ -D_1 & 0 \end{pmatrix} = \begin{pmatrix} T_0 T_1 - D_1 & T_1 \\ -D_0 T_1 & -D_0 \end{pmatrix}$$

and the period two orbit is stable if the modulus of the trace and the modulus of the determinant satisfy equivalent conditions as for the fixed points; i.e., it is stable if

$$|D_0 + D_1 - T_0 T_1| < 1 + D_0 D_1, \quad |D_0 D_1| < 1. \tag{47}$$

So much for the equations – but what combinations of fixed points and periodic orbits can be involved in bifurcations? This is not obvious from the equations. We leave this question as an exercise for the moment, and will return to it in section 10.2.

7.2. Periodic orbits. Although a great deal was known about periodic orbits and the regions of parameter space for which they exist (and may coexist) from the works of Gardini and others [**19, 36**], the more recent approach of Simpson and Meiss [**45, 48**] makes a systematic approach possible.

Let $s_1, \dots s_n$ be a sequence of 0s and 1s, and suppose we wish to look for a periodic orbit of period n such that the k^{th} point of the periodic orbit lies in $x < 0$ if $s_k = 0$ and in $x > 0$ if $s_k = 1$. To find such an orbit it is necessary to solve the fixed point equation for the n^{th} iterate of the map, taking into account the required sequece (s_k), and then to determine whether the fixed point (ia periodic orbit of f) is *real*, i.e., its orbit passes through the regions $x \le 0$ and $x \ge 0$ in the prescribed order, or *virtual*, otherwise, in which case the solution does not correspond to an orbit of the BCNF.

At each iteration $f(\mathbf{x}) = A_{s_k}\mathbf{x} + \mu\mathbf{e}$ and so by induction

$$f^n(\mathbf{x}) = M_s\mathbf{x} + \mu P_s\mathbf{e}$$

where

$$M_s = A_{s_n} \dots A_{s_1}, \quad P_s = I + A_{s_n} + A_{s_n}A_{s_{n-1}} + \dots + A_{s_n} \dots A_{s_2}.$$

The point calculated on the orbit of period n in the half plane determined by s_1 is a solution of the fixed point equation $\mathbf{x}_1 = f^n(\mathbf{x}_1)$, i.e.

$$\mathbf{x}_1 = \mu(I - M_s)^{-1}P_s\mathbf{e}. \tag{48}$$

Of course, this exists and is unique if $I - M_s$ is non-singular, or eqivalently if $\det(I - M_s) \neq 0$.

The same process can be repeated for each point on the orbit: the image of $\mathbf{x}_1$ is $\mathbf{x}_2$ which satisfies a similar equation but with s replaced by $s_1 s_n \dots s_2$. Define the shift σ on these periodic sequences so that

$$\sigma(s_n \dots s_2 s_1) = s_1 s_n \dots s_2$$

then the n points on the orbit of period n corresponding to s are

$$\mathbf{x}_{k+1} = \mu(I - M_{\sigma^k s})^{-1}P_{\sigma^k s}\mathbf{e}, \quad k = 0, 1, \dots, n-1. \tag{49}$$

Simpson and Meiss [**49**] show that the x coordinate of (49) can be written as

$$x_{k+1} = \mu\frac{\det P_{\sigma^k s}}{\det(I - M_s)}, \quad k = 0, 1, \dots, n-1, \tag{50}$$

where we have used the fact that $\det(I - M_{\sigma^k s})$ is independent of k (to see this simply note that $A_{s_1}(I - M_s)A_{s_1}^{-1} = I - M_{\sigma s}$). The remainder of the derivation is far from trivial and details can be found in [**49**].

So far, so much manipulation. But is this solution real or virtual? The answer is very similar to that in the case of the orbit of period two in section 7.1.

Lemma 40. *Fix* $s = s_1 \dots s_n \in \{0,1\}^n$ *and suppose that* $\det(I - M_s) \neq 0$ *and* $\det P_{\sigma^k s} \neq 0$, $k = 0, 1, \dots, n-1$. *If there exists* $g \in \{-1, 1\}$ *such that*

$$\begin{aligned} \operatorname{sign}(\det P_{\sigma^{k-1}s}) &= -g \quad \text{if } s_k = 0 \\ \operatorname{sign}(\det P_{\sigma^{k-1}s}) &= g \quad \text{if } s_k = 1 \end{aligned} \tag{51}$$

then the periodic orbit corresponding to s *exists for* $\mu > 0$ *if* $g\det(I - M_s) > 0$ *and for* $\mu < 0$ *if* $g\det(I - M_s) < 0$.

The proof is straightforward from the definitions and (50). Note that at this stage we have not used the assumption that the map is two-dimensional.

7.3. Resonance tongues and pinching. Lemma 40 and (50) show that the ways by which periodic orbits can be created or destroyed as parameters vary must involve one or other of P_s or $I - M_s$ becoming singular as the parameters are varied.

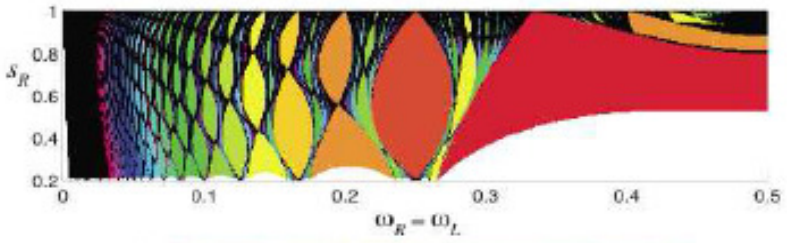

FIGURE 13. Numerically computed regions of parameter with different rotation type periodic orbits, from [**49**].

One fairly general case of this has some interesting and immediately recognisable features. Figure 13 shows regions in the parameter space of the BCNF in which the map has periodic orbits of particular rotation type (i.e., they have rotation numbers and order on a circle reflecting the order described in section 3.2 above). The parameters are chosen so that

$$T_L = 2r_L \cos(2\pi\omega_L), \quad D_L = r_L^2, \quad T_R = \tfrac{2}{s_R}\cos(2\pi\omega_R), \quad D_R = \tfrac{1}{s_R^2}$$

and in the Figure,

$$r_L = 0.2, \quad \mu = 1,$$

and $\omega_R = \omega_L$ is the parameter on the horizontal axis, and s_R is the parameter on the vertical axis. The resonant tongues in which the periodic orbits exist have a 'sausage' shaped pinched structure which can be understood using the methods of the previous section.

The analysis of these bifurcations involves two ingredients. First, the rotation order of the periodic points implies that the points on the periodic orbit can be arranged on a circle (with no self-intersections) so that the order on the circle is $\mathbf{x}_1, \dots, \mathbf{x}_n$ and the effect of the map f is

$$f(\mathbf{x}_k) = \mathbf{x}_{k+m} \tag{52}$$

where the index $k + m$ is interpreted modulo n with the convention that $0 \equiv n$. However, this order does not indicate where the switching surface lies, so the second ingredient specifies the position of the switching surface with

respect to the periodic points. Assume that the switching surface separates the periodic points into two consecutive sets of points on the circle with ℓ points in $x < 0$ and $n - \ell$ in $x > 0$. The orbit is therefore specified by three positive integers: n, m and ℓ, and the labelling can be chosen so that $\mathbf{x}_1, \ldots, \mathbf{x}_{n-\ell}$ lie in $x > 0$ and $\mathbf{x}_{n-\ell+1}, \ldots, \mathbf{x}_n$ lie in $x < 0$. This information is enough to specify the symbolic description s of the orbit (note that it is NOT the rotation-compatible sequences of section 3.2 as the position of the switching surface which determines s is not the same as the coding of the rotations). We shall refer to these orbits as (n, m, ℓ)-orbits.

If this periodic orbit undergoes a border collision bifurcation itself, then one point intersects the switching surface and by continuity this must be either $\mathbf{x}_1$ or $\mathbf{x}_n$ or $\mathbf{x}_{n-\ell}$ or $\mathbf{x}_{n-\ell+1}$.

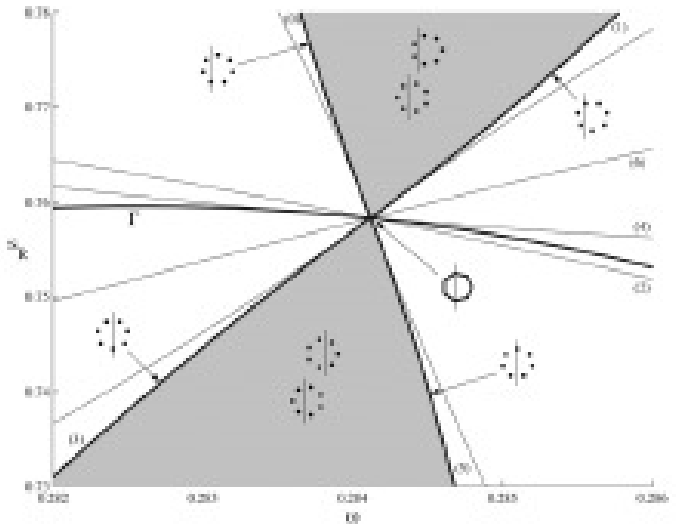

FIGURE 14. Part of the pinched tongue of rotation number 2/7 showing the different border collision bifurcations. This shows the orbit with $\ell = 3$ interacting with the $\ell = 2$ case (upper lobe) and $\ell = 4$ case (lower lobe). From [**48**].

Suppose that it is $\mathbf{x}_1$. Then by the results of section 7.1 the bifurcation will involve two periodic orbits: one with code s and the other with code ${}^0s$, defined to be s with the initial symbol 1 replaced by 0. In other words, the 'partner' orbit has is a $(n, m, \ell + 1)$-orbit. Similarly, if the border collision point is $\mathbf{x}_{n-\ell}$ then it crosses at the border collision creating another code with one of the $1s$ in s replaced by a zero – the partner is again a $(n, m, \ell+1)$-orbit. It turns out (see Figure 14) that these are generalized saddle-node orbits, so there is a lobe in which a (n, m, ℓ)-orbit coexists with a $(n, m, \ell + 1)$-orbit.

Bifurcations involving $\mathbf{x}_n$ or $\mathbf{x}_{n-\ell+1}$ are similar, except each of these involves the existence of a $(n, m, \ell - 1)$-orbit.

The regions (lobes) are thus defined by orbits whose ℓ description differs by one. At the shrinking point (for the piecewise affine BCNF) there is a degenerate invariant circle. This beautiful structure does not persist for

typical nonlinear perturbations of the BCNF: the codimension two pinching point has a natural unfolding, see [**49**] for details.

7.4. Infinitely many sinks. The previous section might give the impression that periodic orbits exist in splendid isolation. However, it has been recognised for many years that complicated regions of multistability exist in the border collision normal form [**19**]. More recently Simpson [**45**] has shown that there are parameter values for the BCNF at which there are infinitely many stable periodic orbits. We will not go into the details here – but Figure 15 show numerically computed basins of attraction at an approximation of the critical parameter. Note that a similar example is explored in [**13**].

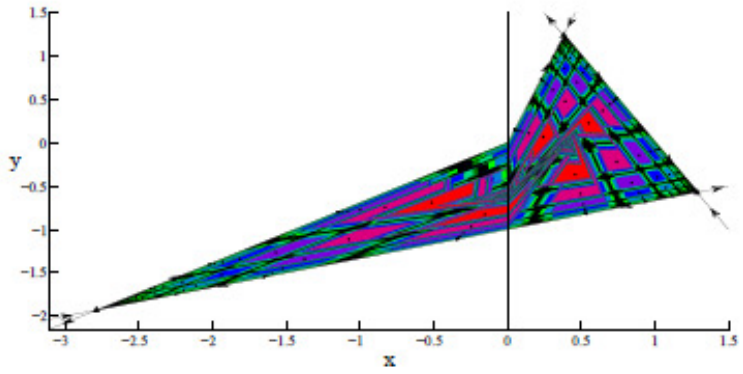

FIGURE 15. Basins of attraction of the lowest period orbits in an example with infinitely many sinks. From [**45**].

8. Robust chaos

The intersection of stable and unstable manifolds of a fixed point (a homoclinic tangle) is one of the classic mechanisms to create chaotic solutions in smooth systems. The mechanism also applies to piecewise smooth systems, and Banerjee *et al.* (1998) use this idea to show that there are robust chaotic attractors in the BCNF, a phenomenon they dubbed 'robust chaos'. Banerjee *et al.* [**4, 5**] provide a brief plausibility argument for the proof of the chaotic attractor, here we will use results of Misieurewicz [**37**] which provide a more direct demonstration of the phenomenon.

8.1. The Lozi map and trapping regions. Consider the restricted problem of the border collision form with

$$T_0 = -T_1 = a > 0, \quad D_0 = D_1 = -b, \quad 0 < b < 1. \tag{53}$$

Taking $\mu = 1$ (i.e., $\mu > 0$ by scaling) we recover the Lozi map (38). Note that the map is a homeomorphism and the left half plane maps to the lower half plane whilst the right half plane maps to the upper half plane. The y-axis, $x = 0$, maps to the x-axis, $y = 0$.

If the constraints of (53) hold and $a + b > 1$ then the system has two fixed points,

$$Y = \left(-\frac{1}{b+a-1}, -\frac{b}{b+a-1} \right), \quad X = \left(\frac{1}{1-b+a}, \frac{b}{1-b+a} \right)$$

as shown in Figure 16. Both are saddles; the Jacobian at Y has an stable negative eigenvalue with an eigenvector of negative slope, and an unstable positive eigenvalue with an eigenvector of positive slope whilst the Jacobian at X has an unstable negative eigenvalue with an eigenvector of negative slope, and a stable positive eigenvalue with an eigenvector of positive slope. The stable and unstable manifolds of X will be particularly important.

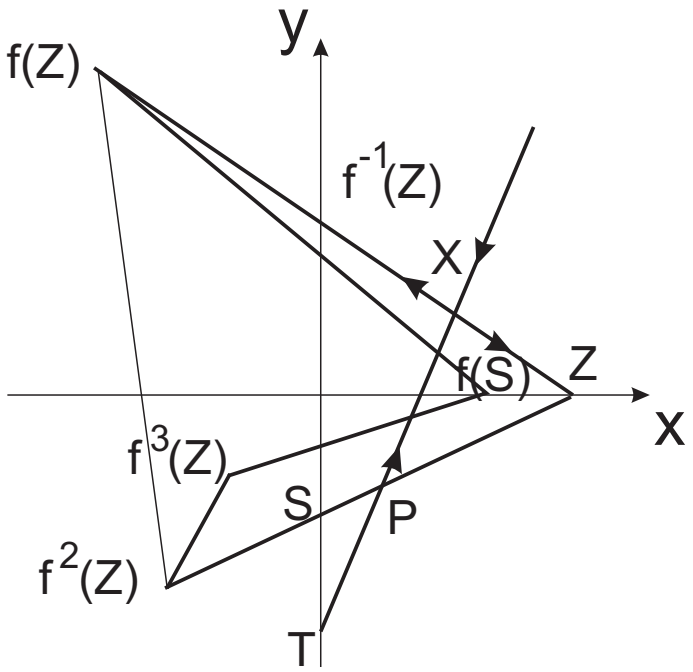

FIGURE 16. Schematic view of the bounding region and geometry of iterates for the Lozi map, after [**37**].

A great deal of the argument used to show the existence of a strange attractor for the Lozi map (38) relies on brute force calculation. We shall keep this to a minimum and try to emphasize the conceptual framework being developed.

The eigenvalues of the Jacobian at X are $s_\pm = \frac{1}{2}(-a \pm \sqrt{a^2+4b})$ with eigenvalues $\begin{pmatrix} s_\pm \\ b \end{pmatrix}$, so by a little elementary geometry the stable direction (with eigenvalue s_+) intersects the y-axis at T where

$$T = \left(0, \frac{2b - a - \sqrt{a^2+4b}}{2(1+a-b)} \right). \tag{54}$$

Since T is on the y-axis $f(T)$ is on the x-axis and since T is on the stable manifold of X, $f(T)$ will be the intersection of TX with the x-axis.

Similarly, the unstable direction of X intersects the (positive) x-axis at Z where

$$Z = \left(\frac{2 + a + \sqrt{a^2 + 4b}}{2(1 + a - b)}, 0 \right). \tag{55}$$

The local unstable manifold of X thus contains the line segment $f(Z)Z$.

Since $f(Z)$ is in $x < 0$, $f^2(Z)$ lies in the lower half plane. There are thus two cases depending on whether $f^2(Z)$ lies on the left or right of the y-axis. In what follows below we consider only the case for which $f^2(Z)$ is on the left of the y-axis; the argument in the other case is a little more complicated (see [**37**]), and we leave it to the reader to find the details if they are interested.

So, by assumption (restricting the cases being considered) $f^2(Z)$ lies in the lower half plane with $x < 0$, and so $f^3(Z)$ can be calculated explicitly. This calculation can be used to show the following lemma from [**37**].

Lemma 41. *Consider the Lozi map* (38) *with parameters as described above. If* $f^3(Z)$ *lies in the triangle* $\triangle = Zf(Z)f^2(Z)$ *then* $f(\triangle) \subset \triangle$.

Proof. The geometry is shown in Figure 16. Let S denote the intersection of $f^2(Z)Z$ with the y-axis and note that $f(S)$ is on the x-axis to the left of Z as S lies below the origin which is below $f^{-1}(Z)$. It is an elementary calculation to show that the x-coordinate of $f^2(Z)$ is larger than that of $f(Z)$ and so the slope of $f(Z)f^2(Z)$ is negative as shown in Fig. 16. Let $f^2(Z) = (p_1, p_2)$ and $S = (0, s_2)$. Then $p_1 < 0$ by assumption and $p_2 < s_2$ by construction. The x-coordinate of $f(S)$ is $1 + s_2$ and the x-coordinate of $f^3(Z)$ is $1 + p_2 + ap_1$ which is clearly less than $1 + s_2$ and hence $f(S)$ is to the right of $f^3(Z)$ as shown.

$\triangle$ is composed of two parts:

$$\triangle_1 = f^{-1}(Z)ZS \text{ in } x \geq 0 \quad \text{and} \quad \triangle_2 = f^{-1}(Z)f(Z)f^2(Z) \text{ in } x \leq 0$$

(note that $\triangle_2$ is not a triangle!). Thus

$$f(\triangle_1) = Zf(Z)f(S) \subset \triangle$$

and

$$f(\triangle_2) = Zf^2(Z)f^3(Z)f(S) \subset \triangle$$

and so $f(\triangle) \subset \triangle$ as required. □

Thus $\triangle$ is a compact invariant set and hence contains an attractor provided $f^3(Z)$ is contained in $\triangle$. Brute calculation establishes that this is true provided a further condition is put on a and b.

Lemma 42. *If* $a > 0$, $0 < b < 1$, $a > b + 1$ *and* $2a + b < 4$ *then* $f(\triangle) \subset \triangle$.

8.2. Strange attractors. Banerjee *et al.* [**4, 5**] provide a plausibility argument for the existence of strange attractors (albeit at different parameters of the border collision normal form, though they also discuss the case here) based on (a) the existence of transverse homoclinic intersections; and (b) the existence of heteroclinic connections between the unstable manifold of Y and the stable manifold of X. Misieurewicz [**37**] takes a more direct route,

and whilst this is more transparent we should say something about the ideas of Banerjee *et al.* [**4, 5**] before continuing.

Since X is a saddle it has stable and unstable manifolds. Suppose that C is curve segment that crosses a part of the stable manifold of X, $W^s(X)$, transversely, then under iteration the intersection point will converge on X and the part of the remainder of the curve near the intersection point will move close to X and then expand close to the unstable manifold of X, $W^u(X)$. The Lambda Lemma [**1**] states that this idea can be stated precisely: in any neighbourhood of any point in $W^u(X)$ there exist a point in the image of C.

In particular, if C is itself a part of $W^u(X)$, so the intersection is a point in $W^u(X) \cap W^s(X)$, i.e., a transverse homoclinic point, then images of $W^u(X)$ lie arbitrarily close to any point in $W^u(X)$, giving a form of recurrence. Similarly, if there is a transverse intersection between $W^u(Y)$ and $W^s(X)$ then images of $W^u(Y)$ also lie arbitrarily close to any point in $W^u(X)$. Banerjee *et al.* [**4, 5**] use this, together with the fact that in $x < 0$ iterates are attracted to $W^u(Y)$ and in $x > 0$ they are attracted to $W^u(X)$ to deduce that the closure of $W^u(X)$ is a chaotic invariant set.

In the case considered here we can have a transverse homoclinic point.

Lemma 43. *If S lies above T on the y-axis than the Lozi map has a transverse homoclinic point.*

Proof. If S lies above T then there exists an intersection point P between XT (part of the stable manifold of X) and $f^2(Z)Z$ (part of the unstable manifold of X). □

The precise condition is messy and will not be pursued here. Misieurewicz [**37**] proves the following.

Theorem 44. *Suppose that $a > 0$, $2a+b < 4$, $a\sqrt{2}-2-b > 0$ and $b < \frac{a^2-1}{2a+1}$. Then the attractor of the Lozi map* (38) *is the closure of $W^u(X)$ and the map is topologically transitive on this set.*

Remark. A subset $\mathcal{A}$ of $\mathbb{R}^2$ is topologically transitive if for all open U_k $k = 0, 1$ with $U_k \cap \mathcal{A} \neq \emptyset$ there exists n such that $f^n(U_0) \cap U_1 \neq \emptyset$.

Sketch Proof. The proof is split into a number of stages which will simply be sketched here.

Step 1: By Lemma 42 $\triangle$ contains an attracting invariant set. It is not conceptually hard (but not an easy calculation) to construct a closed set G such that $\triangle$ is contained in the interior of G and such that the attracting set

$$\tilde{G} = \bigcap_0^\infty f^n(G) = \bigcap_0^\infty f^n(\triangle) = \tilde{\triangle}.$$

So for any $x \in \triangle$ (and in particular, for any x in the attractor) there is an open neighbourhood of x in G.

Step 2: Let $H_0 = XZP$ and $H = \cup_0^\infty f^n(H_0)$. Then the boundary of H, ∂H is contained in $XP \cup W^u(X)$, $f(H) \subset H$, and $\tilde{H} = \cap f^n(H) = \tilde{\triangle}$.

Step 3: That $\tilde{\triangle}$ is the closure of the unstable manifold of X is shown by using G and $\tilde{G}$ to show that $c\ell(W^u(X)) \subseteq \tilde{\triangle}$ and H and $\tilde{H}$ to show that $\tilde{\triangle} \subseteq c\ell(W^u(X))\tilde{\triangle}$.

Step 4: Finally a hyperbolicity argument for expansion on the unstable manifold is used to show that f is topologically mixing on $\tilde{\triangle}$. □

8.3. Young's Theorem. Young's Theorem [**52**] provides an alternative approach to the chaotic attractors of border collision normal forms and their generalizations using invariant measures. This is not the place to give a detailed technical description of the theorem, but it is nonetheless useful to know that such techniques exist and can be applied to examples.

A measure μ on a space is essentially a way of assigning size or probability to subsets (strictly speaking, measureable subsets) of the space. Thus if X is a compact subset of the plane a (probability) measure is a map from (measureable) subsets U of X to the $[0,1]$ such that

- $\mu(\emptyset) = 0$, $\mu(X) = 1$,
- $\mu(U \cup V) \leq \mu(U) + \mu(V)$ with equality if $U \cap V = \emptyset$,

and a measure is an invariant measure of a map $f\colon X \to X$ if for all $U \subseteq X$

$$\mu(f^{-1}(U)) = \mu(U).$$

Invariant measures provide ways of linking spatial and temporal averages: if $g\colon X \to \mathbb{R}$ is a nice (integrable) function then we would like a result of the form

$$\frac{1}{n}\sum_{0}^{n-1} g(f^n(x)) \to \int_X g d\mu$$

as $n \to \infty$ (for μ almost all x). This is true for *ergodic* measures: i.e., invariant probability measures with the property that for every invariant set E (i.e., measureable sets with $f^{-1}(E) = E$) either $\mu(E) = 0$ or $\mu(E) = 1$.

Young's Theorem provides a way of proving that nice measures exist for robust chaos.

Let $R = [0,1] \times [0,1]$ and let $S = \{a_1, \ldots, a_k\} \times [0,1]$ be a set of vertical switching surfaces with $0 < a_1 < \cdots < a_k < 1$. Then $f\colon R \to R$ is a Young map if f is continuous, f and its inverse are C^2 on $R \backslash S$ and $f = (f_1, f_2)^T$ satisfies the expansion properties (H1)-(H3) below on $R \backslash S$.

$$\text{(H1)} \qquad \inf\left\{\left(\left|\frac{\partial f_1}{\partial x}\right| - \left|\frac{\partial f_1}{\partial y}\right|\right) - \left(\left|\frac{\partial f_2}{\partial x}\right| - \left|\frac{\partial f_2}{\partial y}\right|\right)\right\} \geq 0,$$

$$\text{(H2)} \qquad \inf\left(\left|\frac{\partial f_1}{\partial x}\right| - \left|\frac{\partial f_1}{\partial y}\right|\right) = u > 1, \quad \text{and}$$

$$\text{(H3)} \qquad \sup\left\{\left(\left|\frac{\partial f_1}{\partial y}\right| + \left|\frac{\partial f_2}{\partial y}\right|\right)\left(\left|\frac{\partial f_1}{\partial x}\right| - \left|\frac{\partial f_1}{\partial y}\right|\right)^{-2}\right\} < 1.$$

Young's Theorem describes measures that project nicely onto one-dimensions. Technically this is expressed as having absolutely continuous conditional measures on unstable manifolds. Intuitively this means that the measure projects nicely onto on dimension.

Let $Jac(f)$ denote the Jacobian matrix of f and recall that u is defined in (H2).

Theorem 45. [**52**] *If f is a Young map, $|Jac(f)| < 1$ for $x \in R \backslash S$, and there exists $N \geq 1$ s.t. $u^N > 2$ and if $N > 1$ then $f^k(S) \cap S = \emptyset$, $1 \leq k < N$, then f has an invariant probability measure that has absolutely continuous conditional measures on unstable manifolds.*

Since the result is for piecewise C^2 maps and the conditions only depend on derivatives this result has the important corollary that results for the piecewise linear border collision normal form, which should more correctly be called a truncated normal form, persist when small nonlinear terms are added.

Historical note: The theorem as actually published [**52**] has $u^N > 2$ and $f^k(S) \cap S = \emptyset$, $1 \leq k \leq N$ (note the non-strict inequality in the last expression). However, no extra conditions on images of S are required if $N = 1$ and if $N > 1$ then the requirement is that f^N has similar geometry on vertical strips, which only requires non-intersection up to the $(N-1)^{th}$ iterate, so we are confident that Theorem 45 is what was intended.

The criteria for the theorem to hold are easy to verify numerically making it possible to determine regions on which Young's Theorem holds and compare these with theoretical bounds in [**5**], see [**22**] for details.

9. Two-dimensional attractors

The BCNF can also have robust two-dimensional attractors. These results use some beautiful theory for general piecewise linear maps due to Buzzi and Tsujii. These will be described in the second section – first we describe another context in which the existence of two-dimensional attractors can be deduced from first principles. Note that the existence of two-dimensional attractors implies expansion in all directions, so the only way this can occur is through folding, i.e., the map must be non-invertible: $D_0 D_1 < 0$.

9.1. A Markov Partition. In section 1.5 we saw that Markov partitions and their associated graphs provide a good way to analyze dynamics. The idea in this section is to construct an example with a two-dimensional Markov partition and then show that the map (or an iterate of the map) is uniformly expanding on each region defining the Markov partition.

Consider the BCNF with $D_0 < 0$, $D_1 > 0$ and $\mu = 1$. We shall start by constructing a simple bounding region and then try to describe the dynamics in this region. Note that the conditions on D_k, $k = 0, 1$, imply that the images of both the left and the right halsf planes map to the lower half plane.

Let $O = (0, 0)$ so $P_1 = f(0, 0) = (1, 0)$. Suppose that $P_2 = f(P_1)$ is in $x > 0$ and $P_3 = f(P_2)$ lies on the y-axis. so $P_4 = f(P_3)$ lies on the x-axis and we shall assume this can be chosen so that P_4 is in the left half plane as shown in Fig. 17a. To achieve this will require only one real constraint (that P_3 lies the y-axis), the remainder are open conditions.

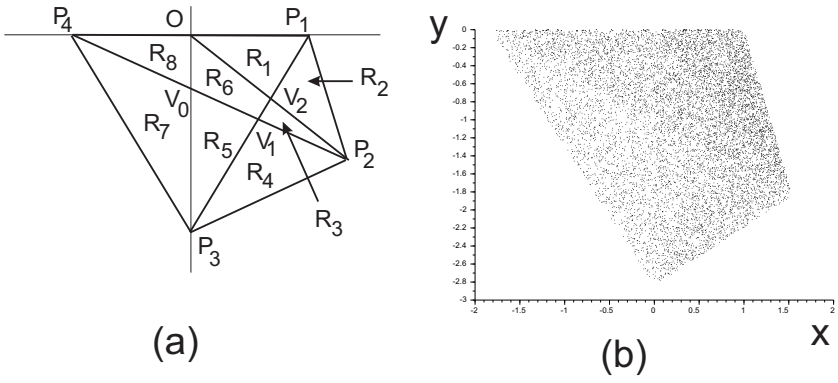

FIGURE 17. (a) Schematic view of the Markov partition; (b) numerical solution for parameters given below.

Next, choose the parameters such that $f(P_4) = P_2$ (two conditions; these will fix T_0 and D_0) and finally arrange it so that the straight line P_4P_2 intersects the y-axis at $V_0 = (0, -1)$, the preimage of O (one real condition). This gives four real conditions for the four parameters $T_k,\ D_k$, $k = 0, 1$. We will show that these can be solved below, but before verifying this let us consider the consequences (see Fig. 17a again).

Let V_1 be the intersection of P_1P_3 with V_0P_2, so its image will lie on the intersection of P_2P_4 and OP_3, i.e., $f(V_1) = V_0$. Similarly let V_2 be the intersection of P_1P_3 and OP_2 so $f(V_2) = V_1$. The lines connecting the points O, $P_1, \ldots, P_4$, V_0, V_1 and V_2 divide the trapping region $OP_1P_2P_3P_4$ into eight sectors

$$\begin{aligned} &R_1 = OV_2P_1, \quad R_2 = P_1V_2P_2 \qquad R_3 = P_2V_1V_2 \quad R_4 = P_2V_1P_3 \\ &R_5 = P_3V_1V_0, \quad R_6 = OV_0V_1V_2, \quad R_7 = P_3V_0P_4 \quad R_8 = P_4V_0O. \end{aligned} \tag{56}$$

These have been chosen so that

$$\begin{aligned} &f(R_1) = R_2 \cup R_3, \qquad f(R_2) = R_4, \qquad f(R_3) = R_5, \\ &f(R_4) = R_4 \cup R_7, \qquad f(R_5) = R_8, \qquad f(R_6) = R_1 \cup R_6, \\ &f(R_7) = R_3 \cup R_6 \cup R_8, \quad f(R_8) = R_1 \cup R_2. \end{aligned} \tag{57}$$

This is therefore a two-dimensional Markov partition and the symbolic description of orbits is easy to describe using a Markov graph in precisely the same way as in section 1.6. A little more work is required to show that the map is transitive on the invariant region, see [**30**] for details.

Let us check that this is possible. By direct calculation

$$P_2 = (T_1 + 1, -D_1), \quad P_3 = (T_1(T_1 + 1) - D_1 + 1, -D_1(T_1 + 1))$$

and hence the first constraint is that

$$D_1 = T_1(T_1 + 1) + 1. \tag{58}$$

In this case set $t = T_1$ so $D_1 = t^2 + t + 1$ and

$$P_3 = (0, -D_1(t^2 + t + 1)), \quad P_4 = (1 - D_1(t + 1), 0)$$

and P_4 is in $x < 0$ provided $D_1(t+1) > 1$ and note that this is certainly true if $D_1 > 1$ and $t > 0$. Now the line P_2P_4 intersects the y-axis at $V_2 = (0, -1)$

if (by similar triangles)

$$\frac{1}{D_1(t+1)-1} = \frac{D_1}{D(t+1)+t}$$

and after a little algebra (involving factorization of a quintic in t) this holds if

$$t^3 + t^2 + t - 1 = 0, \quad D_1 = \tfrac{1}{t}. \tag{59}$$

A simple root finding method shows that this has a positive solution with

$$T_1 = t \approx 0.543689, \quad D_1 \approx 1.839287$$

and solving the equations for T_0 and D_0 gives

$$T_0 = -t^2 \approx -0.295598, \quad D_0 = -1.$$

Figure 17b shows a numerically calculated solution for these parameter values. Glendinning and Wong [**30**] show that an expansion condition holds on iterates of the map which implies transitivity on the whole region $OP_1P_2P_3P_4$. They also derive conditions for a sequence of other parameters having a similar Markov property.

9.2. Piecewise linear maps. A number of general results were proved in around 2000 proving the existence of two-dimensional attractors for piecewise linear maps. These all rely on expansion of each individual map, but the technical assumptions are more general than the BCNF as continuity across boundaries is not assumed. Here we follow Buzzi [**11**] and Tsujii [**50**].

Let $\mathcal{D}$ be a polygonal region in $\mathbb{R}^2$, i.e., a compact connected region whose boundary is a finite union of straight line segments. Let $\mathcal{P}$ be a finite collection of non-intersecting open polygonal regions $\{P_i\}_{i=1}^m$ such that the union of the closures of these polygons is $\mathcal{D}$. Then a map $F\colon \cup P_i \to \mathcal{D}$ is a *piecewise affine map* if $F|_{P_i}$ is an affine map, $i = \{1, \ldots, m\}$. If in addition there exists $\lambda > 1$ and a metric $d\colon \mathbb{R}^2 \to \mathbb{R}$ such that for each $i \in \{1, \ldots, m\}$ $F|_{P_i}$ is expanding, i.e.

$$d(F(x), F(y)) \geq \lambda d(x, y) \quad \text{for all } x \in P_i$$

$i = 1, \ldots, m$, then F is a *piecewise expanding affine map*. The main result that can be applied to the BCNF shows that there are two-dimensional attractors. Like Young's Theorem it uses the idea of invariant measures to describe the dynamics, but it is the existence of open sets in the attractor which implies that the attractor has topological dimension two rather than simply Hausdorff dimension equal to two.

Theorem 46. [**10, 11, 50**] *Suppose F is a piecewise expanding affine map of a planar polygonal region $\mathcal{D}$. Then there exists an attractor in $\mathcal{D}$ such that F has an absolutely continuous invariant measure on the attractor and the attractor contains open sets.*

Unfortunately, the BCNF is not expanding (at least in the standard Euclidean metric), so a little more work needs to be done in order to apply this result.

9.3. Robust bifurcations to two-dimensional attractors. The examples of section 9.1 can be proved to have two-dimensional attractors, but they exist at special values of the parameters. The results of Buzzi and Tsujii of section 9.2 make it possible to prove the existence of such sets for open sets of parameters. It is even possible to construct open conditions so that the border collision bifurcation has a stable fixed point if $\mu < 0$ and a two-dimensional attractor if $\mu > 0$ [**26**]. The proof follows the rather easier path of [**25**]. An example of a two-dimensional attractor with

$$T_L = -0.1, \quad D_L = -8/11, \quad T_R = 0.05, \quad D_R = 1.99$$

and $\mu = 1$ is given in Figure 18.

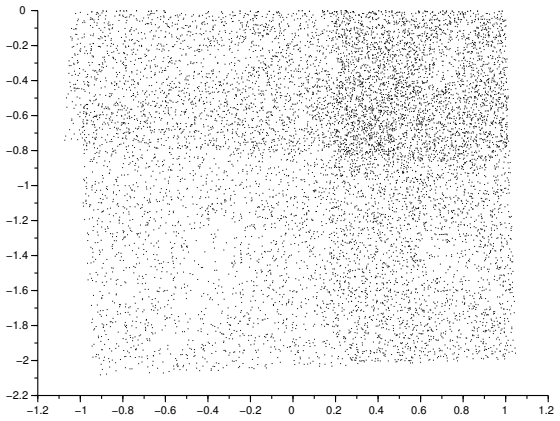

FIGURE 18. Numerically calculated attractor for the BCNF with parameters as given in the text.

Theorem 47. [**26**] *There exists an open region $\mathcal{D} \subset \mathbb{R}^4$ such that if*

$$(T_0, D_0, T_1, D_1) \in \mathcal{D}$$

then the BCNF (39, 40) *has a stable fixed point if $\mu < 0$ and a fully two-dimensional attractor if $\mu > 0$.*

PROOF. From the results of section 7.1 the choices $1 + D_0 - T_0 > 0$ and $1 + D_1 - T_1 > 0$ imply that there is a fixed point in $x < 0$ if $\mu < 0$ and a fixed point in $x > 0$ if $\mu > 0$. The fixed point in $x < 0$ is stable (when it exists) provided the eigenvalues of the Jacobian have modulus less than one, i.e., if

$$|D_0| < 1 \quad \text{and} \quad |T_0| < 1 + D_0. \tag{60}$$

Now consider $\mu > 0$, so by scaling we can assume that $\mu = 1$. The pattern will be similar to proofs of chapter 8: we begin by constructing an absorbing region for well-chosen parameters. Fix $\epsilon > 0$ (to be chosen small enough later) and suppose that

$$|T_k| < \epsilon, \ k = 0, 1, \quad -D_0 \in \left(\frac{6}{11}, \frac{10}{11}\right), \quad D_1 \in (2 - \epsilon, 2). \tag{61}$$

Clearly (60) is satisfied for small ϵ, so if $\mu < 0$ there is a stable fixed point. If $\mu = 1$ consider the rectangular region with

$$-(1 + 0.05 - 4\epsilon) \leq x \leq 1 + 4\epsilon, \quad -(2 + 0.05 - 2\epsilon) \leq y \leq 2\epsilon. \tag{62}$$

If (x, y) is in this rectangle then the image is (x', y') with $x' = 1 + y + T_k x$ and so taking maximum and minimum values

$$1 - (2 + 0.05 - 2\epsilon) - \epsilon(1 + 0.05 - 4\epsilon) \leq x' \leq 1 + 2\epsilon + \epsilon(1 + 4\epsilon)$$

i.e.,

$$-(1 + 0.05 - c_1\epsilon - 4\epsilon^2) \leq x' \leq 1 + 3\epsilon + 4\epsilon^2$$

and so provided ϵ is sufficiently small x' satisfies the same rectangle constraint as x in (62).

Similarly, $y' = -D_0 x$ if $x < 0$, so y' is is negative in this case and takes a minimum value of around $-\frac{10}{11}$ which is small in modulus compared with the boundary of the rectangle and so y' comfortably satisfies the constraints of the rectangle for ϵ small. If $x > 0$ then $y' = -D_1 x$ and so again y' is negative and

$$-2(1 + 4\epsilon) \leq y'.$$

Hence, provided $0.05 - 2\epsilon > 8\epsilon$ this will again lie in the region defined by (62). Thus for small enough $\epsilon > 0$ the region (62) is invariant.

To prove expansion and hence apply results of the preceeding section, section 9.2, we need to know a little more about the dynamics in this region.

Suppose (x, y) lies in the rectangle defined by (62) with $x < 0$. Then the image point (x', y') has $y' = -D_0 x < 0$ and hence the second iterate will have x-coordinate less than $1 - D_0 x + \epsilon|x'|$ which is greater than zero for sufficiently small ϵ as the maximum of x is close to 1.05 so $|D_0 x| \leq \frac{21}{22}$ up to terms of order ϵ. Thus if $x < 0$, the x-coordinate of $f^2(x, y)$ is in $x > 0$.

Note that the linear matrices of the BCNF with $|T_k| \approx 0$ have the form $\begin{pmatrix} 0 & 1 \\ \alpha & 0 \end{pmatrix}$, $\alpha \in \{-D_0, -D_1\}$, suppose we multiply four of these together with $\alpha_1, \ldots, \alpha_4$ as the bottom left coefficients. Straightforward calculation show we obtain

$$\begin{pmatrix} \alpha_2\alpha_4 & 0 \\ 0 & \alpha_1\alpha_3 \end{pmatrix}.$$

Now, the Jacobian of f^4, Df^4, is just a product of BCNF matrices along the orbit, so if $\alpha_1 = -D_0$ then the second iterate is in $x > 0$ and so $\alpha_3 = -D_1$ and similarly for α_2. Thus the only combinations possible are D_1^2 which is close to 4, and $D_0 D_1$ which is close to $-\frac{12}{11}$ or larger. Adding in the order ϵ corrections will not change the fact that thes Jacobian of f^4 is expanding and hence f^4, defined on regions on which it is linear, is an expanding piecewise linear map and has a two-dimensional attractor by Theorem 46. It is straightforward to show that this implies that f itself has a two-dimensional attractor and the result is proved. □

10. Challenges

There are many possible generalizations of th results presented here, and other directions that could have been taken. Here we mention just a few.

10.1. Other classes of maps. In section 1.3 we mentioned Nordmark's square root map [**39**]. Square root maps appear in many contexts in PWS systems [**7**] and so it would be natural to put more attention into the phenomena that can arise in these cases (e.g., [**2**]). Once again though, the issue should be to understand what can be said usefully. It may be that the classes are too large, or the bifurcation phenomena too complicated, to give complete descriptions and therefore the skill is to find useful but finite statements: less is more (cf. section 1.4).

The square root map introduces a particular singularity in the derivative of the map. But in the PWS world it is always possible (at least in principle) to introduce more discontinuities. When is this useful? When is it interesting? What about infinitely many discontinuities? Mathematicians can always think of generalizations, but it is probably best (in general) to allow applications to suggest what is most worthwhile.

The work on the border collision normal form uses the fact that the map is piecewise linear in a number of ways: it means quite a lot of features can be computed by brute force (section 7.2 for example) and it means that iterates of straight lines are straight lines, simplifying geometric arguments considerably (this is key to Buzzi's proofs for piecewise expanding maps in section 9.2). However, apart from Young's theorem (section 8.3) and the original robust chaos argument of [**5**] relatively few results seem to cary over easily. The effect of nonlinear terms and more generally, higher order terms in normal forms, seems an important topic for future research.

The final area, and the one which will occupy the remainder of these lectures, is the effect of higher dimensions. As argued in [**27, 28, 29**] the number of cases can multiply hugely as the dimension of the phase space increases, but there are still examples of results that are either independent of the dimension.

10.2. Higher dimensions: periodic orbits. In section 7.1 it was possible to compute precise criteria for the existence of fixed point and orbits of period two for the border collision normal form in two dimensions, and to give criteria for their stability. This is also possible for the BCNF in $\mathbb{R}^n$, where the normal form is (39) with constant $\mu(1,0,\ldots,0)^T$ and the matrices A_0 and A_1 are in observer canonical form [**6**]

$$A_k = \begin{pmatrix} r_{k1} & 1 & 0 & 0 & ... \\ r_{k2} & 0 & 1 & 0 & ... \\ r_{k3} & 0 & 0 & 1 & ... \\ : & . & . & . & ... \\ r_{kn} & 0 & 0 & ... & 0 \end{pmatrix}, \quad k = 0, 1. \tag{63}$$

Without going through the details, we will state the result, which depends on the *index* of the matrices A_0 and A_1.

Definition 48. The index $\sigma_k^{\pm}$ of the matrix A_k of (63) is defined by σ_k^+ (resp. σ_k^- is the number of real eigenvalues of A_k greater than 1 (resp. less than 1), $k = 0, 1$.

The index gives information about the fixed points and points of period two [**8, 47**].

Theorem 49. *Consider the BCNF in $\mathbb{R}^n$. Let $\mathbf{x}_k$ denote a fixed point of the BCNF in $x < 0$ if $k = 0$ and $x > 0$ if $k = 1$.*

- *If $\sigma_0^- + \sigma_1^-$ is even and $\sigma_0^+ + \sigma_1^+$ is even then $\mathbf{x}_0$ and $\mathbf{x_1}$ exist for different signs of μ and there are no period two orbits if $\mu \neq 0$.*
- *If $\sigma_0^- + \sigma_1^-$ is even and $\sigma_0^+ + \sigma_1^+$ is odd then $\mathbf{x}_0$ and $\mathbf{x_1}$ exist for the same sign of μ and there are no period two orbits if $\mu \neq 0$.*
- *If $\sigma_0^- + \sigma_1^-$ is odd and $\sigma_0^+ + \sigma_1^+$ is even then $\mathbf{x}_0$ and $\mathbf{x_1}$ exist for different signs of μ and an orbit of perioi two orbits exists for one sign of μ.*
- *If $\sigma_0^- + \sigma_1^-$ is odd and $\sigma_0^+ + \sigma_1^+$ is odd then $\mathbf{x}_0$ and $\mathbf{x_1}$ and an orbit of period two orbits exists for one sign of μ.*

If $\mathbf{x}_0$ and $\mathbf{x}_1$ both exist for the same sign of μ then $\sigma_0^+ + \sigma_1^+$ is odd and so at least one of them is non-zero. Hence at least one of the matrices A_0 and A_1 has an eigenvalue with modulus greater tha one.

Corollary 50. *The BCNF cannot have coexisting stable fixed points.*

In fact, with a little more work it can be shown that if the period two orbit if it is stable then the fixed point that coexists with it is unstable [**47**].

Most of the analysis of section 7.2 was actually independent of the dimension of phase space, so the analysis can be used to describe periodic orbits, mode locking and shrinking points in higher dimensional systems. See [**47**] for details.

10.3. Higher dimensions: n-dimensional attractors. The results of Buzzi and Tsujii described in section 9.2 hold in $\mathbb{R}^n$, $n > 2$, but with a slight caveat: the attractors may not have topological dimension n, i.e., they may not contain open sets, though they always have Hausdorff dimension n and topological dimension n on a generic set of parameters. This makes it possible to prove results analogous to Theorem 47 but with that technical restriction.

Theorem 51. [**25**] *There exists an open set $U \subset \mathbb{R}^{2n}$ such that if*

$$(r_{01}, \ldots, r_{0n}, r_{11}, \ldots, r_{1n}) \in U$$

then the border collision normal form in $\mathbb{R}^n$ with matrices (63) *has a stable fixed point if $\mu < 0$ and an attractor with Hausdorff dimension equal to n if $\mu > 0$. This attractor has topological dimension equal to n generically in U.*

It appear harder to generalize Young's results of section 8.3, though a recent result of Zhang [**53**] extends her result to $\mathbb{R}^3$ with two-dimensional unstable manifolds. It would be very interesting to see this extended to higher dimension, and higher dimensional unstable manifolds.

Bibliography

[1] Alligood, K.T., Sauer, T.D. & Yorke, J.A. (1996) *Chaos: An Introduction to Dynamical Systems*, Springer.

[2] Avrutin, V., Dutta, P.S., Schanz, M. & Banerjee, S. (2010) Influence of a square-root singularity on the behavior of piecewise smooth maps, *Nonlinearity* **23** 445–463.

[3] Avrutin, V., Schanz, M. & Banerjee, S. (2006) Multi-parametric bifurcations in a piecewise-linear discontinuous map, *Nonlinearity* **19** 1875–1906.

[4] Banerjee, S. & Grebogi, C. (1999) Border Collision Bifurcations in Two-Dimensional Piecewise Smooth Maps, *Phys. Rev. E* **59**, 4052–4061.

[5] Banerjee, S., Yorke, J.A. & Grebogi, C. (1998) Robust Chaos, *Phys. Rev. Lett.* **80**, 3049–3052.

[6] di Bernardo, M. (2003) Normal forms of border collision in high dimensional non-smooth maps, *Proceedings IEEE ISCAS 2003*, **3**, 76–79.

[7] di Bernardo, M., Budd, C., Champneys, A.R., & Kowalczyk, P. (2008) *Piecewise-smooth Dynamical Systems: Theory and Applications*, Applied Mathematical Sciences, Vol. 163, Springer, London.

[8] di Bernardo, M., Feigin, M.I., Hogan, S.J., & Homer, M.E. (1999) Local Analysis of C-Bifurcations in n-Dimensional Piecewise-Smooth Dynamical Systems, *Chaos, Solitons & Fractals* **10** 1881–1908.

[9] di Bernardo, M., Montanaro, U. & Santini, S. (2011) Canonical Forms of Generic Piecewise Linear Continuous Systems, *IEEE Trans. Automatic Control* **56**, 1911–1915.

[10] Buzzi, J. (1999) Absolutely continuous invariant measures for generic multi-dimensional piecewise affine expanding maps, *Int. J. Bifn. & Chaos* **9**, 1743–1750.

[11] Buzzi, J. (2001) Thermodynamic formalism for piecewise invertible maps: Absolutely continuous invariant measures as equilibrium states, in *Smooth Ergodic Theory and Its Applications*, eds. Katok, A., de la Llave, R., Pesin, Y. & Weiss, H., AMS Proc. Symp. Pure Math. **69**, 749–784.

[12] Devaney, R. (1989) *An Introduction to Chaotic Dynamical Systems (Second Edition)*, Addison-Wesley, Redwood City.

[13] Do, Y. & Lai, Y.-C. (2008) Multistability and arithmetically period-adding bifurcations in piecewise smooth dynamical systems, *Chaos* **18** 043107.

[14] Dobrynskiy, V.A. (1999) On attractors of piecewise linear 2-endomorphisms, *Nonlinear Anal.* **36**, 423–455.

[15] Gambaudo, J.M. (1987) *Ordre, désordre, et frontière des systèmes Morse-Smale*, Thesis, Université de Nice.

[16] Gambaudo, J.M., Glendinning, P. & Tresser, T. (1986) The gluing bifurcation: I. symbolic dynamics of the closed curves, *Nonlinearity* **1** 203–214.

[17] Gambaudo, J.M., Glendinning, P. & Tresser, T. (1987) Stable cycles with complicated structure, in *Instabilities and Nonequilibrium Structures* Eds. Tirapegui, E. & Villarroel, D., Reidel, Dordrecht.

[18] Gambaudo, J.M. & Tresser, C. (1985) Dynamique regulière ou chaotique. Applications du cercle ou de l'intervalle ayant une discontinuité, C.R. Acad. Sci. (Paris) Série I **300** 311–313.

[19] Gardini, L. (1992) Some global bifurcations of two-dimensional endomorphisms by use of critical lines, *Nonlinear Anal.* **18**, 361–399.

[20] Gardini, L., Avrutin, V. & Sushko, I. (2014) Codimension-2 border collision bifurcations in one-dimensional discontinuous piecewise smooth maps., *Int. J. Bif. & Chaos* **24** 1450024.

[21] Glendinning, P. (1985) *Homoclinic Bifurcations in Ordinary Differential Equations*, a Fellowship Dissertation, King's College, Cambridge.

[22] Glendinning, P. (2011) Invariant measures for the border collison normal form, MIMS preprint, Manchester.

[23] Glendinning, P. (2014) Attractors with dimension n for open sets of parameter space in the n-dimensional border collision normal form, *Int. J. Bif. & Chaos* **24** 1450164.
[24] Glendinning, P. (2014) Renormalization for the boundary of chaos in piecewise monotonic maps with a single discontinuity, *Nonlinearity* **27** R143–R162.
[25] Glendinning, P. (2015) Bifurcation from stable fixed point to N-dimensional attractor in the border collision normal form, *Nonlinearity* **28** 3457–3464.
[26] Glendinning, P. (2016) Bifurcation from stable fixed point to two-dimensional attractor in the border collision normal form, *IMA J. Appl. Math.* doi: 10.1093/imamat/hxw001.
[27] Glendinning, P. (2016) Less is More I: a pessimistic view of piecewise smooth bifurcation theory, preprint.
[28] Glendinning, P. (2016) Less is More II: an optimistic view of piecewise smooth bifurcation theory, preprint.
[29] Glendinning, P. & Jeffrey, M.R. (2015) Grazing-sliding bifurcations, border collision maps and the curse of dimensionality for piecewise smooth bifurcation theory, *Nonlinearity* **28** 263–283.
[30] Glendinning, P. & Wong, C.H. (2011) Two-dimensional attractors in the border-collision normal form, *Nonlinearity* **24**, 995–1010.
[31] Granados, A., Alseda, L. & Krupa, M. (2015) The period adding and incrementing bifurcations: from rotation theory to applications, arXiv:1407.1895v3.
[32] Guckenheimer, J. & Williams, R.F. (1979) Structural stability of Lorenz attractors, *Publ. Math. IHES* **50** 59–72.
[33] Jonker, L. & Rand, D.A. (1981) Bifurcations in one-dimension. I. The nonwandering set, *Invent. Math.* **62** 347–365.
[34] Keener, J.P. (1980) Chaotic behavior in piecewise continuous difference equations, *Trans. Amer. Math. Soc.*, **261** 589–604.
[35] de Melo, W. & van Strien, S. (1993) *One-Dimensional Dynamics*, Springer, Berlin.
[36] Mira, C., Gardini, L., Barugola, A. & Cathala, J.C. (1996) *Chaotic Dynamics in Two-Dimensional Noninvertible Maps*, World Scientific, Singapore.
[37] Misieurewicz, M. (1980) Strange attractors for the Lozi mapping, *Ann. NY Acad. Sci.*, **80** 348–358.
[38] Milnor, J. & Thurston, W. (1988) On iterated maps of the interval, in *Dynamical Systems* Ed. Alexander, J.C., LNM 1342 465–563, Springer Berlin Heidelberg.
[39] Nordmark, A.B. (1997) Universal limit mapping in grazing bifurcations, *Phys. Rev. E.*, **55** 266–270.
[40] Nusse, H.E., Ott, E. & Yorke, J.A. (1994) Border-collision bifurcations: an explanation for observed bifurcation phenomena, *Phys. Rev. E* **49**, 1073—1076.
[41] Nusse, H.E. & Yorke, J.A. (1992) Border-collision bifurcation including 'period two to period three' for piecewise-smooth systems, *Physica D* **57**, 39–57.
[42] Palis, J. & de Melo, W. (1982) *Geometric Theory of Dynamical Systems*, Springer.
[43] Rhodes, F. & Thompson, C.L. (1986) Rotation numbers for monotone functions on the circle, *J. London Math. Soc.* **34** 360–368.
[44] Rhodes, F. & Thompson, C.L. (1991) Topologies and rotation numbers for families of monotone functions on the circle, *J. London Math. Soc.* **43** 156–170.
[45] Simpson, D.J.W. (2014) Sequences of Periodic Solutions and Infinitely Many Coexisting Attractors in the Border-Collision Normal Form, *Int. J. Bif. & Chaos* **24**:1430018.
[46] Simpson, D.J.W. (2014) On the Relative Coexistence of Fixed Points and Period-Two Solutions near Border-Collision Bifurcations, *Appl. Math. Lett.* **38** 162–167.
[47] Simpson, D.J.W. (2016) Border-Collision Bifurcations in $\mathbb{R}^N$, to appear in *SIAM Rev.*
[48] Simpson, D.J.W. & Meiss, J.D. (2009) Shrinking Point Bifurcations of Resonance Tongues for Piecewise-Smooth, Continuous Maps, *Nonlinearity* **22** 1123–1144.
[49] Simpson, D.J.W. & Meiss, J.D. (2010) Resonance near Border-Collision Bifurcations in Piecewise-Smooth, Continuous Maps, *Nonlinearity* **23** 3091–3118.

[50] Tsujii, M. (2001) Abolutely continuous invariant measures for expanding piecewise linear maps, *Invent. Math.* **143**, 349–373.
[51] Williams, R.F. (1979) The structure of Lorenz attractors, *Publ. Math. IHES* **50** 73–99.
[52] Young, L.S. (1985) Bowen-Ruelle measures for certain piecewise hyperbolic maps, *Trans. Amer. Math. Soc.* **287**, 41–48.
[53] Zhang, X. (2016) Sinai-Ruelle-Bowen measures for piecewise hyperbolic maps with two directions of instability in three-dimensional spaces, *Discrete Cont. Dyn. Syst.* **36** 2873–2886.

An Introduction to the Dynamics of Piecewise Smooth Flows

by

Mike R. Jeffrey

University of Bristol / Nonsmoothland

mike.jeffrey@bristol.ac.uk

Abstract. Preliminary notes for the Advanced Course on Piecewise Smooth Dynamical Systems 11-15 April 2016 at the CRM, Barcelona, part of the CRM Intensive Research Program in Nonsmooth Dynamics.

1. The Geometrical Theory of Piecewise Smooth Dynamical Systems

This course is about the geometry of piecewise smooth dynamical systems. The solutions of ordinary differential equations can be pictured as trajectories (or *orbits*) in space (the space of whatever independent variables vary under the differential equations). Those trajectories are organized by various singularities, separatrices, and invariant sets, whose geometry can be studied in great generality. A loss of continuity in the differential equations greatly adds to the richness of that geometry.

Piecewise smooth equations are smooth (or at least differentiable) except at isolated thresholds called *switching surfaces*. The solutions of those equations should be continuous, but may 'kink' at a switching surface, becoming non-differentiable, and possibly non-unique.

Nonsmooth dynamics in a nutshell

There are really just a few basic elements you need to build up an understanding of piecewise smooth dynamics. First the vector field.

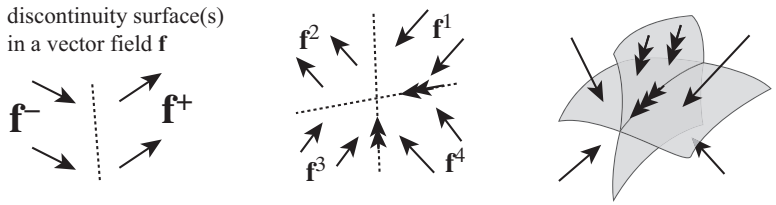

The vector field is discontinuous along certain thresholds. A *sliding* vector field may be induced on those thresholds.

Locally, solutions take certain simple forms. Away from the thresholds they will be smooth (or at least twice differentiable) unique curves. At the thresholds, however, they might cross through the discontinuity, or they might slide along it. We'll learn how to find such solutions.

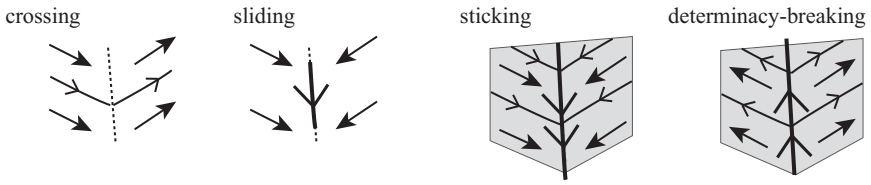

The threshold has a lower dimension than the surrounding space, so if sliding occurs, the number of dimensions the solutions occupy changess. This results in non-uniqueness.

When sliding is:

- attractive, solutions stick to the threshold, and then many solutions will all evolve onto the same trajectory in forward time. The history of any point (shaded in the 3^{rd} figure above) in attractive sliding is therefore non-unique — this is common in physics as mechanical 'sticking'.
- repulsive, solutions escape a threshold, and then the sliding solution has many possible future trajectories (shaded in the 4^{th} figure above). The future of any point in repulsive sliding is therefore non-unique — determinacy is broken.

The only other things we *must* add to these are the elementary singularities. In differentiable vector fields the commonly encountered singularity is a steady state or 'equilibrium'. At a discontinuity we encounter a new kind of steady state, a *sliding equilibrium*.

But in piecewise smooth systems there is much more to local dynamics than this. It is often the transient (i.e., non-stationary) dynamics that creates the most interesting effects. Instead we must consider stationarity relative to the threshold, i.e., *tangency* of solutions to the threshold.

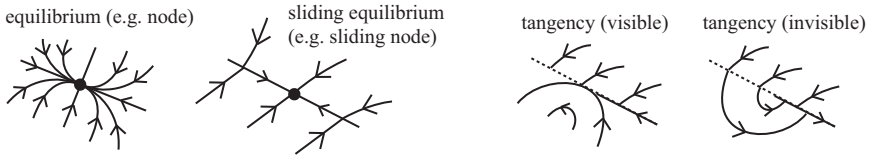

Keep these few elements in mind during this course, and you'll soon gain some intuition for the – at first strange – terrain of what we have come to call informally: *Nonsmoothland*.

2. History & Applications

Ancient History

The theory of the dynamics of smoothly evolving systems has come a long way in the last 100 years or so. All the interesting stuff happens because of nonlinearity. Loosely, this means the equations depend in a nonlinear way on certain unknowns. More important is what this means for the system's behaviour: if we change some variable or parameter in a nonlinear system, then its behaviour may not respond proportionally (unlike a linear system),

and we obtain phenomena like bifurcations, chaos and complexity. Continuity and differentiability of the equations have been vital to dealing with nonlinearity.

Systems which are *not* differentiable or are *not* continuous have been studied as long as there have been dynamical systems. Collisions between rigid bodies result in a discontinuous jump in contact force. Electrical switches discontinuously turn on/off the current in a circuit. People in societies discontinuously switch from following one rule or trend to another.

Discontinuities are often involved when different objects or systems interact.

At a point where the equations are not differentiable, and moreover not even continuous, almost nothing from standard 'smooth' dynamical systems theory can be applied.

You're more familiar with discontinuities than you may realise. One of the most familiar forces to us is also one of the most complex, and a prime example of how discontinuities complicate one of the most fundamental forces of interaction: friction.

The resistance force of friction between two rigid bodies, caused by contact between rough unlubricated contact surfaces, has a long and contentious history. It goes way back to the greek philosophers, but let's start with the seeds of the modern theory:

- in 1500 Leonardo da Vinci shows that friction resistance depends on load, but not on contact area,
- in 1699 Amontons shows that friction depends on surface roughness,
- in 1700 Desagulier shows that friction does *not* depend on surface roughness,
- in 1750 Euler shows that static friction force > kinetic friction force,
- in 1785 Coulomb describes friction as the now commonly adopted

$$m\ddot{x} = -\mu F_N$$

where m is the mass of an object with displacement x, moving at speed $\dot{x}$, on a surface moving at speed v, creating a normal reaction force F_N on the object. The quantity μ is the coefficient of friction, given for some constant μ_k by

$$\mu = \mu_k \operatorname{sign}(\dot{x} - v) = \mu_k \times \begin{cases} +1 & \text{if} \quad \dot{x} > v \ , \\ -1 & \text{if} \quad \dot{x} < v \ . \end{cases}$$

We have in friction our first discontinuous system. It says that as an object changes from slipping right ($\dot{x} > v$) on a surface to slipping left ($\dot{x} < v$), the friction force jumps abruptly between $-\mu_k F_N$ and $+\mu_k F_N$. What happens in between? What complications does the jump introduce into the dynamics? These are the questions of 'piecewise smooth' dynamical systems theory.

The other very common piecewise smooth system, which you probably encountered back in highschool, is a collision. Take a block of mass m, with position x, driven by a force f, colliding with a wall at position c,

$$m\ddot{x} = f \quad : \quad \dot{x} \mapsto -r\dot{x} \text{ if } x = c \ \& \ \dot{x} > 0 \, ,$$

where r is the coefficient of restitution. This is a *hybrid* or *impact* system, composed of a differential equation (left part) and a discrete impact map (right part). We won't study hybrid systems here. However, we can think of the restitution map $\dot{x} \mapsto -r\dot{x}$ as representing a jump through a continuous impact phase, for example introducing a large wall stiffness k,

$$m\ddot{x} = f - k\,\mathrm{step}(x-c) \, , \quad \mathrm{step}(x-c) = \begin{cases} 1 & \text{if} \quad x > c \, , \\ 0 & \text{if} \quad x < c \, . \end{cases}$$

This now has continuous time solutions that are non-differentiable at $x = c$.

History & Applications of Piecewise Smooth Dynamics

Serious attempts to develop the mathematics of dynamical systems with discontinuities go back to the 1930s (at least). They are worth a look, because this is still a young field of research, both in theory and applications, and the ideas in these texts are still central to our thinking today:

- 1934 Kulebakin [**9**]: vibration control for aircraft DC generators.
- 1934 Nikolzky [**12**]: boat rudder as switching controllers.
- 1937 Andronov, Vitt, Khaikin [**1**]: numerous examples are studied of mechanical engines and circuits, analyzing their dynamics and stability.
- 1953 Irmgard Fluegge-Lotz [**5**]: proposes discontinuous control to design missile aiming technologies.
- 1974- Vadim Utkin [**18, 19, 20**][1]: develops a general design method for electronic switching ("variable structure control"), an essential step to our modern approach to solving discontinuous systems.
- 1988 Aleksei Federovich Filippov [**4**][2]: develops the first substantial dynamical theory of "differential equations with discontinuous righthand sides".
- 1990- Marco Antonio Teixeira [**14, 15, 16, 17**][3]: shows how ideas from singularity theory can be applied to study the geometry of flows near discontinuities.
- The modern era: theory (this course) and applications (to electronics, mechanics, especially power control, but also to cell mitosis, economics, predator-prey, climate, ... see guest lectures).

[1] also with more recent books.

[2] representing a substantial Russian literature going back half a century.

[3] note I've written 1990- but one of these references is earlier. Before this Teixeira phrased this work as 'divergent diagrams' or 'pairings of fields and functions' to evade the early skepticism towards discontinuous dynamical systems. Teixeira now leads one of the most fervent and successful communities in geometric piecewise smooth dynamical theory.


Irmgard Fluegge-Lotz


Vadim I. Utkin

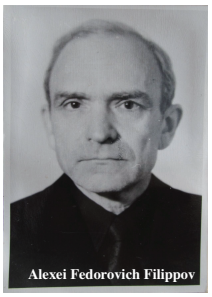
Alexei Fedorovich Filippov


Marco Antonio Teixeira

Content (and things we won't cover that you should ask around about)

We will study an ordinary differential equation $\dot{\mathbf{x}} = \mathbf{f}(\mathbf{x})$, where the vector field $\mathbf{f}$ is smooth almost everywhere, but jumps in value at a surface Σ that partitions space into distinct open regions.

The solutions $\mathbf{x}(t)$ will be continuous curves. Filippov set out methods for solving piecewise smooth differential equations, and these have been adopted as standard. Recently, however, with the discovery of new singularities and singular phenomena, we have understood that more is needed. This series of lectures will provide you with the tools to delve more deeply into the world of nonsmooth dynamics.

We will focus on:

- geometry of piecewise smooth vector fields,
- general methods for solving and analysing them,
- their key notions of stability and bifurcations.

Some important current topics that we will not cover, but you may wish to pursue, include:

- special cases: e.g., piecewise linear or continuous non-differentiable vector fields, hybrid/impact systems;
- modeling non-idealities: e.g., smoothing, noise, delay, etc., and the various types of 'regularization', a word you'll hear a lot as an open problem in current piecewise smooth systems.

You may also want to look into simulation methods: piecewise smooth systems require special consideration when simulating. There are event detection routines built into Matlab and Mathematica. There are ways of making continuation tools like AUTO or MatCont work with discontinuities (often by smoothing them out). Filippov's solving methods (we'll discuss these in the course) have even been built into tools like Mathematica. But these take in to account very little of the current state of the theory. Use them all with care and critical judgement.

3. Inclusions & Combinations

Our first task is to learn how to turn discontinuous vector fields into well formed differential equations, and then to learn how to solve them.

Discontinuous vector fields

We start with a vector $\mathbf{x}=(x_1, x_2, ..., x_n) \in \mathbb{R}^n$, of the variables $x_1, x_2, ..., x_n$. Its time dependence is described by vector fields $\mathbf{f}^i$ such that

$$\dot{\mathbf{x}} = \mathbf{f}^i(\mathbf{x}) \qquad \text{on} \qquad \mathbf{x} \in \mathcal{R}_i$$

or, in components,

$$(\dot{x}_1, \dot{x}_2, ..., \dot{x}_n) = \left(f_1^i, f_2^i, \ldots, f_n^i\right).$$

The index i is taken from a set of labels identifying the regions $\mathcal{R}_i$.

Example 1. The figure shows a system with 2 regions, 4 regions, or 2 regions where the boundary between them is a corner. For a discontinuous system with 4 regions we could label the indices $i = 1, 2, 3, 4$, or $i = ++, +-, -+, --$.

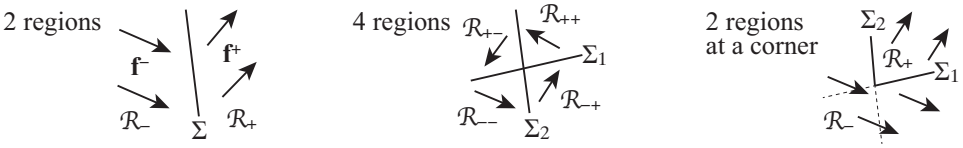

The inclusion

On the boundary Σ, the variation $\dot{\mathbf{x}}$ is not defined. To extend $\dot{\mathbf{x}} = \mathbf{f}^i(\mathbf{x})$ to the boundary Σ, write

$$\dot{\mathbf{x}} \in \mathcal{F} \quad \text{where} \quad \mathbf{f}^i(\mathbf{x}) \in \mathcal{F} \quad \forall\, i \;:\; \lim_{\mathbf{x}' \to \mathbf{x}} \mathbf{f}(\mathbf{x}') = \mathbf{f}^i(\mathbf{x})$$

where $\mathcal{F}$ is set-valued for $\mathbf{x} \in \Sigma$, and $\mathcal{F} = \mathbf{f}^i(\mathbf{x})$ for $\mathbf{x} \in \mathcal{R}_i$.

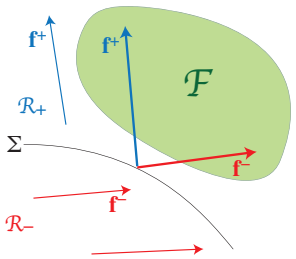

FIGURE 1. The convex set $\mathcal{F}$ at a switching surface Σ between vector fields $\mathbf{f}^+$ on region $\mathcal{R}_+$ and $\mathbf{f}^-$ on region $\mathcal{R}_-$.

Theorem 2 (Existence of solutions)**.** *Solutions of $\dot{\mathbf{x}} = \mathcal{F}$ exist if $\mathcal{F}(\mathbf{x})$ is non-empty, bounded, closed, convex, and upper semicontinuous*. [Filippov 1988 Thm1 p77]*

*Upper semicontinuity is an extension of the notion of continuity for sets. It says $\sup_{b \in \mathcal{F}(\mathbf{x})} \rho(b, a) \to 0$ as $p' \to p$ for $a \in \mathcal{F}(p')$ and $b \in \mathcal{F}(p)$ where $\rho(b, a) = \inf_{a \in A,\, b \in B} |a - b|$ with $|a - b|$ the distance between a & b.

So if solutions to the vector field (the flow) exist, what do they look like?

A classic example: Coulomb friction

Example 3. Consider a block, resting on a surface that moves at velocity v, attached to a spring of stiffness k and a damper with a coefficient c.

$$\text{force} = m\ddot{x} = -c\dot{x} - kx - \lambda F_N \ , \quad \lambda = \begin{cases} +1 & \text{if} \quad \dot{x} > v & \text{“slip right”} \\ +1 & \text{if} \quad \dot{x} < v & \text{“slip left”} \end{cases}$$

Written as a two-dimensional ODE this is

$$\dot{x} = y \ , \qquad \dot{y} = -\frac{c}{m}y - \frac{k}{m}x - \lambda\frac{F_N}{m}$$

The equilibrium at $(x, y) = (-\lambda F_N/k, 0)$ is a focus. Motion along $\dot{x} = v$ represents sticking (i.e., the block and surface stick together).

The block can go from left slip to right slip (or vice versa), from right/left slip to stick and back to slip. All trajectories are attracted to the equilibrium.

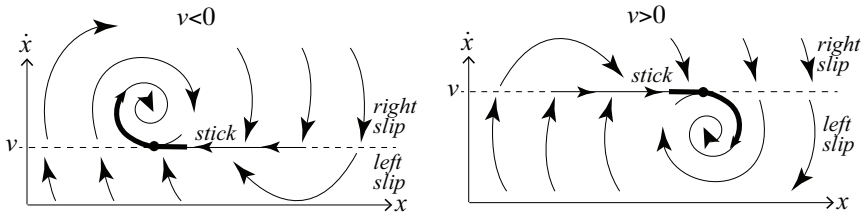

We need a method to describe sticking (on $y = v$). This comes from solving the inclusion.

The switching multiplier λ and switching function σ

Take a single switch at a threshold $\sigma(\mathbf{x}) = 0$, in the bimodal system

$$\dot{\mathbf{x}} = \begin{cases} \mathbf{f}^+(\mathbf{x}) & \text{if} \quad \sigma(\mathbf{x}) > 0 \\ \mathbf{f}^-(\mathbf{x}) & \text{if} \quad \sigma(\mathbf{x}) < 0 \end{cases}$$

in terms of a **switching function** $\sigma : \mathbb{R}^n \mapsto \mathbb{R}$, so $\Sigma = \{\mathbf{x} \in \mathbb{R}^n : \sigma(\mathbf{x}) = 0\}$.

We can re-write this as

$$\dot{\mathbf{x}} = \mathbf{f}(\mathbf{x}; \lambda)$$

replacing each index i with a unique **switching multiplier** λ, such that

$$\mathbf{f}^+(\mathbf{x}) = \mathbf{f}(\mathbf{x}; +1), \ \mathbf{f}^-(\mathbf{x}) = \mathbf{f}(\mathbf{x}; -1), \ \text{i.e.,} \ i = \pm \ \Leftrightarrow \ \lambda = \pm 1.$$

We then define

$$\begin{array}{ll} \lambda = \text{sign}\,(\sigma(\mathbf{x})) & \text{for} \quad \sigma(\mathbf{x}) \neq 0 \\ \lambda \in (-1, +1) & \text{for} \quad \sigma(\mathbf{x}) = 0 \ . \end{array}$$

Combinations

The *combination* $\mathbf{f}(\mathbf{x}; \lambda)$ is differentiable with respect to $\mathbf{x}$ and λ. The discontinuity is now encoded in the multiplier λ.

E.g., Convex combination (Filippov 1988 *Def 4a p50-52*)

$$\dot{\mathbf{x}} = \frac{1+\lambda}{2}\mathbf{f}^+(\mathbf{x}) + \frac{1-\lambda}{2}\mathbf{f}^-(\mathbf{x})$$

E.g., Non-convex combination

$$\dot{\mathbf{x}} = \frac{1+\lambda}{2}\mathbf{f}^+(\mathbf{x}) + \frac{1-\lambda}{2}\mathbf{f}^-(\mathbf{x}) + (\lambda^2-1)\mathbf{g}(\mathbf{x})$$

In both examples $\mathbf{f}(\mathbf{x};\pm 1) \equiv \mathbf{f}^{\pm}(\mathbf{x})$.

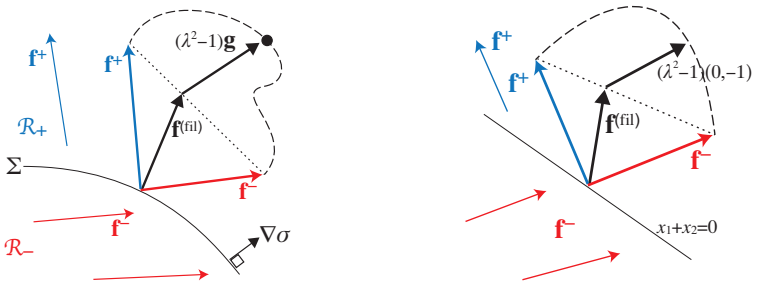

FIGURE 2. The Filippov convex combination (dotted line) and a non-convex combination (dashed curve). The righthand figure shows the quadratic example below.

Example 4. Consider at the point $(x_1, x_2) = (0, 0)$ with a switching multiplier $\lambda = \text{sign}(x_1 + x_2)$, the vector field

$$\mathbf{f}(\mathbf{x};\lambda) = \tfrac{1}{2}(1+\lambda)(2,1) + \tfrac{1}{2}(1-\lambda)(-1,2) + (\lambda^2-1)(0,-1)$$

This switches between $(2, 1)$ and $(-1, 2)$ across $\sigma = x_1 + x_2$.

The term $(\lambda^2 - 1)\mathbf{g}(\mathbf{x})$ is called **hidden**, because it vanishes for $\mathbf{x} \notin \Sigma$ (when $\lambda = \pm 1$). (In fact it is so hidden that you won't find it in most other courses or texts on piecewise smooth dynamics to date).

We'll generalize this for more complex switching later.

4. Types of dynamics

The inclusion... solutions

Filippov's theory tells us that a family of solutions of the equations, the flow, exists. What do the solutions look like?

We concatenate smooth segments of solutions of $\dot{\mathbf{x}} = \mathcal{F}$ in the regions $\mathcal{R}_i$ and on Σ, to form continuous curves that preserve the direction of time.

Definition 5. An **orbit** of the piecewise smooth system through a point $\mathbf{x}_0$ is a maximal ('longest possible') concatenation of trajectories through $\mathbf{x}_0$.

We can solve the equations $\dot{\mathbf{x}} = \mathbf{f}^i(\mathbf{x})$ for the flow inside the regions $\mathcal{R}_i$.

We need a way to find the flow on Σ.

A family of solutions parameterized by initial conditions $\mathbf{x}_0$ forms a flow $\Phi_t(\mathbf{x}_0)$ defined by

$$\mathbf{x}(t) = \Phi_t(\mathbf{x}_0) \quad : \quad \frac{d}{dt}\Phi_t(\mathbf{x}_0) = \mathbf{f}\left(\Phi_t(\mathbf{x}_0);\lambda\right) \ , \quad \Phi_0(\mathbf{x}_0) = \mathbf{x}_0 \ .$$

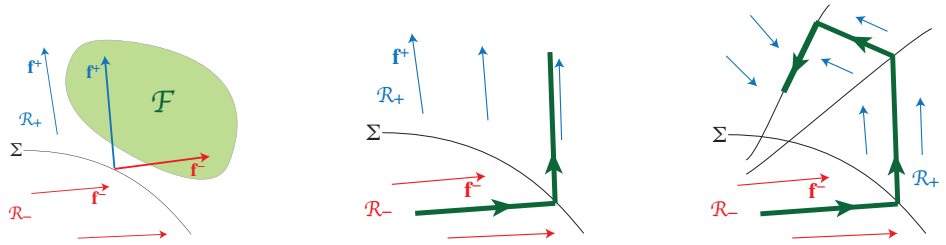

FIGURE 3. The inclusion (left), and a crossing solution (middle). We can concatenate over many discontinuities (right).

We may write the constituent flows in the regions $\mathcal{R}_+$, $\mathcal{R}_-$, as Φ_t^+, Φ_t^-, where

$$\frac{d}{dt}\Phi_t^{\pm}(\mathbf{x}_0) = \mathbf{f}\left(\Phi_t(\mathbf{x}_0); \pm 1\right) \ .$$

Crossing and Sliding

Let Φ_t^+, Φ_t^-, Φ_t^Σ, be the flows on $\mathcal{R}_+$, $\mathcal{R}_-$, Σ, respectively. At Σ an orbit can:

- **cross** through Σ. To cross from $\mathcal{R}_-$ to $\mathcal{R}_+$ at a point $\mathbf{x}_1 = \Phi_\tau^-(\mathbf{x}_0) \in \Sigma$ where $\sigma(\mathbf{x}_1) = 0$ at time τ, it is *necessary* that $\dot\sigma(\Phi^-_{\tau-\delta t}(\mathbf{x}_0))$ and $\dot\sigma(\Phi^+_{\tau+\delta t}(\mathbf{x}_0))$ have the same sign, where δt is a small increment of time. Since $\dot\sigma = \dot{\mathbf{x}}\cdot\nabla\sigma = \mathbf{f}\cdot\nabla\sigma$, crossing requires
$$(\mathbf{f}^+\cdot\nabla\sigma)(\mathbf{f}^-\cdot\nabla\sigma) > 0 \quad \text{on} \quad \Sigma$$
- **slide** along Σ, where the flow Φ_t^Σ must satisfy
$$\mathbf{x}(t) = \Phi_t^\Sigma(\mathbf{x}_0) \quad : \quad \frac{d}{dt}\sigma(\mathbf{x}(t)) = 0 \quad \text{on} \quad \Sigma$$

In the convex combination, sliding occurs where $(\mathbf{f}^+\cdot\nabla\sigma)(\mathbf{f}^-\cdot\nabla\sigma) < 0$, and satisfies

$$0 = \dot\sigma = \dot{\mathbf{x}}\cdot\nabla\sigma = \left\{\frac{1+\lambda}{2}\mathbf{f}^+(\mathbf{x}) + \frac{1-\lambda}{2}\mathbf{f}^-(\mathbf{x})\right\}\cdot\nabla\sigma$$

$$\Rightarrow \quad \lambda = \lambda^\Sigma \equiv \frac{(\mathbf{f}^- + \mathbf{f}^+)\cdot\nabla\sigma}{(\mathbf{f}^- - \mathbf{f}^+)\cdot\nabla\sigma} \quad \Rightarrow \quad \dot{\mathbf{x}} = \frac{(\mathbf{f}^-\cdot\nabla\sigma)\mathbf{f}^+ - (\mathbf{f}^+\cdot\nabla\sigma)\mathbf{f}^-}{(\mathbf{f}^- - \mathbf{f}^+)\cdot\nabla\sigma}$$

Example 6.
(i) An orbit crosses from $\mathcal{R}_-$ to $\mathcal{R}_+$ at time τ,

$$\mathbf{x}(t) = \begin{cases} \Phi_t^-(\mathbf{x}_0) & \text{if} \quad t < \tau \\ \Phi_{t-\tau}^+(\mathbf{x}_1) & \text{if} \quad t > \tau \end{cases}$$

(ii) An orbit in $\mathcal{R}_-$ **stick**s to Σ at time τ:

$$\mathbf{x}(t) = \begin{cases} \Phi_t^-(\mathbf{x}_0) & \text{if} \quad t < \tau \\ \Phi_{t-\tau}^\Sigma(\mathbf{x}_1) & \text{if} \quad t > \tau \end{cases}$$

where $\Phi_t^\pm$ are the flows of $\dot{\mathbf{x}} = \mathbf{f}^\pm$, and $\mathbf{x}_1 = \phi_\tau^-(\mathbf{x}_0)$.

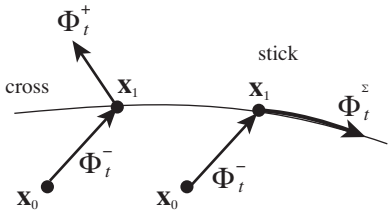

FIGURE 4. Examples of crossing, sliding, and sticking.

Crossing and Sliding – examples I

Example 7 (crossing). Consider the system

$$(\dot{x}_1, \dot{x}_2) = (2 + \lambda, 1) \ , \qquad \lambda = \text{sign}(x_1),$$

so $\sigma(\mathbf{x}) = x_1$. Let $\tau > 0$.

There is an obvious crossing solution

$$x_1(t) = (t - \tau)(2 + \text{sign}(t - \tau)) \ , \qquad x_2(t) = t + x_{20}.$$

Does sliding ($\dot{\sigma} = \sigma = 0$) occur on Σ ($x_1 = 0$)? To find out solve

$$\dot{\sigma} = \dot{x}_1 = 0 \quad \Rightarrow \quad \lambda = -2 \notin (-1, +1) \quad \Rightarrow \quad \text{no sliding.}$$

The value of λ that would give sliding along Σ lies outside of the allowed range $(-1, +1)$, so no sliding solutions exist.

Example 8 (sliding). Consider the system

$$(\dot{x}_1, \dot{x}_2) = (-\lambda, 1) \ , \qquad \lambda = \text{sign}(x_1),$$

so $\sigma(\mathbf{x}) = x_1$. Let $\tau > 0$.

Crossing is impossible, as both vector fields points towards Σ ($x_1 = 0$).

So surely the only possible motions is sliding? Solve

$$\dot{\sigma} = \dot{x}_1 = 0 \quad \Rightarrow \quad \lambda = 0$$

which lies inside $(-1, +1)$, and substituting back into the original system

$$\Rightarrow \quad (\dot{x}_1, \dot{x}_2) = (0, 1)$$

A sticking orbit is given, for example, by

$$x_1(t) = (\tau - t\,\text{sign}(\tau))\,\text{step}(\tau - t) \ , \qquad x_2(t) = t + x_{20}.$$

The local singularities

Any of the constituent systems $\dot{\mathbf{x}} = \mathbf{f}^{\pm}(\mathbf{x})$ may have an equilibrium where $\mathbf{f}^{\pm}(\mathbf{x}) = 0$, or in combination notation, where $\dot{\mathbf{x}} = \mathbf{f}(\mathbf{x}; \pm 1) = 0$.

Two new singularities arise at a (simple) switching surface:

(i) Sliding ("pseudo") equilibria are points where $\mathbf{f}^{\pm}(\mathbf{x}) \neq 0$ but

$$\mathbf{f}(\mathbf{x}; \lambda) = 0 \ \text{ with } \ \sigma(\mathbf{x}) = 0$$

In the convex combination these happen where $\mathbf{f}^{\pm}$ are in opposition, since

$$\mathbf{f}^+ = -\mu\mathbf{f}^- \quad \Rightarrow \quad \dot{\mathbf{x}} = \frac{(\mathbf{f}^- \cdot \nabla\sigma)\mathbf{f}^+ - (\mathbf{f}^+ \cdot \nabla\sigma)\mathbf{f}^-}{(\mathbf{f}^- - \mathbf{f}^+) \cdot \nabla\sigma} = 0$$

for some $\mu > 0$.

(ii) Tangencies of the vector field to Σ are points where:

$$\mathbf{f}^+ \cdot \nabla\sigma = 0 \quad \Rightarrow \quad \dot{\mathbf{x}} = \mathbf{f}^+$$

or similarly for $\mathbf{f}^-$.

Example 9 (Sliding equilibria). In two dimensions consider $\lambda = \operatorname{sign} x_1$ with

$$(\dot{x}_1, \dot{x}_2) = \tfrac{1}{2}(1+\lambda)(-1, -x_2) + \tfrac{1}{2}(1-\lambda)(1, b)$$

or in three dimensions $\lambda = \operatorname{sign} x_1$ with

$$(\dot{x}_1, \dot{x}_2, \dot{x}_3) = \tfrac{1}{2}(1+\lambda)(-1, x_3 - x_2, -x_2) + \tfrac{1}{2}(1-\lambda)(1, b, c)$$

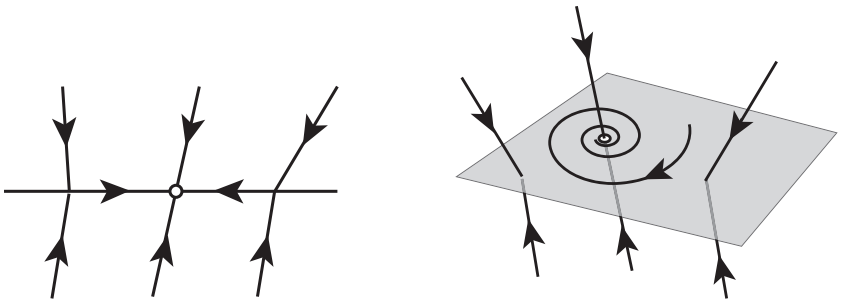

FIGURE 5. Sliding equilibria in two or three dimensions.

Example 10 (Tangencies). The figure below shows quadratic tangencies of types we call 'visible' (curving away) or 'invisible' (curving towards),

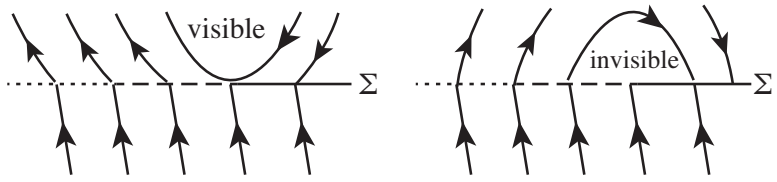

FIGURE 6. Visible and invisible tangencies in the upper vector field.

In higher dimensions, sets of visible and invisible tangencies meet at higher order tangencies, like the cubic tangency, called a 'cusp'.

The examples shown are from the equations

$$(\dot{x}_1, \dot{x}_2) = \tfrac{1}{2}(1+\lambda)(-1, -x_1) + \tfrac{1}{2}(1-\lambda)(0, 1)$$
$$(\dot{x}_1, \dot{x}_2) = \tfrac{1}{2}(1+\lambda)(+1, -x_1) + \tfrac{1}{2}(1-\lambda)(0, 1)$$
$$(\dot{x}_1, \dot{x}_2, \dot{x}_3) = \tfrac{1}{2}(1+\lambda)(x_1^2 + x_2, 1, 0) + \tfrac{1}{2}(1-\lambda)(0, 0, 1)$$

but we could also have cubic, quartic, etc. order.

Above we gave a necessary condition for crossing, but it does not guarantee crossing (it is not necessary *and sufficient*). The shaded region or

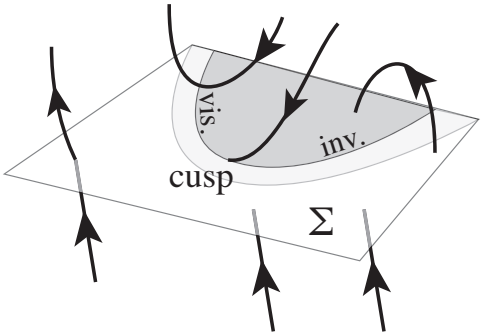

FIGURE 7. A cusp in the upper vector field.

full line on Σ in the figures shows where both vector fields point towards the surface, $\mathbf{f}^+ \cdot \nabla\sigma < 0 < \mathbf{f}^- \cdot \nabla\sigma$, so sliding must occur. In the remaining region trajectories may cross through (indeed in Filippov's convention they *do* cross through), but in non-convex combinations it is possible for the sliding region to 'bleed out' into the crossing region, indicated by the dashed/light-shaded region on Σ.

We've hinted above that crossing or sliding on a switching surface depends on convexity, i.e., whether the dependence on λ is linear. Most courses would assume linearity in λ and hasten onward. Let's hold back a little and consider nonlinear dependence.

Crossing and Sliding – examples II

Let's revisit the crossing example above and add a 'hidden' term.

Example 11 (nonlinear λ). Consider

$$(\dot{x}_1, \dot{x}_2) = (2 + \lambda, 1) + 2(\lambda^2 - 1, 0) \ , \qquad \lambda = \text{sign}(x_1),$$

so $\sigma(\mathbf{x}) = x_1$. Let $\tau > 0$.

The obvious crossing solution is again $x_1(t) = (t - \tau)(2 + \text{sign}(t - \tau))$, $x_2(t) = t + x_{20}$, but turns out to be wrong in the presence of the nonlinear term.

Let's look for sliding solutions by solving $\dot{\sigma} = \sigma = 0$ on Σ ($x_1 = 0$):

$$\dot{\sigma} = \dot{x}_1 = 0 \quad \Rightarrow \quad \lambda = -\tfrac{1}{2} \text{ or } 0 \quad \Rightarrow \quad (\dot{x}_1, \dot{x}_2) = (0, 1) \text{ for both.}$$

Now we seem to have three possible solutions at Σ, the orbit may cross or follow one of two sliding solutions. This kind of ambiguity leads to paradoxes in physics if incorrectly handed. So which is right?

To find out we have to look closer at how λ varies on the interval -1 to $+1$.

5. Switching layers

The dynamics of λ

Switching layers resolve the jump in λ into a continuous (but infinitesimal time) dynamics. A dynamics on λ is introduced such that the sliding dynamics $\dot{\sigma} = 0$ becomes a fixed point of the dynamics on λ.

The multiplier λ is a function of σ, so we may assume $\dot{\lambda} \propto \dot{\sigma}$. Let $\lambda = \lambda(\sigma/\varepsilon)$ for some $\varepsilon \geq 0$, then

$$\dot{\lambda} = \lambda' \dot{\sigma}/\varepsilon = \mathbf{f} \cdot \nabla\sigma/\varepsilon \quad \Rightarrow \quad \varepsilon\dot{\lambda} = \mathbf{f} \cdot \nabla\sigma$$

if we assume ε is such that $\lambda'(\sigma/\varepsilon) = 1$; there are more detailed arguments for the form of ε, but this will suffice since only $\varepsilon \to 0$ is of interest.

Letting $\varepsilon \to 0$ gives an instantaneous switch (instantaneous because the rate of change $\dot{\lambda} \sim 1/\varepsilon$ is then infinitely large), so in piecewise smooth systems, this is the limit we're interested in.

The equilibrium of this is just the sliding solution, since

$$\dot{\lambda} = 0 \qquad \Rightarrow \qquad \dot{\sigma} = 0$$

Example 12 (nonlinear λ . . . continued). On $x_1 = 0$ let

$$\varepsilon\dot{\lambda} = 2 + \lambda + 2(\lambda^2 - 1).$$

This has two equilibria, at $\lambda = -\frac{1}{2}$ or 0. Since

$$\frac{\partial\dot{\lambda}}{\partial\lambda} = 1 + 4\lambda = \begin{cases} -1 & \text{if} \quad \text{at } \lambda = -\frac{1}{2} \\ +1 & \text{if} \quad \text{at } \lambda = 0 \end{cases}$$

the solution $\lambda = -\frac{1}{2}$ is attractive (the other is repelling), so this is the solution the flow follows.

The switching layer

When we take the dynamical equation on λ above, what we actually do is m agnify the *surface* $\sigma = 0$ into a *layer* over which $\lambda \in (-1, +1)$.

Take coordinates so that $\sigma = x_1$, then:

Definition 13. The **switching layer** on $x_1 = 0$ is

$$(\lambda, x_2, ..., x_n) \ \in \ (-1, +1) \times \mathbb{R}^{n-1}.$$

For rigorous theory concerning switching layers see [**13, 8**].

Inside the switching layer the variation is given by a two timescale system:

Definition 14. The switching layer system is

$$\begin{aligned} \varepsilon\dot{\lambda} &= f_1(0, x_2, ..., x_n; \lambda) \\ \dot{x}_i &= f_i(0, x_2, ..., x_n; \lambda) \qquad i = 2, ..., n \end{aligned}$$

in terms of an infinitesimal $\varepsilon \geq 0$ in the limit $\varepsilon \to 0$.

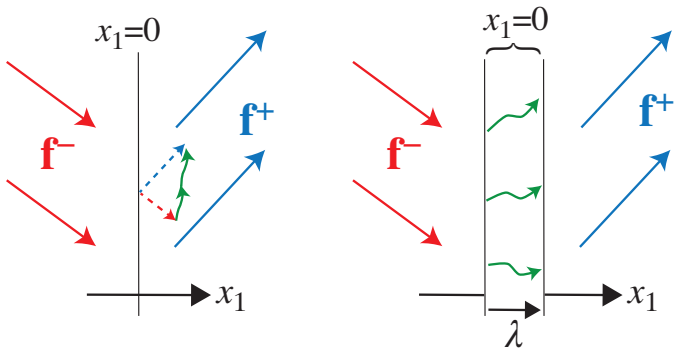

FIGURE 8. A simple crossing (left), blown up to reveal the switching layer (right).

6. Layer variables

The layer system allows us to stretch space to peer inside the discontinuity. But it also gives something more, a way to extend certain local methods from smooth dynamical theory, like linearization, to discontinuities.

Definition 15. In a system where $\lambda = \text{sign}(x_1)$, the switching **layer variable** is the vector

$$(\xi_1, \xi_2, ..., \xi_n) = (\varepsilon\lambda, x_2, ..., x_n)$$

(i.e., the vector $\boldsymbol{\xi}$ given by replacing x_1 by $\varepsilon\lambda$ in coordinates where $\sigma = x_1$).

Layer variables – examples I

Example 16 (I. Linearization).] The planar system

$$\begin{pmatrix} \dot{x}_1 \\ \dot{x}_2 \end{pmatrix} = \begin{pmatrix} -\lambda \\ c - x_2 - \lambda(c + x_2) \end{pmatrix} = \begin{cases} \begin{pmatrix} -1 \\ -2x_2 \end{pmatrix} & \text{if} \quad x_1 > 0 \,, \\ \begin{pmatrix} 1 \\ 2c \end{pmatrix} & \text{if} \quad x_1 < 0 \,, \end{cases}$$

has no equilibria for $x_1 \neq 0$. The switching layer system is

$$\begin{pmatrix} \varepsilon\dot{\lambda} \\ \dot{x}_2 \end{pmatrix} = \begin{pmatrix} -\lambda \\ c - x_2 - \lambda(c + x_2) \end{pmatrix} .$$

This has a sliding equilibrium at $(\lambda, x_2) = (0, c)$.

Is it an attractor? What are it's eigenvalues/vectors?

In layer variables

$$\begin{pmatrix} \dot{\xi}_1 \\ \dot{\xi}_2 \end{pmatrix} = \begin{pmatrix} -\xi_1/\varepsilon \\ c - \xi_2 - \lambda(c + \xi_2) \end{pmatrix} .$$

Find the Jacobian in the layer variables $\boldsymbol{\xi} = (\xi_1, \xi_2) = (\varepsilon\lambda, x_2)$, evaluated at the equilibrium:

$$\mathcal{J} = \begin{pmatrix} \frac{\partial\dot{\xi}_1}{\partial\xi_1} & \frac{\partial\dot{\xi}_1}{\partial\xi_2} \\ \frac{\partial\dot{\xi}_2}{\partial\xi_1} & \frac{\partial\dot{\xi}_2}{\partial\xi_2} \end{pmatrix} = -\frac{1}{\varepsilon}\begin{pmatrix} 1 & 0 \\ c+\xi_2 & \xi_1+\varepsilon \end{pmatrix} = -\frac{1}{\varepsilon}\begin{pmatrix} 1 & 0 \\ 2c & \varepsilon \end{pmatrix}$$

with eigenvalues γ_i and eigenvectors $\boldsymbol{\gamma}_i$ (solutions of $\mathcal{J}\boldsymbol{\gamma}_i = \gamma_i\boldsymbol{\gamma}_i$):

$$\begin{array}{lll} \gamma_1 = -1/\varepsilon \to -\infty & : & \boldsymbol{\gamma}_1 \to (1, 2c)^{\mathsf{T}} \\ \gamma_2 = -1 & : & \boldsymbol{\gamma}_2 = (0,\ 1\ )^{\mathsf{T}} \quad \Leftrightarrow \quad \text{in line of } \Sigma \end{array}$$

Both are attracting (agreeing with this being a node, since $\det\mathcal{J} = 1/\varepsilon > 0$).

Attraction along the $(0, 1)^{\mathsf{T}}$ direction is at unit rate $x_2 - c \sim (x_{20} - c)e^{-t}$.

Attraction along the $(1, 2c)^{\mathsf{T}}$ direction is infinitely fast $(-1/\varepsilon)$, so the contraction to $\xi_1 = 0$ is in finite time, $\xi_1 \sim e^{-t/\varepsilon}$ (i.e., it takes a finite time to reach $x_1 = 0$, but once there, in any time instant t, we find ξ_1 contracts immediately to the equilibrium at $e^{-t/\varepsilon} \to 0$ as $\varepsilon \to 0$).

Layer variables – examples II

Example 17 (II. Linearization). The planar system

$$\begin{pmatrix} \dot{x}_1 \\ \dot{x}_2 \end{pmatrix} = \begin{pmatrix} 1 - x_2 - \lambda(1+x_2) \\ c - 1 - \lambda(c+1) \end{pmatrix} = \begin{cases} 2\begin{pmatrix} -x_2 \\ -1 \end{pmatrix} & \text{if} \quad x_1 > 0\,, \\ 2\begin{pmatrix} 1 \\ c \end{pmatrix} & \text{if} \quad x_1 < 0\,, \end{cases}$$

has no equilibria for $x_1 \neq 0$. The switching layer system is

$$\begin{pmatrix} \varepsilon\dot{\lambda} \\ \dot{x}_2 \end{pmatrix} = \begin{pmatrix} 1 - x_2 - \lambda(1+x_2) \\ c - 1 - \lambda(c+1) \end{pmatrix}\,.$$

This has a equilibrium at $(\lambda, x_2) = (\frac{c-1}{c+1}, \frac{1}{c})$.

Is it an attractor? What are it's eigenvalues/vectors?

Find the Jacobian in the layer variables $\boldsymbol{\xi} = (\xi_1, \xi_2) = (\varepsilon\lambda, x_2)$, evaluated at the equilibrium:

$$\mathcal{J} = \begin{pmatrix} \frac{\partial\dot{\xi}_1}{\partial\xi_1} & \frac{\partial\dot{\xi}_1}{\partial\xi_2} \\ \frac{\partial\dot{\xi}_2}{\partial\xi_1} & \frac{\partial\dot{\xi}_2}{\partial\xi_2} \end{pmatrix} = -\frac{1}{\varepsilon}\begin{pmatrix} 1+\xi_2 & \xi_1+\varepsilon \\ c+1 & 0 \end{pmatrix} = -\frac{1}{\varepsilon}\begin{pmatrix} 1+\frac{1}{c} & \frac{2c\varepsilon}{c+1} \\ c+1 & 0 \end{pmatrix}$$

with eigenvalues/vectors (where $R = (c+1)^2 + 8c^3\varepsilon$):

$$\begin{array}{lll} \gamma_1 = \frac{c+1+\sqrt{R}}{-4c\varepsilon} \to -\infty & : & \boldsymbol{\gamma}_1 \to (1, c)^{\mathsf{T}} \\ \gamma_2 = \frac{c+1-\sqrt{R}}{-4c\varepsilon} \to \frac{c^2}{c+1} & : & \boldsymbol{\gamma}_2 = (0,\ 1\ )^{\mathsf{T}} \quad \Leftrightarrow \quad \text{direction of } \Sigma \end{array}$$

One is attracting, one repelling (implying a saddle, agreeing with $\det\mathcal{J} = -2c/\varepsilon < 0$).

Repulsion along the $(0, 1)^{\mathsf{T}}$ direction is as $x_2 - \frac{1}{c} \sim (x_{20} - \frac{1}{c})e^{+tc^2/(c+1)}$.

Along the $(1, c)^{\mathsf{T}}$ direction the rate of attraction is infinitely fast, so the contraction to $\xi_1 = 0$ is instantaneous, $\xi_1 - \frac{c-1}{c+1} \sim (\xi_{10} - \frac{c-1}{c+1})e^{-t(c+1)/2c\varepsilon}$.

Layer variables – examples III

Example 18. (III. Linearization). The three dimensional system

$$\begin{pmatrix} \dot{x}_1 \\ \dot{x}_2 \\ \dot{x}_3 \end{pmatrix} = \begin{cases} \begin{pmatrix} -1 \\ ax_2 + bx_3 \\ cx_2 + dx_3 \end{pmatrix} & \text{if} \quad x_1 > 0 \,, \\ \begin{pmatrix} 1 \\ e \\ 0 \end{pmatrix} & \text{if} \quad x_1 < 0 \,, \end{cases}$$

has no equilibria for $x_1 \neq 0$. Taking the convex combination, the switching layer system simplifies to

$$\begin{pmatrix} \varepsilon\dot{\lambda} \\ \dot{x}_2 \\ \dot{x}_3 \end{pmatrix} = \tfrac{1}{2} \begin{pmatrix} -2\lambda \\ (1+\lambda)(ax_2 + bx_3) + (1-\lambda)e \\ (1+\lambda)(cx_2 + dx_3) \end{pmatrix} .$$

This has an equilibrium at $(\lambda, x_2, x_3) = (0, -d, c)e/(ad - bc)$.

The Jacobian at this point is

$$\underline{\underline{J}} = \tfrac{1}{2} \begin{pmatrix} -2/\varepsilon & 0 & 0 \\ -2e/\varepsilon & a & b \\ 0 & c & d \end{pmatrix}$$

with eigenvalues and corresponding eigenvectors as $\varepsilon \to 0$

$$\begin{array}{lll} \gamma_1 = -1/\varepsilon \to -\infty & : & \boldsymbol{\gamma}_1 \to (1, e, 0)^{\mathsf{T}} \\ \gamma_2 = \frac{a+d}{4} - \sqrt{R} & : & \boldsymbol{\gamma}_2 = (0, 2\gamma_2 - d, c)^{\mathsf{T}} \quad — \quad \text{inside } \Sigma \\ \gamma_3 = \frac{a+d}{4} + \sqrt{R} & : & \boldsymbol{\gamma}_3 = (0, 2\gamma_3 - d, c)^{\mathsf{T}} \quad — \quad \text{inside } \Sigma \end{array}$$

where $R = \left(\frac{a+d}{4}\right)^2 + bc - ad$.

The eigenvalues $\gamma_{2,3}$ are finite and confined to the (x_2, x_3) plane of Σ, where the equilibrium is: a saddle if $ad - bc < 0$, focus if $ad - bc > 0 > R$, node if $ad - bc > 0$ & $R > 0$, attracting if $a + d < 0$ and repelling if $a + d > 0$.

The eigenvalue γ_1 says the sliding region $x_1 = 0$ is attracting with an infinite rate (i.e., in zero time) along the direction $(1/e, 1, 0)$, i.e., along the directions of the two constituent vector fields $\mathbf{f}^{\pm}$ at the equilibrium.

Example 19 (A saddlenode bifurcation in the plane). Take a smooth system

$$\begin{pmatrix} \dot{x}_1 \\ \dot{x}_2 \end{pmatrix} = \begin{pmatrix} x_1^2 - c \\ -x_2 \end{pmatrix}$$

which has equilibria at $(x_1, x_2) = (\pm\sqrt{c}, 0)$, which exist only for $c > 0$.

The Jacobian is $\mathcal{J} = \begin{pmatrix} \pm\sqrt{c} & 0 \\ 0 & -1 \end{pmatrix}$ at $(x_1, x_2) = (\pm\sqrt{c}, 0)$, with

$$\begin{array}{lll} \gamma_1 = -1 & : & \boldsymbol{\gamma}_1 \to (0, 1)^{\mathsf{T}} \\ \gamma_2 = \pm 2\sqrt{c} & : & \boldsymbol{\gamma}_2 = (1, 0)^{\mathsf{T}} \end{array}$$

The '+' gives a saddle and the '−' gives an attracting node.

A saddlenode bifurcation occurs as c changes sign: the two equilibria (for $c > 0$) annihilate each other and leave a non-vanishing flow (for $c < 0$).

Let's contrast this with a similar boundary equilibrium bifurcation...

Example 20 (A discontinuity-induced saddlenode bifurcation). Take a piecewise-smooth system

$$\begin{pmatrix} \dot{x}_1 \\ \dot{x}_2 \end{pmatrix} = \tfrac{1}{2}(1+\lambda)\begin{pmatrix} 1 \\ b \end{pmatrix} + \tfrac{1}{2}(1-\lambda)\begin{pmatrix} -\frac{1}{2}x_1 \\ -x_2 \end{pmatrix}$$

where $\lambda = \operatorname{sign}\sigma$ and $\sigma = x_1 - x_2 - c$, the bifurcation parameter is c, and b is a small nominal constant. For the layer system we rotate coordinates, so let $(y_1, y_2) = (x_1 - x_2 - c, x_1 + x_2)/4$, giving

$$\begin{pmatrix} \dot{y}_1 \\ \dot{y}_2 \end{pmatrix} = \tfrac{1}{2}(1+\lambda)\begin{pmatrix} 1-b \\ 1+b \end{pmatrix} + \tfrac{1}{2}(1-\lambda)\begin{pmatrix} y_2 - 3y_1 - \frac{3}{4}c \\ y_1 - 3y_2 + \frac{1}{4}c \end{pmatrix}$$

in which the node lies at $(y_1, y_2) = (-\frac{c}{4}, 0)$, with

$$\mathcal{J} = \begin{pmatrix} -3 & 1 \\ 1 & -3 \end{pmatrix} \quad \Rightarrow \quad \begin{array}{lll} \gamma_1 = -4 & : & \boldsymbol{\gamma}_1 \to (-1,1)^{\mathsf{T}} \\ \gamma_2 = -2\sqrt{c} & : & \boldsymbol{\gamma}_2 = (1,1)^{\mathsf{T}} \end{array}$$

The layer system on $y_1 = 0$ is

$$\begin{pmatrix} \varepsilon\dot{\lambda} \\ \dot{y}_2 \end{pmatrix} = \tfrac{1}{2}(1+\lambda)\begin{pmatrix} 1-b \\ 1+b \end{pmatrix} + \tfrac{1}{2}(1-\lambda)\begin{pmatrix} y_2 - 3y_1 - \frac{3}{4}c \\ y_1 - 3y_2 + \frac{1}{4}c \end{pmatrix}$$

with an equilibrium at $(\lambda, y_2) = \left(\frac{c+b-2}{c-b+2}, \frac{c(2+b)}{4(2-b)}\right)$, where the Jacobian in layer variables is

$$\mathcal{J} = \begin{pmatrix} \frac{\partial\dot{\xi}_1}{\partial\xi_1} & \frac{\partial\dot{\xi}_1}{\partial\xi_2} \\ \frac{\partial\dot{\xi}_2}{\partial\xi_1} & \frac{\partial\dot{\xi}_2}{\partial\xi_2} \end{pmatrix} = \begin{pmatrix} \frac{(b-1)(c-b+2)}{2\varepsilon(b-2)} & \frac{2-b}{c-b+2} \\ \frac{2+c+b+cb-b^2}{2\varepsilon(2-b)} & \frac{3(2-b)}{b-c-2} \end{pmatrix}$$

with eigenvalues and corresponding eigenvectors as $\varepsilon \to 0$

$$\begin{array}{lll} \gamma_1 = \frac{1}{\varepsilon}\frac{(1-b)(c-b+2)}{2(2-b)} \to +\infty & : & \boldsymbol{\gamma}_1 \to (1-b, 1+b)^{\mathsf{T}} \\ \gamma_2 = \frac{2(2-b)^2}{(b-1)(c-b+2)} < 0 & : & \boldsymbol{\gamma}_2 = (0,1)^{\mathsf{T}} \quad \text{—} \quad (\text{along } \Sigma) \end{array}$$

(for small c and b.)

Hence this equilibrium is a saddle, with an infinite rate of repulsion along the $(1-b, 1+b)$ direction out of the switching surface, and asymptotic attraction along the vertical inside the surface.

As in the previous example, the two equilibria exist only for $c > 0$. As c becomes negative the two equilibria leave their domains of definition:

- the node leaves the $x_1 = -\frac{c}{4} < 0$ region ($x_1 > 0$ for $c < 0$),
- the saddle leaves the $\lambda \in (-1, +1)$ layer ($\lambda = \frac{c+b-2}{c-b+2} < -1$ for $c < 0$).

7. Multiple switches

Combinations for r switches

We wrote $\dot{\mathbf{x}} = \mathbf{f}(\mathbf{x};\lambda)$ for a single switch with $\lambda = \text{sign}(\sigma)$.

Now let the switching surface Σ be comprised of m transversally intersecting sub-manifolds $\Sigma = \Sigma_1 \cup \Sigma_2 \cup ... \cup \Sigma_m$, where

$$\begin{aligned} \Sigma_i &= \{\, \mathbf{x} \in \mathbb{R}^n \;:\; \sigma_i(\mathbf{x}) = 0 \,\} \\ \Sigma &= \{\, \mathbf{x} \in \mathbb{R}^n \;:\; \sigma(\mathbf{x}) = \sigma_1(\mathbf{x})\sigma_2(\mathbf{x})...\sigma_m(\mathbf{x}) = 0 \,\} \end{aligned}$$

The multiplier λ becomes a vector $\boldsymbol{\lambda} = (\lambda_1, ..., \lambda_m)$ where each $\lambda_i = \text{sign}(\sigma_i)$.

The combination becomes

$$\dot{\mathbf{x}} = \mathbf{f}(\mathbf{x};\boldsymbol{\lambda}) \quad : \quad \begin{array}{ll} \lambda_i = \text{sign}\,(\sigma_i(\mathbf{x})) & \text{for} \quad \sigma_i(\mathbf{x}) \neq 0 \\ \lambda_i \in (-1,+1) & \text{for} \quad \sigma_i(\mathbf{x}) = 0\,. \end{array}$$

E.g., $\mathbf{f}^{+---}(\mathbf{x})$ corresponds to $\mathbf{f}(\mathbf{x};+1,-1,-1,-1)$.

If we have m surfaces $\sigma_1 = 0$, ..., $\sigma_m = 0$, this results in 2^m different vector fields $\mathbf{f}^{\pm_1 \cdots \pm_m}$.

Canopy combination

If we are given constituent vector fields $\mathbf{f}^1$, $\mathbf{f}^2$, ..., or in binary indices $\mathbf{f}^{++\cdots}$, $\mathbf{f}^{-+\cdots}$, ..., how do we form a combination $\mathbf{f}^(\mathbf{x};\lambda_1,\lambda_2,...)$ from them?

The direct extension of the convex combination to multiple switches is the *convex hull*,

$$\dot{\mathbf{x}} = \mathbf{f}(\mathbf{x};\boldsymbol{\lambda}) = \sum_i \lambda_i \mathbf{f}^i\,(\mathbf{x}) \;\;,$$

summing over all the indices i labelling regions, and subject to a normalization condition $\sum_i \lambda_i = 1$. This means typically for m switching surfaces, we have 2^m vector fields $\mathbf{f}^i$, and $2^m - 1$ unknown multipliers λ_i. If we seek sliding motion on those surfaces we will solve m conditions $\sigma_1 = ... = \sigma_m = 0$. Such a problem is only well posed if the number of unknowns matches the number of conditions, $2^m - 1 = m$, which is only satisfied in the trivial case $m = 1$, i.e., a single switch. The convex hull, therefore, does not give a well posed expression of the piecewise smooth system. Fortunately there is a resolution.

We can extend the combinations from earlier as the 'canopy' of $\mathbf{f}^{\cdots}$ values:

$$\dot{\mathbf{x}} = \mathbf{f}(\mathbf{x};\boldsymbol{\lambda}) = \sum_{i_1=\pm} ... \sum_{i_m=\pm} \lambda_j^{(i_j)} \lambda_2^{(i_2)} ... \lambda_m^{(i_m)} \mathbf{f}^{i_1 i_2 ... i_m}\,(\mathbf{x}) \;\;,$$

using shorthand

$$\lambda_j^{(\pm)} \equiv \tfrac{1}{2}(1 \pm \lambda_j)\;.$$

We can also add a hidden term $\mathbf{k}$ which satisfies

$$\sigma_1(\mathbf{x})...\sigma_m(\mathbf{x})\;\mathbf{k}(\mathbf{x}) = 0\;.$$

Theorem 21. If we assume $\dot{\mathbf{x}}$ depends multi-linearly on m independent switching multipliers $\lambda_1, ..., \lambda_m$, it can be written uniquely as $\dot{\mathbf{x}} = \mathbf{f}(\mathbf{x}; \lambda_1, ..., \lambda_m)$ using the canopy combination.

E.g., For $m = 1$: $\dot{\mathbf{x}} = \mathbf{f}(\mathbf{x}; \boldsymbol{\lambda}) = \frac{1+\lambda_1}{2}\mathbf{f}^{+}(\mathbf{x}) + \frac{1-\lambda_1}{2}\mathbf{f}^{-}(\mathbf{x})$

E.g., For $m = 2$: $\dot{\mathbf{x}} = \mathbf{f}(\mathbf{x}; \boldsymbol{\lambda}) = \frac{1+\lambda_2}{2}\left\{\frac{1+\lambda_1}{2}\mathbf{f}^{++}(\mathbf{x}) + \frac{1-\lambda_1}{2}\mathbf{f}^{-+}(\mathbf{x})\right\}$
$+\frac{1-\lambda_2}{2}\left\{\frac{1+\lambda_1}{2}\mathbf{f}^{+-}(\mathbf{x}) + \frac{1-\lambda_1}{2}\mathbf{f}^{--}(\mathbf{x})\right\}$.

8. *r*-Switching layers

The switching layer for *r* switches

Extending the method for a single switch, magnify each sub-manifold $\sigma_i = 0$ into a *layer* over which each $\lambda_i \in (-1, +1)$.

Take coordinates so that $\sigma_j = x_j$ for $j = 1, ..., r$, with $0 < r \leq m \leq n$:

Definition 22. The **switching layer** on $x_1 = x_2 = ... = x_r = 0$ is

$$(\lambda_1, ..., \lambda_r, x_{r+1}, ..., x_n) \in (-1, +1)^r \times \mathbb{R}^{n-1}$$

Inside the layer the variation is given by the $r + 1$ timescale system:

Definition 23. The switching layer system is

$$\begin{aligned} \varepsilon_j \dot{\lambda}_j &= f_j(0, ..., 0, x_{r+1}, ..., x_n; \lambda_1, ..., \lambda_m) \qquad j = 1, ..., r \\ \dot{x}_i &= f_i(0, ..., 0, x_{r+1}, ..., x_n; \lambda_1, ..., \lambda_m) \qquad i = r+1, ..., n \end{aligned}$$

in terms of (*different*) infinitesimals $\varepsilon_j > 0$ in the limit $\varepsilon_j \to 0$.

Codimension *r* sliding

Definition 24. The (codimension r) sliding manifold is the set of points in the switching layer where

$$0 = f_j(0, ..., 0, x_{r+1}, ..., x_n; \lambda_1, ..., \lambda_m) \quad \forall \ j = 1, ..., r$$

on which the sliding dynamics is given by the differential algebraic equations

$$\begin{aligned} 0 &= f_j(0, ..., 0, x_{r+1}, ..., x_n; \lambda_1, ..., \lambda_m) \qquad j = 1, ..., r \\ \dot{x}_i &= f_i(0, ..., 0, x_{r+1}, ..., x_n; \lambda_1, ..., \lambda_m) \qquad i = r+1, ..., n \end{aligned}$$

Example 25 (Sliding equilibrium). For a system with two switches, take coordinates such that $\sigma_i = x_i$, so $\lambda_i = \operatorname{sign} x_i$ for $i = 1, 2$, and consider vector fields

$$\begin{pmatrix} \dot{x}_1 \\ \dot{x}_2 \end{pmatrix} = \begin{pmatrix} a_1 \\ a_2 \end{pmatrix} + \begin{pmatrix} b_{11} & b_{12} \\ b_{21} & b_{22} \end{pmatrix} \begin{pmatrix} \lambda_1 \\ \lambda_2 \end{pmatrix} .$$

where the a_i and b_{ij} may be functions of $\mathbf{x}$.

There is codimension $r = 1$ (i.e., 'normal') sliding:
on $x_1 = 0$:

$$\lambda_1^\Sigma = -\frac{a_1 + b_{12}\operatorname{sign} x_2}{b_{11}} \quad \Rightarrow \quad \dot{x}_2 = a_2 - \frac{b_{21}}{b_{11}}\left(a_1 + b_{12}\operatorname{sign} x_2\right) + b_{22}\operatorname{sign} x_2 \ ,$$

on $x_2 = 0$:

$$\lambda_2^\Sigma = -\frac{a_2 + b_{21}\operatorname{sign} x_1}{b_{22}} \quad \Rightarrow \quad \dot{x}_1 = a_1 - \frac{b_{12}}{b_{22}}\left(a_2 + b_{21}\operatorname{sign} x_1\right) + b_{11}\operatorname{sign} x_1 \ ,$$

and elsewhere the flow crosses $x_1 = 0$ and $x_2 = 0$ transversally.

The intersection we must treat separately.

There is codimension $r = 2$ sliding where

$$\begin{pmatrix} \lambda_1^\Sigma \\ \lambda_2^\Sigma \end{pmatrix} = \frac{1}{b_{11}b_{22} - b_{12}b_{21}} \begin{pmatrix} b_{12}a_2 - b_{22}a_1 \\ b_{21}a_1 - b_{11}a_2 \end{pmatrix}$$

which exists if it lies in $(-1,+1) \times (-1,+1)$ (which we can more concisely write as $(-1,+1)^2$).

The attractivity of the sliding solution can be derived either from the eigenvectors and eigenvalues of $\frac{d\mathbf{f}}{d\boldsymbol{\lambda}} = \begin{pmatrix} b_{11} & b_{12} \\ b_{21} & b_{22} \end{pmatrix}$, and in simple cases from the directions of the flows along the manifolds $x_1 = 0$ and $x_2 = 0$.

Example 26 (Sliding equilibrium in 3D). Eigenvectors of an equilibrium in codimension 2 sliding.

Consider the three dimensional system

$$\begin{pmatrix} \dot{x}_1 \\ \dot{x}_2 \\ \dot{x}_3 \end{pmatrix} = \begin{pmatrix} a_1 \\ a_2 \\ -x_3 \end{pmatrix} + \begin{pmatrix} b_{11} & b_{12} & 0 \\ b_{21} & b_{22} & 0 \\ 0 & 0 & 0 \end{pmatrix} \begin{pmatrix} \lambda_1 \\ \lambda_2 \\ 0 \end{pmatrix}$$

where $\lambda_i = \operatorname{sign} x_i$, for nonzero constants a_i, b_{ij}. The system outside Σ (which is made up of $x_1 = 0$, $x_2 = 0$, and $x_3 = 0$) is non-vanishing, so there are no equilibria outside the switching surface.

Taking the intersection first, the switching layer system is

$$\begin{pmatrix} \varepsilon_1\dot{\lambda}_1 \\ \varepsilon_2\dot{\lambda}_2 \\ \dot{x}_3 \end{pmatrix} = \begin{pmatrix} a_1 + b_{11}\lambda_1 + b_{12}\lambda_2 \\ a_2 + b_{21}\lambda_1 + b_{22}\lambda_2 \\ -x_3 \end{pmatrix} \qquad \text{on } \ x_1 = x_2 = 0 \ .$$

This has a unique equilibrium at

$$(\lambda_1, \lambda_2, x_3) = \frac{(a_2b_{12} - a_1b_{22}, a_1b_{21} - a_2b_{11}, 0)}{b_{11}b_{22} - b_{12}b_{21}} \ ,$$

the first two components of which must lie inside $(-1,+1)$, otherwise the equilibrium ceases to exist.

When that happens, where does it go? We return to this question in the next section.

The layer Jacobian of the equilibrium is

$$\mathcal{J} = \begin{pmatrix} \varepsilon_1^{-1} b_{11} & \varepsilon_2^{-1} b_{12} & 0 \\ \varepsilon_1^{-1} b_{21} & \varepsilon_2^{-1} b_{22} & 0 \\ 0 & 0 & -1 \end{pmatrix}$$

with eigenvalues and corresponding eigenvectors

$$\begin{array}{lll} \gamma_1 = (\frac{b_{11}+\mu b_{22}}{2} + \sqrt{R})/\varepsilon_1 & : & \boldsymbol{\gamma}_1 = (\gamma_1 - \mu b_{22}, b_{21}, 0)^{\mathsf{T}} \\ \gamma_2 = (\frac{b_{11}+\mu b_{22}}{2} - \sqrt{R})/\varepsilon_1 & : & \boldsymbol{\gamma}_2 = (\gamma_2 - \mu b_{22}, b_{21}, 0)^{\mathsf{T}} \\ \gamma_3 = -1 & : & \boldsymbol{\gamma}_3 = (0, 0, 1)^{\mathsf{T}} \end{array}$$

where $\mu = \varepsilon_1/\varepsilon_2$ and $R = \left(\frac{b_{11}+\mu b_{22}}{2}\right)^2 + \mu b_{12} b_{21} - \mu b_{11} b_{22}$.

The eigenvector γ_3 gives a finite rate of attraction along the intersection.

The eigenvalues $\gamma_{1,2}$ have a magnitude that is infinite as $\varepsilon_{1,2} \to 0$, since they describe dynamics in the plane transverse to the intersection, i.e., in the directions out of the codimension 2 sliding region. Their eigenvectors, however, are finite, assuming that the ratio $\mu = \varepsilon_1/\varepsilon_2$ is finite and nonzero as $\varepsilon_{1,2} \to 0$.

Thus the parameters b_{ij} and the ratio μ determine whether the equilibrium is a node, focus, or saddle in the $\lambda_{1,2}$ plane. This closely mirrors what happens outside the intersection, and if $\mu = 1$ it corresponds directly.

Boundary equlibrium bifurcations

The layer system is defined only on $\boldsymbol{\lambda} \in (-1, +1)^2$.

If any of the λ_j's satisfying $\mathbf{f}_j = 0$ ($\forall\, j = 1, ..., r$) sits at $\lambda_j^{\Sigma} = \pm 1$, then the point lies on a boundary of codimension r sliding.

Example 27 (Boundary equilibrium bifurcation between codimension 1 and 2 sliding). Consider again the three dimensional system above. There are no equilibria outside the switching surface, and we saw that an equilibrium exists inside the intersection $x_1 = x_2 = 0$ at

$$(\lambda_1, \lambda_2, x_3) = \frac{(a_2 b_{12} - a_1 b_{22}, a_1 b_{21} - a_2 b_{11}, 0)}{b_{11} b_{22} - b_{12} b_{21}} \,,$$

only for

$$\left| \frac{a_2 b_{12} - a_1 b_{22}}{b_{11} b_{22} - b_{12} b_{21}} \right| < 1 \,, \quad \left| \frac{a_1 b_{21} - a_2 b_{11}}{b_{11} b_{22} - b_{12} b_{21}} \right| < 1 \,.$$

When the parameters lie outside this region, the equilibrium inside the intersection no longer exists. Bifurcations occur at

$$\left| \frac{a_2 b_{12} - a_1 b_{22}}{b_{11} b_{22} - b_{12} b_{21}} \right| = 1 \quad \& \quad \left| \frac{a_1 b_{21} - a_2 b_{11}}{b_{11} b_{22} - b_{12} b_{21}} \right| = 1 \,.$$

Where does the equilibrium go?

There are sliding regions on the switching manifolds $x_1 = 0$ or $x_2 = 0$ outside the intersection. The bifurcation that actually occurs at these values will be degenerate, with the entire sliding vector field along $x_2 = 0$ and

$x_1 = 0$ vanishing respectively at these two parameter values. A more generic system is easily obtained, say by perturbing this system to

$$\begin{pmatrix} \dot{x}_1 \\ \dot{x}_2 \\ \dot{x}_3 \end{pmatrix} = \begin{pmatrix} a_1 + c_1 x_1 \\ a_2 + c_2 x_2 \\ -x_3 \end{pmatrix} + \begin{pmatrix} b_{11} & b_{12} & 0 \\ b_{21} & b_{22} & 0 \\ 0 & 0 & 0 \end{pmatrix} \begin{pmatrix} \lambda_1 \\ \lambda_2 \\ 0 \end{pmatrix}$$

which does not change the system on the intersection, hence our analysis so far stands.

On the switching manifolds $x_1 = 0$ or $x_2 = 0$ outside the intersection, the layer systems are

$$\begin{pmatrix} \varepsilon_1 \dot{\lambda}_1 \\ \dot{x}_2 \\ \dot{x}_3 \end{pmatrix} = \begin{pmatrix} a_1 + b_{11}\lambda_1 + b_{12}\,\mathrm{sign}(x_2) \\ a_2 + c_2 x_2 + b_{21}\lambda_1 + b_{22}\,\mathrm{sign}(x_2) \\ -x_3 \end{pmatrix} \quad \text{on } \; x_1 = 0 \neq x_2 \; ,$$

$$\begin{pmatrix} \dot{x}_1 \\ \varepsilon_2 \dot{\lambda}_2 \\ \dot{x}_3 \end{pmatrix} = \begin{pmatrix} a_1 + c_1 x_1 + b_{11}\,\mathrm{sign}(x_1) + b_{12}\lambda_2 \\ a_2 + b_{21}\,\mathrm{sign}(x_1) + b_{22}\lambda_2 \\ -x_3 \end{pmatrix} \quad \text{on } \; x_2 = 0 \neq x_1 \; .$$

Sliding (where the $\dot{\lambda}_i$ subsystems vanish) occurs for $\lambda_1^\Sigma = -\frac{a_1 + b_{12}\,\mathrm{sign}(x_2)}{b_{11}}$ and $\lambda_2^\Sigma = -\frac{a_2 + b_{21}\,\mathrm{sign}(x_1)}{b_{22}}$ respectively, giving dynamics

$$\dot{x}_2 = c_2 x_2 + \tfrac{a_2 b_{11} - a_1 b_{21}}{b_{11}} - \tfrac{b_{21} b_{12} - b_{11} b_{22}}{b_{11}}\,\mathrm{sign}(x_2) \quad \text{on } \; x_1 = 0 \neq x_2 \; ,$$

$$\dot{x}_1 = c_1 x_1 + \tfrac{a_1 b_{22} - a_2 b_{12}}{b_{22}} - \tfrac{b_{12} b_{21} - b_{11} b_{22}}{b_{22}}\,\mathrm{sign}(x_1) \quad \text{on } \; x_2 = 0 \neq x_1 \; .$$

At the bifurcation values, as the equilibrium vanishes from codimension two sliding on the intersection, it either passes into one of these two systems, or collides with another equilibrium and the two annihilate in another example of a discontinuity-induced saddlenode bifurcation. We leave it as an exercise to explore the different scenarios.

9. A 'thorny issue': Stability, equivalence, & bifurcation

The notions of equivalence between systems, and structural stability of a system within a given class, are incredibly important in smooth systems, and are quite easy to extend to piecewise smooth systems, but use them with care.

There are three notions of equivalence between systems that are useful.

Definition 28. Orbital, differentiable, and topological equivalence:

(i) **Orbital equivalence**: If two vector fields $\mathbf{f}$ and $\hat{\mathbf{f}}$ are related by $\mathbf{f}(\mathbf{x};\boldsymbol{\lambda}) = \mu(\mathbf{x};\boldsymbol{\lambda})\hat{\mathbf{f}}(\mathbf{x};\boldsymbol{\lambda})$ for some continuous positive definite scalar function $\mu(\mathbf{x};\boldsymbol{\lambda})$, the orbits of the systems $\dot{\mathbf{x}} = \mathbf{f}(\mathbf{x};\boldsymbol{\lambda})$ and $\dot{\mathbf{x}} = \hat{\mathbf{f}}(\mathbf{x};\boldsymbol{\lambda})$ are identical up to a time rescaling.

(ii) $q-$**Conjugacy**: If two vector fields $\mathbf{f}$ and $\hat{\mathbf{f}}$ are related by a q-times differentiable mapping $\mathbf{h}$ which takes orbits of $\dot{\mathbf{x}} = \mathbf{f}(\mathbf{x};\boldsymbol{\lambda})$ to those of $\dot{\mathbf{x}} = \hat{\mathbf{f}}(\mathbf{x};\boldsymbol{\lambda})$, preserving direction but not necessarily scaling of time, then the vector fields $\mathbf{f}(\mathbf{x};\boldsymbol{\lambda})$ and $\hat{\mathbf{f}}(\mathbf{x};\boldsymbol{\lambda})$ are said to be q-conjugate (or q-differentiably equivalent, sometimes called C^q equivalence).

(iii) **Topological equivalence**: If $q = 0$ in (ii) and the switching surface is preserved, the vector fields $\mathbf{f}(\mathbf{x};\boldsymbol{\lambda})$ and $\hat{\mathbf{f}}(\mathbf{x};\boldsymbol{\lambda})$ are said to be *topologically equivalent*. That is, topological equivalence between the vector fields $\mathbf{f}(\mathbf{x};\boldsymbol{\lambda})$ and $\hat{\mathbf{f}}(\mathbf{x};\boldsymbol{\lambda})$ means that $\mathbf{f}$ and $\hat{\mathbf{f}}$ are related by a continuous mapping $\mathbf{h}$ which takes orbits of $\dot{\mathbf{x}} = \mathbf{f}(\mathbf{x};\boldsymbol{\lambda})$ to those of $\dot{\mathbf{x}} = \hat{\mathbf{f}}(\mathbf{x};\boldsymbol{\lambda})$, preserving direction but not necessarily scaling of time, and maps the switching surface of one system to that of the other preserving orientation with respect to orbits.

It is important to include the switching surface explicitly in the definition of topological equivalence, otherwise, for example, a system that crosses a switching surface is equivalent to a smooth system with no switching surface at all.

A q-conjugacy with:

- q infinite preserves the eigenvalues associated with any equilibria,
- $q > 1$ preserves only the relative sizes of eigenvalues,
- $q = 0$ preserves spatial and temporal topology of orbits themselves, but does not preserve eigenvalues.

So a node and a focus are topologically equivalent if they have the same attractivity, but only on a region that does not include the switching surface.

At a switching surface, a node and a focus of the same attractivity are not topologically equivalent, because all orbits hit the switching surface in both forward and backward time around a boundary focus, while some orbits (shaded in figure) contact the switching surface only in one direction near a boundary node.

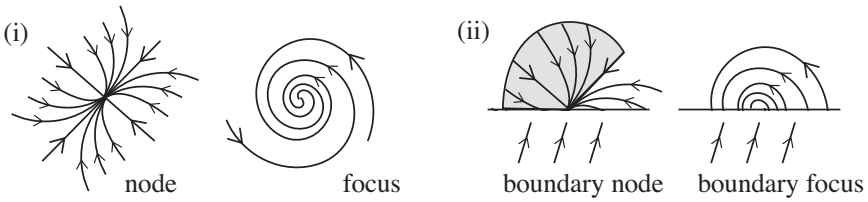

FIGURE 9. The node and focus in (i) are topologically equivalent, the boundary node and focus in (ii) are not.

Note that systems may be equivalent but have very different functional expressions, and conversely, two systems that appear similar in their functional expressions may in fact not be equivalent.

A system is considered robust in its behaviour — or **structurally stable** — if small changes in its expression produce equivalent systems. Intuitively, a small perturbation involves the addition of a small term in the equations, but does not qualitatively alter the dynamics. The precise definitions (see e.g., Guckenheimer & Holmes 2002) can be extended (see e.g., Filippov 1988) formally, for example:

Definition 29. If $\mathbf{f} \in \mathbb{R}^n$ and $\sigma \in \mathbb{R}$ are r times differentiable (vector and scalar valued resp.) functions, in which the level set $\sigma = 0$ is the switching surface Σ of $\mathbf{f}$, then for some $0 < q \leq r$ and $\varepsilon > 0$, the functions $\tilde{\mathbf{f}}$ and $\tilde{\sigma}$ are a perturbation of f and σ of size ε, of differentiability class q, if there

is a compact set $K \subset \mathbb{R}^{n+1}$ such that $\mathbf{f} = \tilde{\mathbf{f}}$ and $\sigma = \tilde{\sigma}$ on the complement set $K_c = \mathbb{R}^{n+1} - K$ and for all $i_1, i_2, ..., i_n$, with $i = i_1 + i_2 + ... + i_n \leq q$ we have $\left| \left(\partial^i / \partial x_1^{i_1} ... \partial x_n^{i_n} \right) (\mathbf{f} - \tilde{\mathbf{f}}) \right| < \varepsilon$ and $\left| \left(\partial^i / \partial x_1^{i_1} ... \partial x_n^{i_n} \right) (\sigma - \tilde{\sigma}) \right| < \varepsilon$.

But it is more important to understand what this means. Perturbing a piecewise smooth systems is a subtle act. But it is vital to our notion of 'robustness' of a system, or *structural stability*.

Definition 30. A vector field $\mathbf{f} \in \mathbb{R}^n$ is **structurally stable** if there is an $\varepsilon > 0$ such that all differentiable ($q = 1$) ε perturbations of $\mathbf{f}$ are topologically equivalent to $\mathbf{f}$.

In a smooth system we typically consider only continuous or continuously differentiable perturbations. We could insist on this in piecewise smooth systems, just to be safe, but this seems a little *too* safe.

If we write

$$\dot{\mathbf{x}} = \mathbf{f}^+(\mathbf{x}) \text{ on } \mathcal{R}_+, \quad \dot{\mathbf{x}} = \mathbf{f}^-(\mathbf{x}) \text{ on } \mathcal{R}_-, \quad ...$$

then can we perturb in one region (say $\dot{\mathbf{x}} = \mathbf{f}^+(\mathbf{x}) + \delta$) but not another? This means introducing a perturbation that is δ in $\mathcal{R}_1$ and zero elsewhere, i.e., the perturbation is discontinuous.

Normally we don't allow discontinuous perturbations. Even a simple smooth system with a stable equilibrium isn't structurally stable under discontinuous perturbations, for example $\dot{x}_1 = x_1$ is equivalent to $\dot{x}_1 = x_1 - \delta$ (the equilibrium is slightly shifted), but not to $\dot{x}_1 = x_1 - \delta \operatorname{sign} x_1$ (the equilibrium splits into three!), even though these all tend to the same thing as $\delta \to 0$.

Even if we disallow such obviously absurd perturbations, what conditions must we place on the perturbation at the switching surface to make sure sliding dynamics is preserved? You'll find partial answers to these in Filippov 1988, Guardia Seara Teixeira 2011, and Budd Champneys di Bernardo Kowalczyk 2008, which seem to suggest only differentiable perturbations should be allowed — we can't perturb $\mathbf{f}^+$ without perturbing $\mathbf{f}^-$ the same amount.

Because we have expressed our system in the form $\dot{\mathbf{x}} = \mathbf{f}(\mathbf{x}; \boldsymbol{\lambda})$, however, we can do a little more, and allow perturbations that are at least differentiable in $\mathbf{x}$ or $\boldsymbol{\lambda}$. Intuitively, small changes in the dependence on $\boldsymbol{\lambda}$ will make only small changes in the equations for sliding, for example, and preserve equivalence. This is despite the fact that adding, say, $\delta\boldsymbol{\lambda}$, means adding a perturbation that is different in different regions. The discontinuity of the perturbation with respect to $\mathbf{x}$ is implicitly hidden inside $\boldsymbol{\lambda}$.

So if we want to perturb $\dot{x}_1 = x_1$ with respect to λ_1, where $\lambda_1 = \operatorname{sign} x_1$ (for $x_1 \neq 0$ at least), we must first consider this to be a system $\dot{x}_1 = f(x_1; \lambda_1)$, i.e., with λ_1 defined even if it doesn't appear in the dynamical equation, and hence the switching surface $x_1 = 0$ is defined.

We can now see immediately that this system is structurally unstable, because x_1 lies on the switching surface, and any small perturbation will kick it off, giving a non-equivalent system. The switching surface matters even if we can't see it!

In the system $\dot{x}_1 = x_1 - 1$ with $\lambda = \operatorname{sign} x_1$ (for $x_1 \neq 0$), however, the equilibrium lies at $x_1 = 1$ away from the switching surface at $x_1 = 0$. If we perturb as before, to $\dot{x}_1 = x_1 - 1 - \delta\lambda$ for small δ, the resulting system is equivalent, so $\dot{x}_1 = x_1 - 1$ with a switching surface at $x_1 = 0$ is structurally stable to perturbations proportional to $\lambda = \operatorname{sign} x_1$.

Both Filippov [**4**] and Teixeira consider pseudo-orbits to be a determining factor in the equivalence of systems. It depends what you want to study about a system, but I prefer to exclude them. A pseudo-orbit is a concatenation of trajectories that does not preserve the direction of time, therefore it is of no dynamical (or as far as we know physical) significance.

Example 31 (Stable or not?). In the figure below:

- A fused centre is not structurally stable. It is comprised entirely of closed orbits that cross through a switching surface, formed by the piecewise smooth fusing of two parabolic systems.
- Perturbation results in a (repelling or attracting) fused focus, which typically is structurally stable, possibly surrounded by one or more isolated closed orbits.
- If we ignore pseudo-orbits, then a pseudo fused centre (similar to the centre but the orbits travel the 'wrong way' on one side of the surface) is typically structurally stable, and is dynamically no different from a ...
- ... pseudo fused focus.

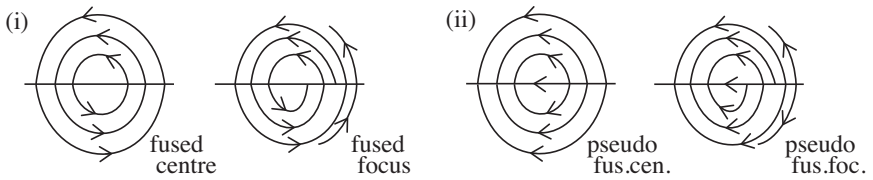

FIGURE 10. (i) The fused centre and fused focus are not equivalent, only the centre is structurally unstable. (ii) Whether the same is true for for the corresponding pseudo-singularities is a matter of interpretation.

Example 32. The system $\dot{x} = -\lambda$ with $\Sigma = \{x = 0\}$ and $\lambda = \operatorname{sign}(x)$ is structurally stable. The system $\dot{x} = -x$ is stable, but the system defined as $\dot{x} = -x$ for $x \gtrless 0$ about a switching surface $\Sigma = \{x = 0\}$ is not structurally stable, a perturbation $\dot{x} = \delta c - x$ or $\dot{x} = \delta\lambda - x$ when $\lambda = \operatorname{sign}(x)$ creates a non-equivalent system. The similar system defined as $\dot{x} = b - x$ for $x \gtrless 0$ about a switching surface $\Sigma = \{x = 0\}$ is structurally stable for b bounded away from zero.

The systems we will study generally depend on variables $\mathbf{x} = (x_1, x_2, ..., x_n)$, switching multipliers $\boldsymbol{\lambda} = (\lambda_1, \lambda_2, ..., \lambda_m)$, and parameters $\mathbf{p} = (a, b, c, ...)$. Structurally unstable systems may occur at particular values of the parameters.

Definition 33. A **bifurcation set** is the set of parameters $\mathbf{p} = (a, b, c, ...)$ for which the system $\dot{\mathbf{x}} = \mathbf{f}(\mathbf{x}; \boldsymbol{\lambda}; \mathbf{p})$ is structurally unstable. Any point $\mathbf{x}$ in a neighbourhood of which the system is structurally unstable is a **singularity** (or singular point).

A bifurcation of the system – a topological change – takes place as we vary parameters through the bifurcation set.

Bifurcations can take place in a region where $\dot{\mathbf{x}} = \mathbf{f}^i$ is smoothly varying, which may be outside the switching surface, or may be inside the surface if $\mathbf{f}^i$ is one of the sliding vector fields. These are covered by the bifurcation theory of smooth dynamical systems.

Then there are a whole new array of bifurcations that cannot occur in differentiable dynamical systems, because they involve the discontinuity in a non-trivial way.

Definition 34. A bifurcation is said to be **discontinuity-induced** in a system $\dot{\mathbf{x}} = \mathbf{f}(\mathbf{x}; \boldsymbol{\lambda})$ if it involves a singular point on the boundary of a sliding region.

This tightens a definition given in [**2**] which would permit any bifurcation in a discontinuity system to be considered discontinuity-induced. The definition almost certainly is still not perfect.

10. Discontinuity-induced phenomena

We end this course with a brief survey of fun things you now have the foundations to explore.

Local bifurcation points

Tangencies

Above we looked a tangencies as the boundaries of sliding regions. We also defined a *discontinuity-induced bifurcation* as one occurring at such a boundary. This means that tangencies lie at the heart of most of the interesting phenomena in piecewise smooth flows.

One particular singularity has caused much confusion and misunderstanding over the last 30 years. Yet it could hardly be more simple!

Example 35 (The two-fold singularity). Consider the piecewise linear system

$$(\dot{x}_1, \dot{x}_2, \dot{x}_2) = \begin{cases} (-x_2, a, v) & \text{if} \quad x_1 > 0 \ , \\ (\ x_3, w, b) & \text{if} \quad x_1 > 0 \ , \end{cases}$$

Exercise: see what you can find out about this! There are three main 'flavours' depending on whether each fold is visible or invisible. Then there are lots of sub-cases depending on the sliding dynamics, determined by v and w.

Tangencies are a rich source of bifurcations. Already in the plane they have a number of cases (see next page).

You can derive the fold cases from:

$$\dot{\mathbf{x}} = \mathbf{f}(\mathbf{x};\lambda) = \tfrac{1}{2}(1+\lambda)\begin{pmatrix} a(x_2-1)+bx_1 \\ -1 \end{pmatrix} + \tfrac{1}{2}(1-\lambda)\begin{pmatrix} \alpha_1+\alpha_2 x_2 \\ a \end{pmatrix}$$

and the cusp cases from:

$$\dot{\mathbf{x}} = \mathbf{f}(\mathbf{x};\lambda) = \tfrac{1}{2}(1+\lambda)\begin{pmatrix} x_2^2+b \\ \pm 1 \end{pmatrix} + \tfrac{1}{2}(1-\lambda)\begin{pmatrix} 1 \\ 0 \end{pmatrix}$$

with $\lambda = \text{sign}(x_1)$, where a, b, α_i, are constants.

These become much richer still in three (or some higher) dimensions, of course; see the ongoing work of Teixeira starting with [**17**].

Tangencies are much more than singularities in their own right. Any object — any attractor or orbit — that acquires or loses a connection with the switching surface must do so via a tangency. We will see a few examples below.

Boundary equilibria

Definition 36. An equilibrium of a vector field $\mathbf{f}^i$ lying on the switching surface (or of a codimension r sliding vector field lying on a codimension $r+1$ switching intersection) is a **boundary equilibrium**.

A boundary equilibrium is structurally unstable, and is typically a bifurcation point. A prototype for boundary equilibria is quite easy to write down: a general equilibrium on one side of the switching surface, a constant but *sufficiently general* vector field on the other side. For example:

$$\dot{\mathbf{x}} = \mathbf{f}(\mathbf{x};\lambda) = \tfrac{1}{2}(1+\lambda)\underline{\underline{A}}\begin{pmatrix} x_1-\mu \\ x_2 \\ x_3 \\ \vdots \end{pmatrix} + \tfrac{1}{2}(1-\lambda)\begin{pmatrix} 1 \\ d_1 \\ d_2 \\ \vdots \end{pmatrix}$$

with $\lambda = \text{sign}(x_1)$, where the $n \times n$ matrix $\underline{\underline{A}}$ and n-vector $(1, d_1, ..., d_{n-1})$ are constants.

A boundary equilibrium occurs at $\mu = 0$, when the equilibrium of the $\lambda = +1$ system lies at $(x_1, x_2) = (0, 0)$ on the switching surface $x_1 = 0$.

As we change μ, a *boundary equilibrium bifurcation* occurs. For $\mu > 0$ the equilibrium lies in $x_1 > 0$. For $\mu < 0$ this equilibrium no longer exists.

Exercise: where did the equilibrium of this dynamical system go?

I promised you that tangencies lay at the heart of discontinuity-induced bifurcations. The tangency in the system above can only occur in the $\lambda = +1$ system (exercise: why?), so it lies where

$$x_1 = \dot{x}_1 = 0 \;\;\&\;\; \lambda = +1 \quad \Rightarrow \quad a(-\mu) + bx_2 = 0 \quad \Rightarrow \quad x_2 = \mu a/b$$

Is it visible or invisible? A visible tangency curves away from the surface, an invisible curves towards it. In $x_1 \geq 0$ this means $\ddot{x}_1 > 0$ for visible or $\ddot{x}_1 < 0$ for invisible (in $x_1 \leq 0$ the conditions are means $\ddot{x}_1 < 0$ for visible or $\ddot{x}_1 > 0$ for invisible), so evaluate

$$\ddot{x}_1 = a\dot{x}_1 + b\dot{x}_2 = a\left\{a(x_1-\mu) + bx_2\right\} + bcx_2 = \mu a^2 c$$

The tangency therefore switches between visible and invisible as μ changes sign, i.e., as the bifurcation 'unfolds', and as the equilibrium contacts the boundary. $\ddot{x}_1$ is zero at $\mu = 0$, so at the bifurcation point itself the tangency is degenerate.

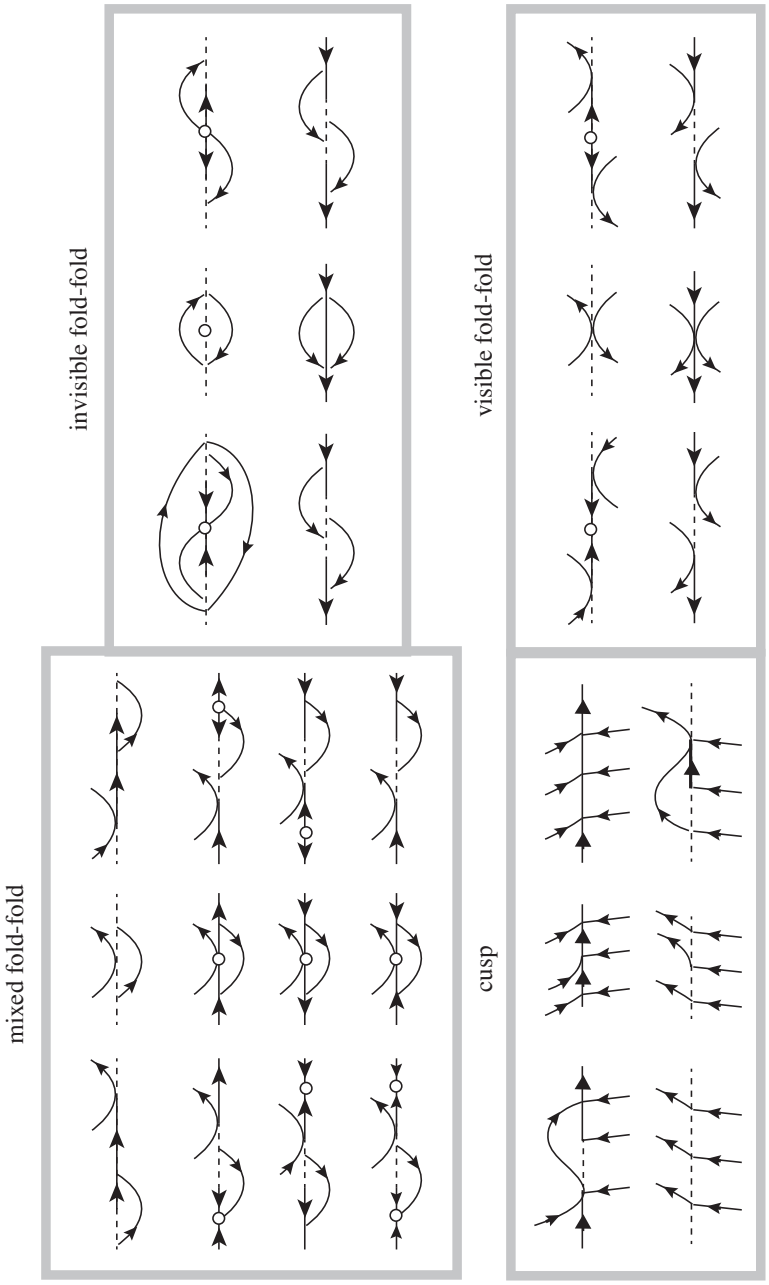

FIGURE 11. Codimension 1 tangencies and their unfoldings.

Exercise: see if you can recreate all of the cases below, using the prototype above for two dimensions, with $\lambda = \text{sign}(x_1)$ and

$$\dot{\mathbf{x}} = \mathbf{f}(\mathbf{x};\lambda) = \tfrac{1}{2}(1+\lambda)\begin{pmatrix} a(x_1-\mu)+bx_2 \\ cx_2 \end{pmatrix} + \tfrac{1}{2}(1-\lambda)\begin{pmatrix} 1 \\ d \end{pmatrix}$$

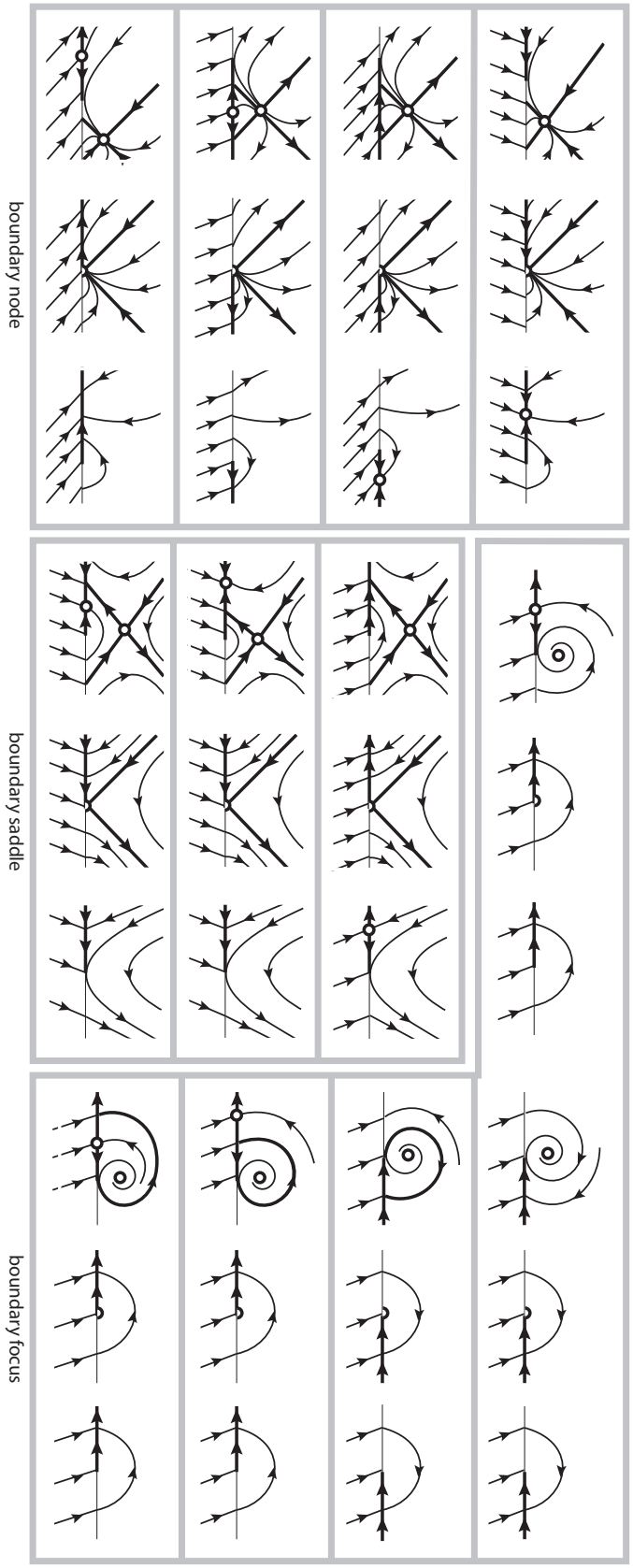

FIGURE 12. Codimension 1 boundary equilibria and their unfoldings.

Each triplet shows the unfolding as μ changes sign. The middle portrait in each shows the bifurcation point – the boundary equilibrium. You can find most of these (some were missed!) in [**10**] and later references. You'll find the bifurcation points themselves (all of them!) only in Filippov's book [**4**].

Because these unfold as a single parameter (μ) changes, they are called *codimension one* bifurcations.

Filippov (1988) classified the bifurcation points of boundary equilibria, of tangencies, and of more exotic things like line singularities. (To clarify the remark above, Kuznetsov Rinaldi Gragnani (2003) also classified boundary equilibria, claiming their list to be "complete", and provided "normal forms", but beware of the terms in quotes when you see them, because these and other authors missed some important cases! These are not easy notions in piecewise smooth dynamics)

Global bifurcation points

Global bifurcation points consist of orbital connections between singularities: equilibria, sliding equilibria, and tangencies. The latter of course come into play only in piecewise smooth systems, and give rise to global discontinuity-induced bifurcations.

These may arise when distinguished orbits (those already connected to an equilibrium or periodic orbit, for example) have connections to visible or invisible tangencies. In the figure, the ★ denotes some other singularity.

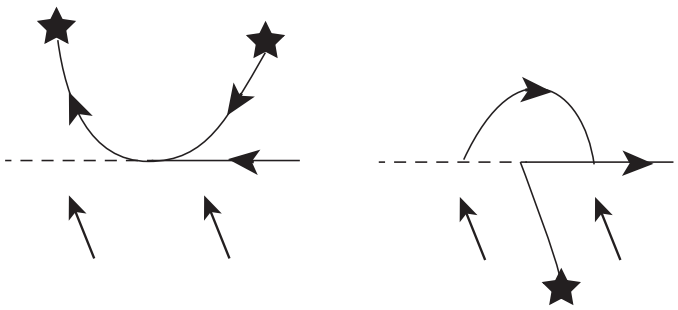

FIGURE 13. Connections to a visible (left) or invisible (right) tangency are structurally unstable.

The following figure shows various connections that give rise to bifurcations, though many more are possible, particularly when we consider multiple dimensions, and multiple switches.

The first row shows heteroclinic connections between a smooth equilibrium and a tangency. The second row shows heteroclinic connection between a smooth equilibrium and a sliding equilibrium, the last two shows two ways that a visible tangency can facilitate a homoclinic connection to a smooth equilibrium or a sliding equilibrium.

Under perturbation of any of these the connection typically will be broken, and a bifurcation takes place. See [**2, 10**] for further examples.

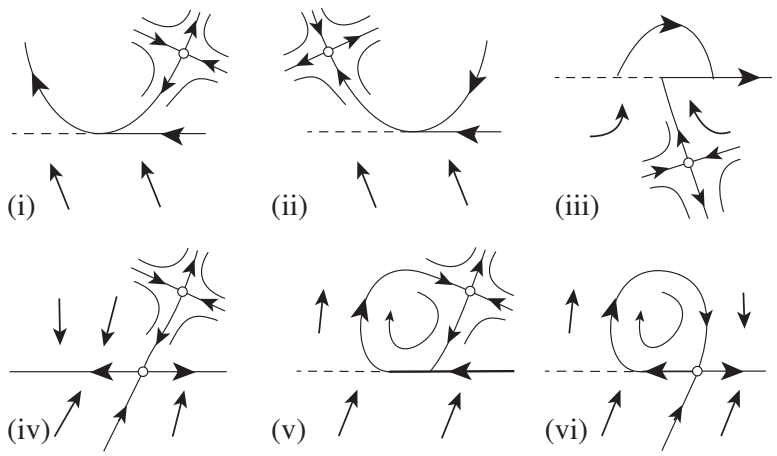

FIGURE 14. Codimension one connections: Heteroclinic connection between a saddle and a visible tangency (i-ii), a saddle and invisible tangency (iii), a saddle and sliding saddle (iv). Homoclinic connection via visible tangency to a saddle (vi) or a sliding saddle (vii).

A visible tangency may connect to itself, forming a periodic orbit. Let's unfold this particular bifurcation, known as a *grazing-sliding* bifurcation). On one side of the bifurcation is a smooth limit cycle, on the other side is a so-called "stick-slip" oscillation.

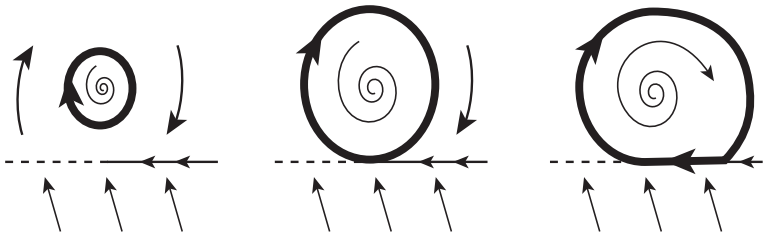

FIGURE 15. Unfolding of a grazing-sliding bifurcation.

When repelling sliding is involved, bifurcations can take another, more dramatic form. We call these sliding *explosions*.

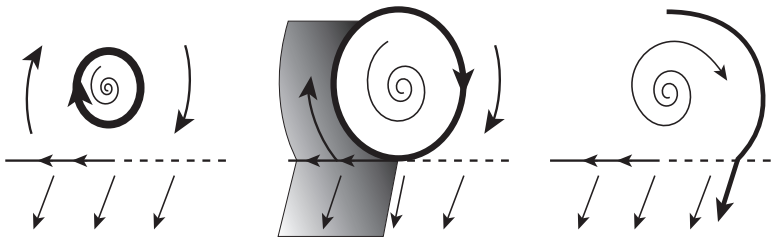

FIGURE 16. Unfolding of a grazing-sliding explosion [**6**].

Determinacy-breaking

An explosion is one example of *determinacy-breaking*, a general phenomenon that occurs when the flow is somehow able to enter a region of repelling sliding.

The only robust way this can happen is when a sliding region changes attractivity, so the flow passes from attracting sliding to repelling sliding. (Notice in the grazing sliding explosion above that the explosion happens only at a special parameter value, i.e., it doesn't happen at a general parameter value, hence it is not 'robust').

One way this can happen is at a two-fold singularity (see earlier example). A simpler way is at a switching surface made of two intersecting manifolds. For example:

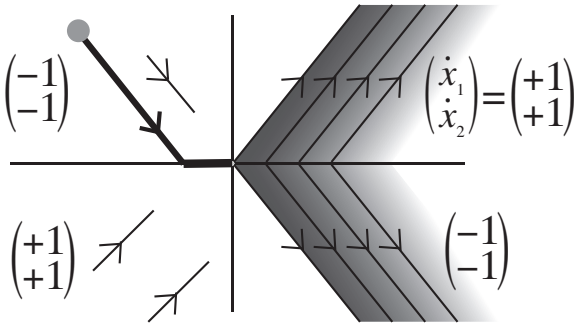

FIGURE 17. Determinacy-breaking at a switching intersection. The system has two switches creating four regions. The loss of determinacy at the intersection can be partially resolved using layer analysis, see [**7**].

Because of the presence of determinacy-breaking points like these, piecewise smooth systems are *almost* deterministic, at best.

Hidden attractors

The dynamics inside a switching surface can do strange things in seemingly simple systems. Consider

$$\begin{aligned}
\dot{x}_1 &= 5(\lambda_2 - \lambda_1) - 75x_1 \ , \\
\dot{x}_2 &= -\lambda_1 - 15\lambda_1\lambda_3 - \tfrac{1}{2}\lambda_2 - 75x_2 \ , \\
\dot{x}_3 &= 15\lambda_1\lambda_2 - \tfrac{4}{3} - \tfrac{4}{3}\lambda_3 - 75x_3 \ , \\
\dot{x}_4 &= \lambda_1 - 75x_4 \ ,
\end{aligned}$$

where $\lambda_j = \text{sign}(x_j)$ for $j = 1, 2, 3$.

This has three switches, and eight regions, but the dynamics is seemingly almost trivial. Outside the switching surface each row looks like $\dot{x}_i = \text{const} - 75x_i$, giving strong attraction towards $\frac{1}{75} \times \text{const}$, which ultimately results in collapse towards the origin. Once at $(x_1, x_2, x_3) = (0, 0, 0)$, where all three switches intersect, however, things become interesting.

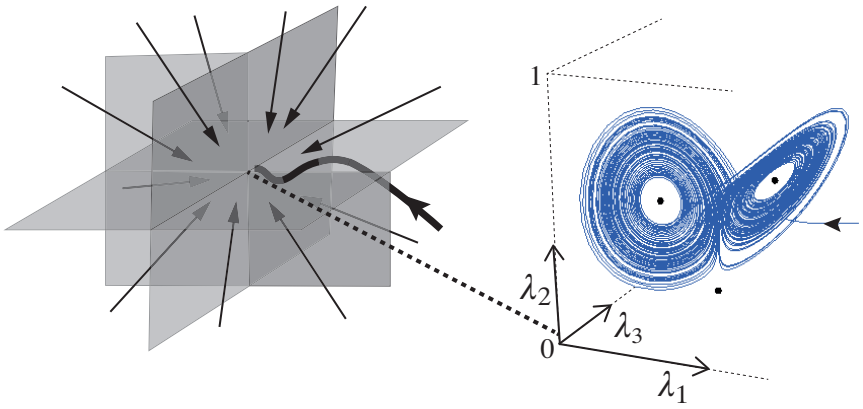

FIGURE 18. Hidden Lorenz attractor at the intersection of three switches. This example was inspired by gene regulatory networks [**11**].

When $(x_1, x_2, x_3) = (0, 0, 0)$, the layer system (if we let $\varepsilon_i = \varepsilon$ for $i = 1, 2, 3$) becomes the Lorenz system in $\lambda_1, \lambda_2, \lambda_3$,

$$\begin{aligned} \varepsilon\dot{\lambda}_1 &= 5(\lambda_2 - \lambda_1) \,, \\ \varepsilon\dot{\lambda}_2 &= -\lambda_1 - 15\lambda_1\lambda_3 - \tfrac{1}{2}\lambda_2 \,, \\ \varepsilon\dot{\lambda}_3 &= 15\lambda_1\lambda_2 - \tfrac{4}{3} - \tfrac{4}{3}\lambda_3 \,, \end{aligned}$$

so the 3 switching multipliers behave chaotically inside the switching layer $(\lambda_1, \lambda_2, \lambda_3) \in (-1, +1)^3$. The variables x_1, x_2, x_3, remain at zero. The variable x_4, however, is coupled to the λ_1 switching multiplier, and will follow a chaotic trajectory.

Hidden bifurcations

Hidden attractors can undergo their own bifurcations, including any bifurcations that are possible in smooth systems, and many more that remain to be discovered. Consider

$$\begin{aligned} \dot{x}_1 &= \tfrac{1}{2}(1 - \lambda_1\lambda_2) - \gamma_1(x_1 + \theta_1) \\ \dot{x}_2 &= \tfrac{1}{4}(3 - \lambda_1 - \lambda_2 - \lambda_1\lambda_2) - \gamma_2(x_2 + \theta_2) \end{aligned}$$

where $\lambda_j = \text{sign}(x_j)$ for $j = 1, 2$.

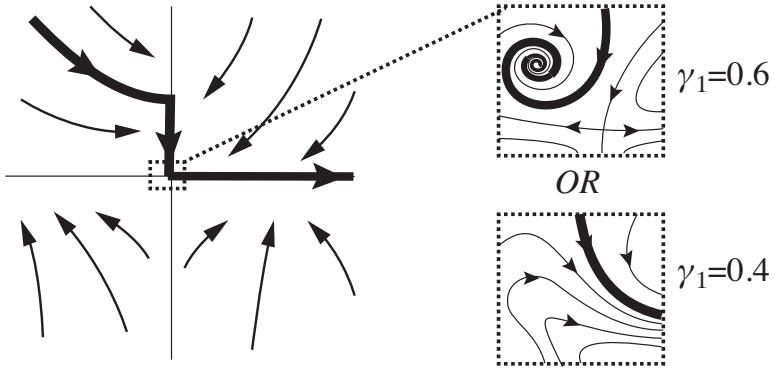

FIGURE 19. Hidden saddlenode bifurcation at the intersection of two switches. This example was derived from models of gene regulatory networks [**3**].

This has two switches that intersect at the origin $(0,0)$. There is attraction towards $(0,0)$ from some directions, either directly or via sliding, but also repulsion from $(0,0)$ via sliding. To find out what the flow does we must look inside the switching layer.

The layer system for $x_1 = x_2 = 0$ undergoes a saddlenode bifurcation as γ_1 changes value. There is an attracting focus for higher values of γ_1, which traps solutions at $(0,0)$, but as γ_1 decreases the focus collides with a saddle and annihilates, leaving no attractor, so solutions pass through $(0,0)$ onto the righthand half line of the switching surface.

11. In closing

Piecewise smooth dynamics has a long history, but it is still a young, rapidly growing and exciting area full of new ideas. Let me just end by picking out – quite arbitrarily – a few of the many highlights of recent years.

Two big breakthroughs from recent years:

- The two-fold singularity – Is it stable or not? Is it an attractor or not? For the beginnings of the problem see Filippov 1988, Teixeira 1990, CRM Program 2007. This was eventually solved around 2008-2011, extended to many dimensions in 2013, and to many switches in 2015.
- "Hilbert's 16^{th} for nonsmooth systems" was thrown open when it was shown (in 2015) that infinitely many cycles are possible even in a piecewise linear system.

Two big challenges outstanding:

- Regularization / Non-ideal switching – how do we deal with effects of smoothing, hysteresis, stochastics, discretization, delay, ...
- Higher dimensions – what new attractors/bifurcations/chaos or entirely new phenomena appear in higher dimensions? What new concepts do we need to describe them?

Applications:

climate	power control	economy	cell biology
social behaviour	process engineering	earthquakes	biscuits
robotics	classical mechanics	chemical reactions	neuroscience
superconductors	friction/impact	etc. . .	

There are many more breakthroughs, open challenges, and emerging applications to list here, but I'll leave them for you to discover for yourselves ....!

Bibliography

[1] A.A. Andronov, A.A. Vitt, and S.E. Khaikin. *Theory of oscillations*. Moscow: Fizmatgiz (in Russian), 1959.

[2] M. di Bernardo, C.J. Budd, A.R. Champneys, and P. Kowalczyk. *Piecewise-Smooth Dynamical Systems: Theory and Applications*. Springer, 2008.

[3] R. Edwards, A Machina, G. McGregor, and P. van den Driessche. A modelling framework for gene regulatory networks including transcription and translation. *Bull. Math. Biol.*, 77:953–983, 2015.

[4] A.F. Filippov. *Differential Equations with Discontinuous Righthand Sides*. Kluwer Academic Publ. Dortrecht, 1988 (Russian 1985).

[5] I. Flügge-Lotz. *Discontinuous Automatic Control*. Princeton University Press, 1953.

[6] M.R. Jeffrey. Non-determinism in the limit of nonsmooth dynamics. *Physical Review Letters*, 106(25):254103, 2011.

[7] M.R. Jeffrey. Exit from sliding in piecewise-smooth flows: deterministic vs. determinacy-breaking. *Chaos, in press*, 2015.

[8] M.R. Jeffrey. Hidden degeneracies in piecewise smooth dynamical systems. *Int. J. Bif. Chaos, in press*, 2015.

[9] V. Kulebakin. On theory of vibration controller for electric machines. *Theor. Exp. Electon (in Russian)*, 4, 1932.

[10] Yu. A. Kuznetsov, S. Rinaldi, and A. Gragnani. One-parameter bifurcations in planar Filippov systems. *Int. J. Bif. Chaos*, 13:2157–2188, 2003.

[11] A. Machina, R. Edwards, and P. van den Dreissche. Singular dynamics in gene network models. *SIADS*, 12(1):95–125, 2013.

[12] G. Nikolsky. On automatic stability of a ship on a given course. *Proc Central Commun Lab (in Russian)*, 1:34–75, 1934.

[13] D.N. Novaes and M.R. Jeffrey. Regularization of hidden dynamics in piecewise smooth flow. *J. Differ. Equ.*, 259:4615–4633, 2015.

[14] J. Sotomayor and M.A. Teixeira. Regularization of discontinuous vector fields. *Proceedings of the International Conference on Differential Equations, Lisboa*, pages 207–223, 1996.

[15] M.A. Teixeira. Structural stability of pairings of vector fields and functions. *Boletim da S.B.M.*, 9(2):63–82, 1978.

[16] M.A. Teixeira. Stability conditions for discontinuous vector fields. *J. Differ. Equ.*, 88:15–29, 1990.

[17] M.A. Teixeira. Generic bifurcation of sliding vector fields. *J. Math. Anal. Appl.*, 176:436–457, 1993.

[18] V.I. Utkin. Variable structure systems with sliding modes. *IEEE Trans. Automat. Contr.*, 22:212–222, 1977.

[19] V.I. Utkin. *Sliding modes and their application in variable structure systems*, volume (Translated from the Russian). MiR, 1978.

[20] V.I. Utkin. *Sliding modes in control and optimization*. Springer-Verlag, 1992.

Abstracts

Jaume Llibre, Universitat Autònoma de Barcelona
Analytic Computation of Periodic Solutions of Piecewise Differential Systems.

Abstract: We present four different techniques for computing analytically the periodic solutions of piecewise differential systems, based on the Newton-Kantorovich Theorem, on the Poincaré map, on the averaging theory, and on the first integrals.

Contact address: `jllibre@mat.uab.cat`

Abdelali El Aroudi, Universitat Rovira i Virgili
Sliding-Mode Control and Stability Analysis of DC-DC Switching Converters.

Abstract: The sliding-mode control of DC-DC switching converters is presented in contrast to the traditional pulse width modulation approach. The method of the equivalent control is illustrated in the design of a two-loop control for the voltage regulation of a switching boost converter which is characterized by a bilinear power stage. The theoretical predictions are validated by means of numerical simulations using a circuit-level model implemented in PSIM software. Applications of the method reported are also discussed.

Contact address: `abdelali.elaroudi@urv.cat`

Gerard Olivar, Universidad Nacional de Colombia
Sustainable Development.

Abstract: We show modeling and numerical simulation of the long-run dynamic interaction between the exploitation of natural environment and population growth in a society economically dependent on renewable resources and agriculture. Different mathematical models of development are presented and analysed through bifurcation theory and state space simulations. We obtain parameter settings that yield positive values of resources and population (thus sustainability), and parameter settings where resources become extinct. Results show that one-parameter bifurcations of equilibria and limit cycles exist when we consider a planar system, and quasiperiodic and chaotic behaviour is observed when endogenous technological progress is introduced as an extra dynamical variable. Alternatively, self-regulation of labour force employed in harvesting shows a positive effect in resources conservation. Sliding and pseudo-equilibria are obtained when a reserve is created to protect a certain amount of resources from human exploitation.

Contact address: `golivar@unal.edu.co`

Enrique Ponce, Universidad de Sevilla
Characterizing the Compound Bifurcation in the Teixeira Singularity for Piecewise Linear Systems.

Abstract: We consider 3D piecewise linear Filippov differential systems with a separation plane, having a two-fold point with invisible tangencies, that is, the so-called Teixeira singularity. For some parameter values this singularity undergoes a compound bifurcation: there appears a sliding bifurcation involving a pseudo-equilibrium point and, simultaneously, a bifurcation associated to the birth of a crossing limit cycle.

After determining a generic canonical form, we show how to characterize such a compound bifurcation. Several examples, including realistic applications, will be addressed.

The presentation comes from a joint work with Rony Cristiano and Daniel J. Pagano (both from UFSC Florianópolis, Brasil), and Emilio Freire (U. Sevilla).

Bibliography

[1] M.A. Teixeira, *Stability conditions for discontinuous vector fields.* Journal of Differential Equations 88 (1990), 15–29.

[2] M.A. Teixeira, *Generic bifurcation of sliding vector fields.* J. Math. Anal. Appl. 176 (1993), 436–457.

[3] M.R. Jeffey, A. Colombo, *The two-fold singularity of discontinuous vector fields.* SIAM J. Applied Dynamical Systems 8 (2009), no. 2, 624–640.

[4] S. Fernandez-Garcia, D.A. Garcia, G.O. Tost, M. di Bernardo, M.R. Jeffrey, *Structural stability of the two-fold singularity.* SIAM Journal on Applied Dynamical Systems 11 (2012), no. 4, 1215–1230.

[5] A. Colombo, M.R. Jeffey, *Nondeterministic chaos, and the two-fold singularity in piecewise smooth flows.* SIAM J. Applied Dynamical Systems 10 (2011), no. 2, 423–451.

[6] A. Colombo, M. di Bernardo, E. Fossas, M.R. Jeffrey, *Teixeira singularities in 3d switched feedback control systems.* Systems & Control Letters 59 (2010, 615–622.

Contact address: `eponcem@us.es`

Campus de Bellaterra, Edifici C
08193 Bellaterra, Spain
Tel.: +34 93 581 10 81
Fax: +34 93 581 22 02
crm@crm.cat
www.crm.cat